GEORGIA INSTITUTE OF TECHNOLOGY — OFFICE OF CONTRACT ADMINISTRATION

PROJECT ADMINISTRATION DATA SHEET

[X] ORIGINAL [ ] REVISION NO. ____

Project No. E-25-610 GTRI/~~GIT~~ DATE 9 / 23 / 83

Project Director: Dr. Wayne J. Book School/~~EMK~~ ME

Sponsor: National Science Foundation

Type Agreement: Grant No. MEA-8303539

Award Period: From 9/15/83 To ~~2/28/85~~ 8-31-85 * (Performance) 5/28/85 * (Reports)

Sponsor Amount:	This Change	Total to Date
Estimated:	$ 79,698	$ 79,698
Funded:	$ 79,698	$ 79,698

Cost Sharing Amount: $ ____ Cost Sharing No: E-25-313

Title: "The Bracing Approach to High Speed Manipulation with Lightweight Robot Arms."

ADMINISTRATIVE DATA — OCA Contact Brian J. Lindberg X4820

1) Sponsor Technical Contact:	2) Sponsor Admin/Contractual Matters:
Dr. Elbert Marsh	Lois A. Shapiro
Mechanical Systems Program	National Science Foundation
National Science Foundation	Washington, D.C. 20550
1800 G Street, N.W.	
Washington, D.C. 20550	
(202)357-7386	(202)357-9626

Defense Priority Rating: N/A Military Security Classification: None

(or) Company/Industrial Proprietary: ____

RESTRICTIONS

See Attached NSF Supplemental Information Sheet for Additional Requirements.

Travel: Foreign travel must have prior approval – Contact OCA in each case. Domestic travel requires sponsor approval where total will exceed greater of $500 or 125% of approved proposal budget category.

Equipment: Title vests with GIT - see section 8 of Grant General Conditions

COMMENTS:

* Includes usual six-month unfunded flexibility period.

COPIES TO:

Project Director (Book)	Procurement/EES Supply Services	GTRI
Research Administrative Network	Research Security Services	Library
Research Property Management	(Reports Coordinator (OCA))	Project File
Accounting	Research Communications (2)	Other I. Newton

FORM OCA 4-79R

GEORGIA INSTITUTE OF TECHNOLOGY OFFICE OF CONTRACT ADMINISTRATION

SPONSORED PROJECT TERMINATION/CLOSEOUT SHEET

Date 9/19/86

Project No. E-25-610 School/~~Lab~~ ME

Includes Subproject No.(s) N/A

Project Director(s) Wayne Book GTRC / ~~GIT~~

Sponsor National Science Foundation

Title "The Bracing Approach to High Speed Manipulation with Lightweight Robot Arms."

Effective Completion Date: 8/31/85 (Performance) 11/30/85 (Reports)

Grant/Contract Closeout Actions Remaining:

- [ ] None
- [ ] Final Invoice or Final Fiscal Report
- [ ] Closing Documents
- [XX] Final Report of Inventions – Sent Questionnaire to P.I.
- [ ] Govt. Property Inventory & Related Certificate
- [ ] Classified Material Certificate
- [ ] Other

Continues Project No. Continued by Project No.

COPIES TO:

Project Director
Research Administrative Network
Research Property Management
Accounting
Procurement/GTRI Supply Services
Research Security Services
Reports Coordinator (OCA)
Legal Services

Library
GTRC
Research Communications (2)
Project File
Other I. Newton
A. Jones
R. Embry

FORM OCA 69.285

FINAL REPORT

THE BRACING APPROACH TO HIGH SPEED MANIPULATION WITH LIGHTWEIGHT ROBOT ARMS

By

Wayne J. Book (Principal Investigator)

Prepared for

NATIONAL SCIENCE FOUNDATION
Washington, D.C. 20550

Under

NSF Award Number: MEA-8303539

Report Period from 9/15/83 to 8/31/85

May 1986

GEORGIA INSTITUTE OF TECHNOLOGY
A UNIT OF THE UNIVERSITY SYSTEM OF GEORGIA
SCHOOL OF MECHANICAL ENGINEERING
ATLANTA, GEORGIA 30332

APPENDIX VII

NATIONAL SCIENCE FOUNDATION
Washington, D.C. 20550

FINAL PROJECT REPORT
NSF FORM 98A

PLEASE READ INSTRUCTIONS ON REVERSE BEFORE COMPLETING

PART I–PROJECT IDENTIFICATION INFORMATION

1. Institution and Address	2. NSF Program	3. NSF Award Number
Georgia Tech Research Corp. (formerly Georgia Tech Research Institute) Atlanta, GA 30332	Mechanical Systems	MEA-8303539
	4. Award Period From 9/15/83 To 8/31/85	5. Cumulative Award Amount $79,698

6. Project Title: The Bracing Approach to High Speed Manipulation with Lightweight Robot Arms

PART II–SUMMARY OF COMPLETED PROJECT *(FOR PUBLIC USE)*

The concept of bracing a robot arm to increase its rigidity during small, accurate motions of its end point is studied in this research. This approach eliminates the conflict between fine motion speed, which is enhanced by rigidity, and large motion speed, which is enhanced by light weight. With bracing the arm is temporarily attached at a bracing point to a stationary supporting structure or the workpiece (if it is large) during the fine motion phase of the task. Motion is carried out by additional degrees of freedom such as an end effector. The anthropomorphic analogy is often observed in human manipulation of objects. The human braces the heel of his hand against a work surface while manipulating small objects with his fingers. By enabling robot arms to work in an analagous manner, lighter, faster, less expensive, and more accurate robot arms may be possible.

The work performed was as follows: (a) Survey and characterize potential tasks which would benefit most from the bracing capability; (b) develop an experimental arm to test the enabling research in one or more of these task environments; (c) explore control algorithms for lightweight arms that are compatible with the flexible dynamics; and (d) implement the most promising techniques on the experimental arm. The initial experiments were carried out on a single link arm to obtain a basic understanding. By measuring the deflection of the arm with strain gages the joint actuators can be controlled to rapidly damp out arm vibrations. Motions that avoid exciting vibrations in the first place were also studied. A large (6 m.) arm with two links was constructed for more advanced studies.

PART III–TECHNICAL INFORMATION *(FOR PROGRAM MANAGEMENT USES)*

1. ITEM *(Check appropriate blocks)*	NONE	ATTACHED	PREVIOUSLY FURNISHED	TO BE FURNISHED SEPARATELY TO PROGRAM	
				Check (√)	Approx. Date
a. Abstracts of Theses		X			
b. Publication Citations		X			
c. Data on Scientific Collaborators	X				
d. Information on Inventions	X				
e. Technical Description of Project and Results		X			
f. Other *(specify)*					

2. Principal Investigator/Project Director Name *(Typed)*	3. Principal Investigator/Project Director Signature	4. Date
Wayne J. Book	Wayne J. Book	5/12/86

NSF Form 98A (3-83) Supersedes All Previous Editions

Form Approved OMB No. 3145-0058

Final Report: The Bracing Approach to High Speed Manipulation with Lightweight Robot Arms

NSF Grant No. MEA-8303539

This report will describe results obtained under the research grant MEA-8303539 during the period September 15, 1983 through the extended completion date, August 31, 1985. Detailed reporting of the technical results is found in the technical papers that have been presented in conferences. They are included in the Appendix. The body of this report will summarize the work performed and related to the proposed work.

Expansion of the Research Area of Flexible Arm Control

Since the initiation of the NSF sponsored project to which this report pertains, the problems of flexibility in robot arms has become much more widely recognized. The author organized one session on this topic at the 1985 American Society of Mechanical Engineers Winter Annual Meeting. Two sessions on related topics were held at the 1986 IEEE International Conference on Robotics and Automation. Additional sessions are planned at the forth coming IEEE Conference for Decision and Control and the ASME Winter Annual Meeting, in all of which the author is participating. The support from the National Science Foundation has been very helpful in not only the research described below, but through that research and other channels, helpful in exposing the needs and research opportunities in control of lightweight, flexible arms.

Summary of Proposed Research

The proposal originally written for this grant described a three year research program, the first year of which was funded and is reported here. As described in the Modified Research Plan submitted in a revision to the initial proposal, the following activities were to be pursued:

Design Studies and Bread board Design

1. Survey potential applications of bracing
2. Characterize a promising task and determine parameters for the bread board designs.
3. Design and construct a single axis bread board.
4. Test bread board operation.
5. Extend the bread board to two axes.

Modeling and Control of Lightweight Arms

1. Consider the minimum time and regulator problems for simple (one link) flexible arms.
2. Program algorithms for the bread board systems.

3. Test the algorithms.

4. Model and simulate more complex flexible arms.

These tasks have been undertaken and the results on several topics reported in the papers attached to the body of this report. It is not accurate to say that each task has been completed since they remain active research projects. In addition to the work proposed for year one, some of the topics proposed for years two and three have been undertaken, and papers are also included on these results. Arm trajectories for minimum excitation of vibrational arm modes is one such topic. Research has been initiated on adaptive strategies for flexible arm control that has spawned out of the NSF grant but which is not NSF supported at this time.

Design Studies and Bread board Design

A survey of potential applications for the bracing strategy has identified to a number of important tasks which are difficult to automate. As described in the proposal previous papers by the P.I., tasks with large workspaces and light payloads and requiring relatively high precision in a dynamic sense seem to have the most to gain from a bracing strategy. A spectrum of applications for which these conditions exist include:

- Welding of pressure vessels, buildings, ships, and bridges.

- Inspection of the structural integrity of pressure vessels, aircraft, and bridges by nondestructive methods.

- Assembly of aerospace vehicles, space structures.

- Service applications such as window washing, servicing nuclear reactors, utility lines, transformers, connections, etc.

A single link arm was constructed and used in a number of experiments. (See attached papers for details.) Gordon Hastings was supported during much of his Ph.D. work to conduct experiments on this system. He will complete his Ph.D. degree in the Summer Quarter of 1986. The single link test bed that he constructed was also used in experiments by other Ph.D. students working with Gordon to test the effects of constrained layer passive damping treatments on the robustness of the control algorithms implemented. The experiments held some surprises in terms of the dynamics that must be modeled to accurately represent the behavior of lightly damped feedback control systems. These surprises were explained analytically, but reinforce the need for experimental verification in this type of work.

A two link, two degree of freedom lightweight, flexible arm has been designed and partially constructed, and a three degree of freedom "rigid" arm also has been constructed for mounting on the end of the flexible arm in bracing studies. These two design projects were carried out by two Master's degree students, Thomas Wilson and Ray Holden, and two Master's Theses resulted. While these students were not supported by the NSF Grant, the construction was supplemented by the grant. The flexible arm consists of two 3.04 meter (ten foot) links driven by rotary joints in a plane. Actuation was

designed to be by brushless dc motors but initial tests will be powered by hydraulic rams. The braced arm to be placed on the end of the large arm consists of two links 0.608 m. (2 ft.) long and powered by brushless d.c. motors. Figures of both designs appear with the abstracts of these theses in the Appendix. Experimentation on the appropriate model to represent the behavior of this system is now underway. The actuation of the second joint by means of a four-bar linkage complicates the model over previous nonlinear multi-link cases the author has modeled.

Modeling and Control of Lightweight Arms.

Results on the regulator control problem for flexible arms with consideration of the flexible states was a major contribution of the research performed under this grant. Gordon Hastings extended our prior theoretical and analytical work on single link arms to a physically implemented form. It forms the basis for our further work in this area applied to more complex cases. This work has been described in several conference papers (attached), in his forthcoming Ph.D. Dissertation, and is expected to result in refereed journal publications. The controller design was based on a linear quadratic optimal regulator with guaranteed stability margin. Two strain gages sensed deflection and amplitudes of two assumed mode shapes were reconstructed. The rate of change of these amplitudes were estimated by a reduced order Luenberger observer. The application of these techniques to robot arms and verification of the performance on a physical system is the major contribution of his work.

Our prior work on minimum time control of single link arms pointed out the extreme sensitivity of these methods to errors in the switching times. Consequently, efforts under the NSF Grant were oriented to more robust near optimal techniques. This work was performed by Sabri Cetinkunt, who was supported under the grant. He is pursuing his Ph.D. degree with research in this area. The nonlinear and flexible effects combine to make this an extremely complex problem. Extensions of works by other authors (e.g. Bobrow and Dubowsky, and Shin) on rigid arms in an approximate sense seemed feasible. A modification of the switching times of those works to account for the flexible behavior was implemented. The new method insures that actuator constraints are not violated but are no longer guaranteed optimal. Modification of the discontinuous nature of the control has also been considered so that flexible modes are not excited as much.

Modeling and simulation of two link flexible arms was also implemented by Mr. Cetinkunt. His model was based on the recursive Lagrangian method with assumed modes previously proposed by the P.I. This model is implemented on the VAX 11/750 and has been verified in several special cases. The program does not attempt to be general, but does verify this modeling approach and provides the simulation tool for the two link studies on trajectory planning.

Conclusions and Recommendations for Further Work

Substantial progress in controlling lightweight arms has been achieved as the first step to producing a practical braced arm. The importance of physical experiments has been reinforced with these studies. The control method for damping the flexible motion has been established to be robust,

especially when combined with passive damping treatments. Studies on two link, two joint flexible arms should continue along these lines with verification of regulator controls and trajectory planning. Adaptive techniques utilizing multiple time scale analysis should also be pursued as a means to produce a robust control in the face of uncertainties in the arm, the task, and the environment.

Papers Published Based on Work Performed

1. Book, W., S. Le, and V. Sangveraphunsiri, "The Bracing Strategy for Robot Operation," Proceedings of the 5th Symposium on Theory and Practice of Robots and Manipulators, sponsored jointly by CIMS and IFToMM, 1984, Udine, Italy.

2. Cetinkunt, S. and W. Book, "Optimum Control of Flexible Robot Arms on Fixed Paths," Transactions of the Third Army Conference on Applied Mathematics and Computing, Atlanta, GA, May 13, 1985.

3. Hastings, G.G., and W. Book, "Experiments in the Control of a Flexible Robot Arm," Proceedings of ROBOTS 9 Conference, Society of Manufacturing Engineers, June 2-6, 1985, pp. 20-45 to 20-56.

4. Hastings, G.G., and W. Book, "Experiments in optimal Control of a Flexible Arm," Proceedings of the 1985 American Control Conference, Boston, MA, June, 1985 pp. 728-729.

5. Alberts, T.E., G.G. Hastings, W.J. Book and S.L. Dickerson, "Experiments in Optimal Control of a Flexible Arm with Passive Damping," VPI&SU Symposium on Dynamics and Control of Large Flexible Structures, Blacksburg VA, June, 1985.

6. Book, W., S. Dickerson, G. Hastings, S. Cetinkunt, and T. Alberts, "Combined Approaches to Lightweight Arm Utilization," in Robotics and Manufacturing Automation ASME, M.Donath and M. Leu, ed. 1985, pp 97-107. Also presented at the 1985 ASME Winter Annual Meeting.

7. Book, W. and S. Cetinkunt, "Near Optimum Control of Flexible Robot Arms on Fixed Paths," Proceedings of the 1985 IEEE Conference on Decision and Control, Dec. 11-13, 1985.

8. Hastings, G.G. and W. Book, "Verification of a Linear Dynamic Model for Flexible Robotic Manipulators," Proceedings of the 1986 IEEE International Conference on Robotics and Automation, April 7-10, San Francisco, CA, pp 1024-1029.

9. Holden, R., "A Braced End Effector for a Flexible Robot Manipulator," M.S. Thesis, Georgia Institute of Technology, School of Mechanical Engineering, Feb., 1986. (only abstract attached)

10. Wilson, T., "The Design and Construction of a Flexible Manipulator," M.S. Thesis, Georgia Institute of Technology, School of Mechanical Engineering, March, 1986. (only abstract attached)

APPENDIX
Copies of Papers Published Based on Work Performed

Papers appear in the order cited in the final section of the main report. The two Master's theses have only abstracts and some key figures included.

Presented at the 5th Symposium on Theory and Practice of Robots and Manipulators 1984, Udine, Italy, sponsored by CISM-IFToMM.

THE BRACING STRATEGY FOR ROBOT OPERATION[1]

Wayne J. Book, Sanh Le, and Viboon Sangveraphunsiri
School of Mechanical Engineering
Georgia Institute of Technology
Atlanta, GA 30332
U.S.A.

Summary

A new strategy of robot operation, the bracing strategy, is presented. Under this strategy an arm is moved into position then rigidized by bracing against either the work piece or an auxiliary, static structure. Subsequent precision motion does not involve the entire arm, but only degrees of freedom at the end of the arm. The advantage of this strategy is that it allows high speed, precision motion with a light weight, flexible arm. Light arms require smaller actuators, less energy, may be faster, are safer, and are less expensive.

Four means of clamping to the structure are considered: A simple normal force, mechanical clamping, vacuum attachment, and magnetic attachment. Each means has restrictions and advantages. Arm control with the bracing strategy requires four modes: gross motion control, rendezvous with the bracing structure, control of gross actuators after bracing and control of fine motion actuators distal to the bracing point.

---

1. This work is partially supported by the National Science Foundation of the U.S.A., Grant No. MEA-8303539

The Rationale for a Bracing Strategy

Ultimately, one must have fast motion to have the highest performance for a robot arm. Most robot tasks consist of gross motion and fine motion phases. Gross motion involves large movements with a relatively predictable destination enabling trajectory planning. These motions require a high force to inertia ratio for rapid completion. Fine motion involves smaller, more precise movements which are less predictable. They could arise from sensory or joint angle feedback in response to disturbances, statistical variation in dimensions, or changes in the environment. To accomplish these motions quickly a high bandwidth servo system is required. Such bandwidth typically requires rigidity in the actuated structure, hence additional structural mass. The traditional approach accomplishes both gross and fine motions with the same actuators and linkage. Thus the structural mass required for the fine motion speed detracts from the gross motion speed.

The research underway seeks to eliminate the conflict between gross and fine motion speed. The configurations studied effectively reduce the distance from the end point to a "fixed" base during the fine motion phase by "**bracing**" it against a static structure or the work piece itself. This approach is especially relevant to long arms with light payloads as documented by the author previously[1]. This is analogous to the strategy of human workers who steady their hand for precise work by bracing their arm against a work bench. It is also a variation of the strategy of extending the range of an arm by providing it with mobility. For mobile robots the strategy is typically to transport the arm to the vicinity of the work piece, deactivate the mobility subsystem, and activate the arm. Both cases are examples of allocation of the motion responsibilities to the most appropriate degrees of freedom. Similar approaches have been proposed by Hogan[2] and applied specifically to drilling.

The advantages and disadvantages of bracing compared to other strategies for using lightweight arms are being considered. Particular consideration is given to the mechanical design and joint control consequences of employing this strategy as opposed to conventional rigid arm strategies. The increased control complexity, additional degrees of freedom, and end point location issues penalize the bracing strategy.

Alternative Means of Bracing

For a bracing mechanism design, the following parameters are evaluated for comparison purposes: holding force/unit weight, size, required working environment, power consumption, reliability, maintenance.

In all cases the controllable force for clamping is applied normal to the surface of the bracing structure. Consequently, the coefficient of friction between the robot and structure is an important parameter.

Simple Normal Force

The most simple and least reliable means of bracing for robots is the one used extensively by humans. By simply applying a normal force to the bracing structure as shown in Fig. 1, rigidization can be achieved. Unlike the other methods, a net force is imparted to the bracing structure which may be unacceptable. Since the joint actuators would apply this force, a means of force control would be necessary in addition to position and/or velocity control. A continuous actuation would mean substantial energy consumption. Brakes or other means of locking the joints would circumvent this consumption. As observed in the human, an appropriate design can be effective and require low levels of actuation or rely totally on gravity. The mobile robot typically relies on gravity to achieve bracing. This method can also be used to supplement other bracing means. The only additional mechanical design consideration is to provide an durable, high friction surface for contact with the bracing surface.

Mechanical Clamping Device

This type of device requires edges, holes, or other features of a bench or work piece for attachment. The general design force/weight ratio is limited by the strain/stress relation of the material. Commercially available clamping devices achieve a force to weight ratio of up to 1000. This estimate does not include the weight of the actuating solenoid or hydraulic cylinder. The latter may dominate the total system weight and may reduce the ratio by one-half. Hydraulic, pneumatic, or electromagnetic actuation devices may be employed. A hydraulic ram may be used directly as in Fig. 2 with quite favorable size and weight advantages. Pneumatic and electromechanical actuation would likely require some type of mechanical linkage to provide mechanical advantage.

The energy consumption of the hydraulic clamping device is proportional to the stroke and area of the piston. Additional energy is consumed by the valving. If hydraulic actuators are used in the joints of the arm, the additional cost of hydraulic clamping will be greatly reduced. Simple on-off control of the clamping actuator will produce fast clamping with but

with high impacts on the work piece and high pressure transients. A more complex control circuit will be necessary to produce fast clamping without these adverse effects.

One obvious limitation of mechanical clamping is that the point of clamping must be near an edge so that opposing forces can be applied. A practical limitation on the range of separation of the opposing surfaces (thickness) for fast bracing exists. Positioning the arm to engage the clamping mechanism requires more complex maneuvers in the gross motion.

Vacuum Attachment

By providing suction to a cup with a pliable rubber-like material on its lip, a normal bracing force can be achieved as shown in Fig. 3. Suction will provide a normal force to the bracing surface limited by the atmospheric pressure around the arm and the area to which a vacuum is applied. Consequently, it is appropriate only where fairly large, smooth surfaces are available. The weight of such a system is derived from its mechanical structure and the vacuum fixtures such as connecting hoses and the cup. Thus, based on strength its force/weight ratio will be on the same order of the mechanical clamping devices. Because of the limit on negative pressure the force is proportional to area. The resulting large size may dictate that stiffness of the bracing point be increased by adding material to the cup. The energy consumption will depend on the strategy of controlling the air flow. Consequently the bulk and mass is expected to be larger than for mechanical clamping.

Permanent Magnets

Magnetic forces can be used to attach to ferrous clamping structures. Because of the constant current requirements for electromagnets, they have not been considered for providing the normal force directly. The permanent magnet is popular in temporary holding applications. A strong holding force is provided once good contact is established with the working surface. The force is strongly dependent on the gap between the magnet and the working surface. In general a permanent magnet circuit is designed with pole pieces to concentrate the flux density in the gap so as to increase the holding force as in Fig. 4. With a rare earth magnet a force to weight ratio of about 200 can be achieved in a small volume (5 cm^3 for 900 N.). For a given geometry, the magnetic holding force is proportional to K^2 where K is the scale factor of the geometry.

There are basically two methods for releasing a work piece: flux diversion and depolarization. In flux diversion, an alternative return

path is connected to the magnetic circuit to divert flux going through the work piece, thereby releasing it from the magnet. This diversion may be actuated by a separate actuator or by the arm motion. In depolarization, a high impulse of unidirectional current is passed through the pole pieces to temporarily reverse the polarity of the poles and thus disrupt the flow path of the magnetic circuit and allow release. For a 2.5 cm diameter $SeCo_5$ rare earth magnet, a 10 ms pulse of 100 amp current is required for depolarization. This is a substantial complication to the method but one that is being explored.

Comparison of Bracing Means

All the candidate bracing means have advantages which could dominate in certain applications. Table 1 summarizes the characteristics which have been largely discussed above.

Table 1. Summary of clamping designs producing a holding force (normal) of 900 N.

Characteristic	Magnet	Vacuum	Mechanical
Material	$SeCo_5$	metal + rubber	steel
Work environment	surface ferrous	surface smooth	edge or hole
Size (cm)	3x2.5x1.3	(10 dia)	2.5 dia or less
Force/weight	200	500	500
Action (speed)	good	fair	excellent
Energy consumption	low	moderate	moderate
Maintenance	low	moderate	high
Reliability	excellent	good	good
Other	compact	noisy bulky	difficult rendezvous

Control Issues in Bracing

To implement the bracing strategy several control issues must be addressed:

1. Gross motion control of a lightweight arm.

2. Rendezvous of the bracing mechanism with the bracing structure.
3. Control of the actuators between the base and the bracing point after bracing.
4. Control of the actuators distal to the bracing point after bracing.

It should also be clarified that the ability to successfully perform the first two tasks above does not constitute the ability to successfully manipulate with a flexible arm. The accuracy needed to rendezvous can be made less than required for the final manipulation task. Certainly the speed of manipulation after bracing can be made higher. Perhaps most importantly, the effect of disturbances on the braced arm are not as troublesome as for the unbraced arm.

Issues one and two above are quite challenging and have been treated by Truckenbrot[3], Book[1] and others. The two may be treated together or separately, but separate treatment may allow for a robust treatment of errors and uncertainty in rendezvous while maintaining high speed gross motions.

After bracing has begun the arm is no longer an open loop kinematic chain and dynamics of the links between the base and the point of bracing are quite different than before bracing. If clamping prevents all translation and rotation the joints may move only by deforming the structure. If only some translations or rotations are restricted the arm has become a closed loop mechanism. The remaining degrees of freedom are available for positioning the end effectors. A force control mode is envisioned for the actuators in this case, and application of a downward force to enhance the clamping action will be helpful.

The control of distal joints after bracing contends with dynamics similar to conventional manipulation. The short links are essentially rigid. The exact position of the end effector may be poorly known based on the joint angles alone. A decreased emphasis on this source of information and increased reliance on direct measurements of the end point, either absolute or relative to the work piece is appropriate.

Ongoing Work

Research underway is constructing alternative bracing mechanisms and simple light weight arms and devising control algorithms. This will allow

practical evaluation of the bracing strategy.

---

1. Book, W.J. and M. Majette, "Controller Design for Flexible Distributed Parameter Mechanical Arms Via Combined State Space and Frequency Domain Techniques," to appear in J. Dynamic Systems, Measurement, and Control

2. Moore, S.R. and N. Hogan, "Part Referenced Manipulation--A Strategy Applied to Robotic Drilling," in Control of Manufacturing Processes and Robotic Systems, D. Hardt and W.J. Book, eds. American Society of Mechanical Engineers, New York, pp. 183-191, 1983.

3. Truckenbrot, A., "Modelling and Control of Flexible Manipulator Structures," Proc. of the Symposium on the Theory of Robots and Manipulators, September, 1981, Zabarow, Poland.

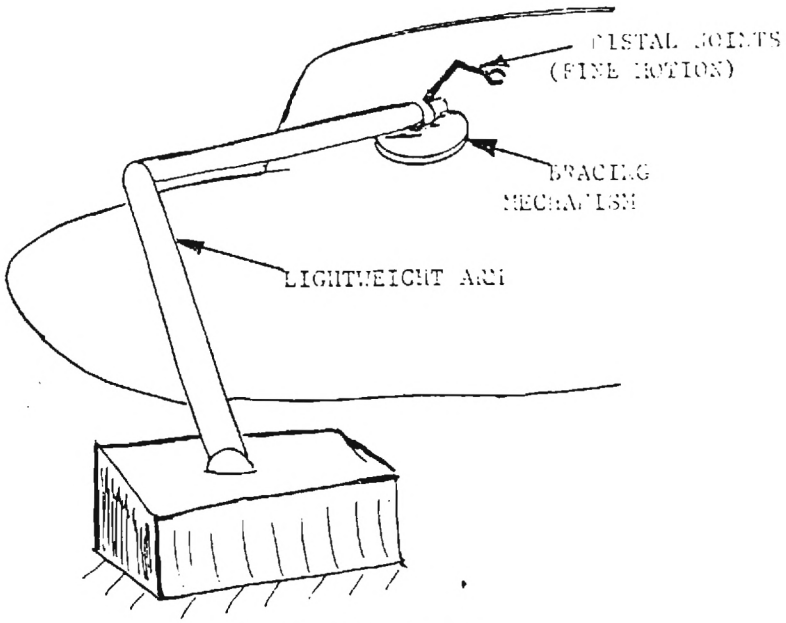

Fig. 1 The Bracing Strategy

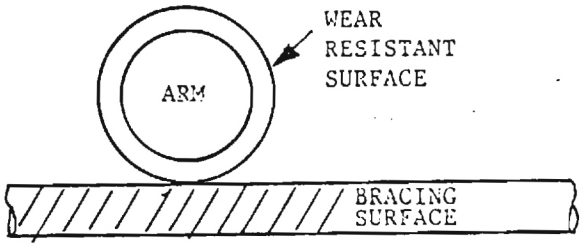

Fig. 2 Simple Normal Force for Bracing

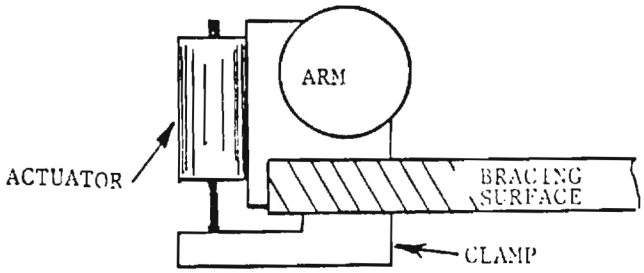

Fig. 3 Mechanical Clamping for Bracing

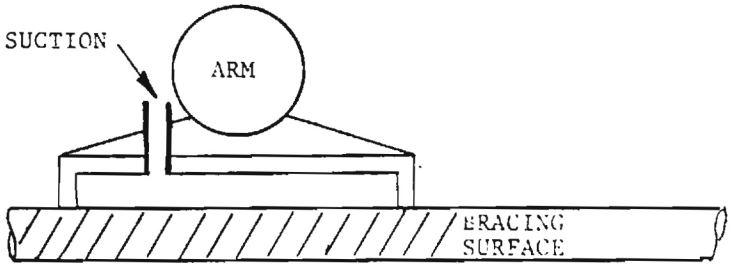

Fig. 4 A Vacuum Attachment for Bracing

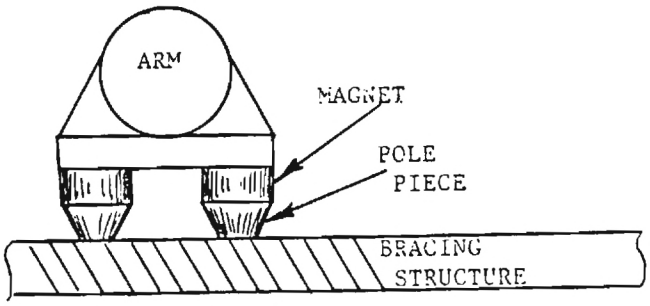

Fig. 5 A Magnetic Bracing Mechanism

ARO Report 86-1

TRANSACTIONS OF THE THIRD ARMY

CONFERENCE ON APPLIED MATHEMATICS AND COMPUTING

Sponsored by

The Army Mathematics Steering Committee

on behalf of

THE CHIEF OF RESEARCH, DEVELOPMENT

AND ACQUISITION

OPTIMUM CONTROL OF FLEXIBLE ROBOT ARMS ON FIXED PATHS.

Sabri Cetinkunt
Wayne J. Book
School of Mechanical Engineering
Georgia Institute of Technology
Atlanta, GA 30332

ABSTRACT

Productivity of the industrial robots are directly related to the speed of the task execution. The speed of the robots can be drastically improved by using better control algorthims and reducing the weight of the manipulator.

The speed of a robotic manipulator is constrained by manipulator dynamics and actuator capabilities. Increasing the size of the actuators is not a solution since that will increase the weight of the the overall system leading to a relatively heavier system.The more realistic approach to the problem is to find the optimum control solution for a manipulator to follow a pre-defined path in minimum time, with limited actuator capabilities.

In terms of the dynamic constraints, the weight of the arms may be the most important factor. If a light-weight arm structure is used, actuators will be able to afford higher speeds during the task execution than they would for rigid arm structure. On the other hand using flexible-arms has a major draw-back which is the flexible vibrations, while increasing the speed.

This paper presents the minimum time control solution of a two link flexible arm with actuator constraints . We solved the minimum time problem with no constraints on the flexible modes and show the time improvement due to the use of light-weight arms. The objective is to modify the trajectory, such that flexible vibrations are bounded while changing the solution from the previous one as little as possible. Practical ways of trajectory modifications for flexible arms are discussed.

INTRODUCTION

Today, most trajectory planning algorithms do not consider the dynamics of the manipulators, rather constant and/or piece wise constant accelerations for the overall task are used and an overall maximum allowable speed is set [5,6,7]. However, robotic manipulators are highly nonlinear dynamic systems, so it is expected that affordable accelerations and decelerations and maximum speeds will vary as a function of states. For the traditional schemes to work, the trajectory must be planned for the worst possible case. The capabilities of the system will be used only a small part of the time. Bobrow et.al. [1] first reported that for every point on the path there is an associated maximum allowable speed and maximum affordable acceleration and

---

This material is based in part on work supported by the National Science Foundation under grant MEA-8303539.

deceleration, and these values can drastically vary from one state to another. Incorporating the manipulator dynamics into the trajectory planning level, they found the minimum time trajectories for different manipulator models [1,2] with limited actuator capabilities moving along pre-defined paths. Shin and McKay [3] solved the same problem independently.

Light-weight manipulators with the same actuator capabilities will be faster. The main problem associated with the light-weight structures is the flexible vibrations. Fig. 1 conceptually shows the performance improvement in terms of increased speed.

In this paper we show the performance improvements due to

1. use of light-weight arms

2. incorporating the manipulator dynamics into trajectory planning level

3. Discuss flexible vibrations during a minimum time trajectory execution and considerations of path modifications such that flexible vibrations will be bounded. This problem is similar in nature to the one raised by Hollerbach [8].

FLEXIBLE MANIPULATOR DYNAMIC MODEL IN JOINT AND PATH VARIABLES

A general dynamic modelling technique for flexible robotic manipulators was developed by Book using recursive Lagrangian-assumed modes method. Homogeneous transformation matrices are used for kinematic relations of the system [4]. A two link flexible robotic manipulator is modelled using that technique (Fig. 2). In the model no actuator dynamics is considered, rather the net torque input to the links is considered as the input variable. No friction at joints nor in the structural vibrations is considered. Flexibility of each link is approximated with one assumed mode for each link. The dynamic model of the manipulator may be expressed in general terms as :

$$[J]_{4\times4}\ \ddot{\underline{q}} = \underline{f}(\underline{q},\dot{\underline{q}}) + \underline{Q} \qquad (2\text{-}1)$$

where

$\underline{q}^T$: $[\theta_1, \theta_2, \delta_1, \delta_2]$ Joint angle and flexible mode time variables

$\underline{Q}^T$: $[T_1, T_2, 0, 0]$ Net input torques

$[J]_{4\times4}$: Generalized Inertia Matrix ,symmetric, positive definite.

$\underline{f}^T$: $[f_1, f_2, f_3, f_4]$ Nonlinear dynamic terms including centrifugal gravitational,effective spring and Coriolis.

The problem is to find the minimum time trajectories for a given manipulator with limited actuator capabilities moving along a fixed path, with state constraints (bounded flexible vibration constraint). Once the path to be moved along is specified

$$S = S(x,y) \qquad (2\text{-}2)$$

From inverse kinematic formulation, the corresponding joint angles can be found as

$$\underline{\theta} = \underline{\theta}(s) \quad , \quad \underline{\theta}^T = [\theta_1, \theta_2,] \qquad (2\text{-}3)$$

Similarly, once the speed along the path is known S(S)

$$\underline{\theta}=\underline{\theta}\,(s,\dot{s}) \tag{2-4}$$

and

$$\underline{\delta}=\underline{\delta}\,(s,\dot{s},\ddot{s}) \tag{2-5}$$

Knowing the relations (2-3)-(2-5) analytically form or numerically the manipulator dynamics in part can be expressed in path variables.

$$\begin{bmatrix} C_{11}(s,\underline{\delta}) \\ C_{12}(s,\underline{\delta}) \end{bmatrix}_{2x1} \ddot{s} = \begin{bmatrix} T_1 \\ T_2 \end{bmatrix}_{-1} - \begin{bmatrix} C_{21}(s,\dot{s},\underline{\delta},\dot{\underline{\delta}},\vec{e}_t,\vec{e}_n,\rho) \\ C_{22}(s,\dot{s},\underline{\delta},\dot{\underline{\delta}},\vec{e}_t,\vec{e}_n,\rho) \end{bmatrix} \tag{2-6a}$$

$$\begin{bmatrix} \ddot{\delta}_1 \\ \ddot{\delta}_2 \end{bmatrix} = \begin{bmatrix} J_{33} & J_{34} \\ J_{43} & J_{44} \end{bmatrix} \begin{bmatrix} f_3-g_3+h_1(s,\dot{s},\vec{e}_t) \\ f_4-g_4+h_2(s,\dot{s},\vec{e}_t) \end{bmatrix} \tag{2-6b}$$

where $f_i=f_i(s,\dot{s},\underline{\delta},\dot{\underline{\delta}})$ (2-7)

$g_i=g_i(s,\dot{s},\vec{e}_t,\vec{e}_n,\rho)$ (2-8)

$J_{ij}=J_{ij}(s,\underline{\delta})$ (2-9)

$\vec{e}_t,\vec{e}_n$: Unit tangent and normal vectors along the path.

ρ : Curvature of the path at a point.

Notice that flexible modes also affect the position of the end effector, but are not included in the definition of the path. This is mainly due to the fact that we do not have a "direct" control on the flexible vibrations and would like to keep them as small as possible in general.

FORMULATION OF THE NEAR MINIMUM TIME TRAJECTORY PROBLEM FOR FLEXIBLE MANIPULATORS

Using the classical variational calculus principles, the optimum control/ programming problem may be stated as:

Minimize $$J = \int_0^{t_f} dt = \int_{so}^{s_f} \frac{ds}{\dot{s}} \tag{3-1}$$

$S(So) = So$

$\dot{S}(s_f) = \dot{S}_f$ Initial and final states in path variables.

Subject to :

System dynamics, equations (2-6a) and (2-6b)

Actuator constraints

$$T_{i_{min}}(\underline{\theta},\dot{\underline{\theta}}) \le T_i \le T_{i_{max}}(\underline{\theta},\dot{\underline{\theta}}) \qquad i = 1,2 \tag{3-2}$$

Dynamic inequality constraints on flexible modes

$$a_i(t) \le \delta_i(t) \le b_i(t) \qquad i=1,2 \tag{3-3}$$

The constraints (3-3) naturally arise in flexible structures. If such a constraint is not imposed there is no guarantee on the accuracy of the end point along the path. At first the problem will be solved without considering these constraints. This solution will be used as a nominal solution for the trajectory modification step so that (3-3) are satisfied.

The solution method we use closely follows Bobrow et.al.'s method with some modifications for flexible manipulators. The solution of the above stated optimization problem follows: for any path $S(x,y)$ with given $\dot{S}_o(S_o), \dot{S}_f(S_f)$ to minimize J, $\dot{S}$ should be as large as possible while satisfying the system dynamics and actuator constraints. In order to do so at any state on the path one should use maximum acceleration or deceleration. Then, the problem is reduced to finding the maximum accelerations and decelerations associated with each state of interest. It can be seen from equation (6a) that for each $(S, \dot{S})$

$$\ddot{S}_d \leq \ddot{S} \leq \ddot{S}_a \qquad (3\text{-}4)$$

$$\ddot{S}_a = \min \{ \ddot{S}_{ai} \}$$

$$\ddot{S}_d = \max \{ \ddot{S}_{di} \}$$

Obviously there may be some range of speeds associated with every point on the path that system can no longer afford to satisfy all conditions (the S range that above inequality is violated). Collection of these ranges defines the forbidden region on $(S, \dot{S})$ plane. The boundary between allowed and forbidden regions is constant for a given rigid manipulator for a given task. In the case of flexible manipulators, due to the coupling between equations (6a) and (6b) this boundary is also a function of flexible modes,not only $(S, \dot{S})$. So, depending on the time history of flexible modes and unpredictable disturbances the boundary will vary. This is not true in the rigid case where the true extremum can be found. At this point the problem is to find when to use maximum accelerations and when maximum decelerations (i.e. to find the switching point(s)).See Fig. 3a-3b.

Finding switching points for flexible manipulators:

1.Integrate $\ddot{S}=\ddot{S}(x,y)$ from final state backward in time until it crosses forbidden region or initial position, using maximum deceleration.

2. Integrate $\ddot{S}(x,y)$ Forward in time with maximum acceleration until the boundary is reached or the two curves crossed each other. If the two curve crossed each other before they enter forbidden region, then find that point. This is the last switching point and terminate the search. If not, then

3.Backup on the forward integrated curve and integrate forward with maximum deceleration until a the trajectory passes tangent to the boundary.

4.Then using the point as new starting point go to step two.

Notice that the last switching point is not the exact switching points, because the flexible modes will not match at this point. That will

cause one to miss the final state somewhat. Also, when searching for the switching points one has to move in a continuous manner in order to keep track of the flexible mode histories accurately. In that sense, the algorithm given at [1] has been modified for flexible robotic manipulators.

SIMULATION RESULTS AND DISCUSSION

The two-link flexible manipulator model for task one (shown in Fig. 4a) was simulated for the two different cases in order to show the performance improvement achieved due to light-weight system. In both cases actuators have same capabilities. It is found that weight reduction by a factor of 2 results in approximately 60 % time improvements (Fig. 5a and 6a). This improvement, of course, slightly varies depending on the task. Joint actuator histories are shown in Fig. 5b-6c and flexible mode responses are shown in Fig. 5c-6d.

Task 2 (Shown in Fig. 4b) simulated for light-weight manipulator and results are shown Fig 7 a-d. The final trajectory is shown in heavy lines. One interesting point in this simulation is the fact that as soon as the manipulator end point enters the curvature the system must accelerate along the path in order to obey the constraints. In Fig. 5a the curve ab shows that right before the curvature the system is able to afford deceleration (aa' curve), but as end point enters the curvature, then the sudden appearance of a normal acceleration term in the dynamics of the system makes the difference.The other point in the case of flexible arms is that at the last switching point flexible modes are not same,since thay have different histories. This will cause error in the final state reached. See Fig. 6a, 7a. The last switching point needs to be varied from the original result of the above algorithm. This can be done on trial and error basis at the trajectory planning level.

5.CONCLUSION AND FURTHER WORK

In this paper we showed ways to improve performance and productivity of Robotic manipulators With Flexible arms.One way was to use light-weight structures and the other was to incorporate the dynamics of manipulators in to trajectory planning level and make optimum utilization of given manipulator. This method can be used with any path.Application of the method requires manipulator model,Geometric path in work space,and actuator capabilities. Obvoiusly as trajectory gets closer to the forbiden region boundary system capabilities are being used to the limits and any disturbance or uncertainty can easliy put the system into forbiden region .The situation is more dramatic for flexible manipulators.While this analysis is nice in terms of knowing the ultimate capabilities , in practice there will be a saftey factor that will require to keep the optimal trajectory away from the forbideen region certain amount.Research is in progress on the Optimum modification of the trajectories found by above described method so that inequality constraints on the flexible modes will be satisfied.

REFERENCES

1.Bobrow,J.E., Dubowsky,S., Gibson,J.S. " On the Optimal Control of Robotic Manipulators with Actuator Constraints" Proc.of 1983 ACC,San Fransisco,CA June 1983,pp 782-787

2.Dubowsky,S, Shiller,Z. " Optimal Dynamic Trajectories For Robotic Manipulators" Fifth CISM-IFToMM Symposium On The Theory And Practice Of Robotic Manipulators Preprints,June 26-29 1984,Udine,Italy ,pp 96-103.
3.Shin, K.G., McKay, M.D. " Minimum-Time Control Of Robotic Manipulators With Geometric Path Constraints". IEEE Trans. on Automatic Control,Vol AC-30 No.6,June 1985 pp 531-541.
4.Book, W.J. " Recursive Lagrangian Dynamics of Flexible Manipulators " The International Journal of Robotic Research,MIT Press,V.3,N.3 pp. 87-101, Fall, 1984 .
5. Kahn, M.E., Roth,B. " The Near-Minimum time Control of Open-loop Articulated Kinematic Chains " Journal of Dynamic Systems,Measurement, and Control.ASME Trans.,Vol.93,No.3,Sept 1971,pp 141-171.
6. Luh, J.Y.S., Lin, C.S. " Optimum Path Planning For Mechanical Manipulators" Journal of Dyn.Syst.and Measurement and Control,ASME Trans.,Vol.102,No.2, June 1981 ,pp 142-151
7. Luh, J.Y.S., Walker, M.W.," Minimum-time Along the Path for a Mechanicel Manipulator", Proc.of IEEE Conf. on Decision and Control , Dec.1977, New Orleans, LA, pp 755-759.
8. Hollerbach, J.M. " Dynamic Scalling Of Manipulator Trajectories" Proc.of ACC , June 1983, San Fransisco, CA.

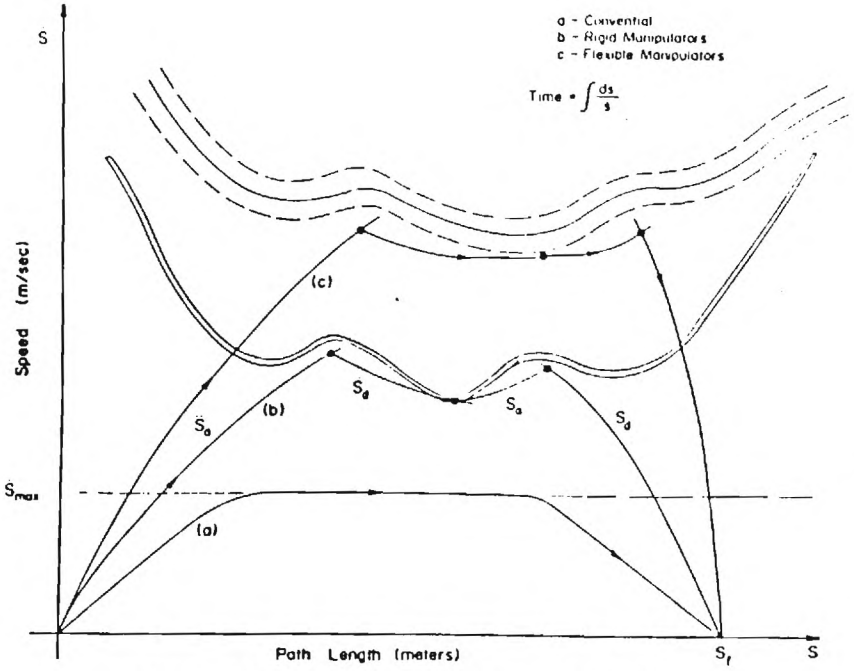

Fig.1 Different trajectory plans.

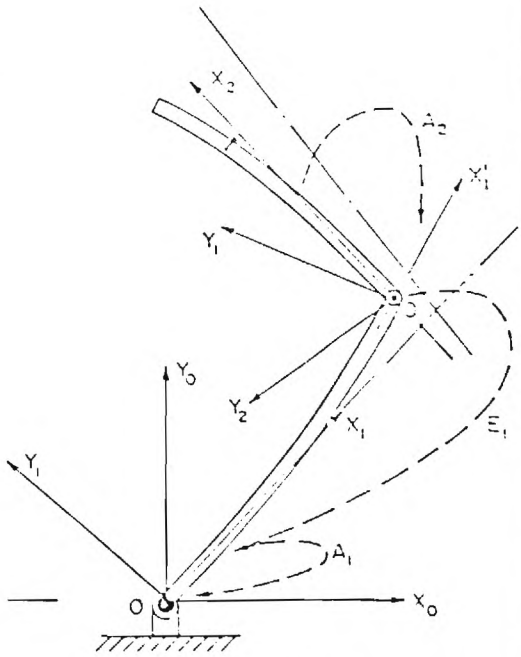

Fig.2 Manipulator Model.

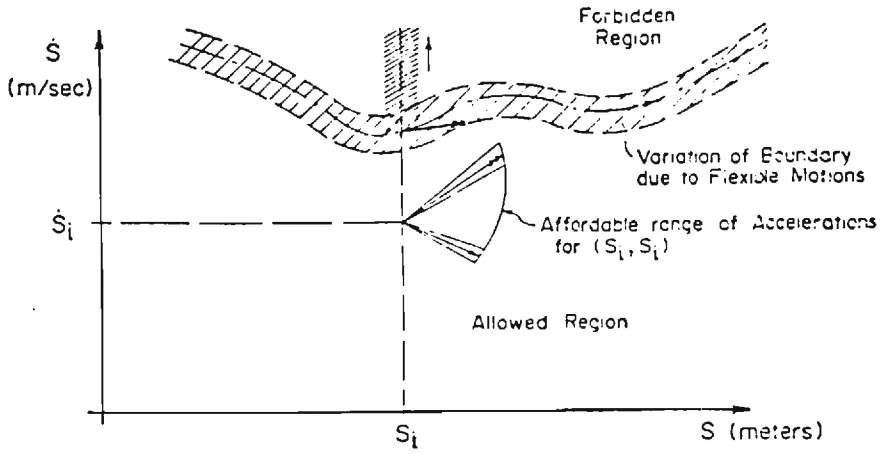

Fig. 3.a (S,Ṡ) Plane

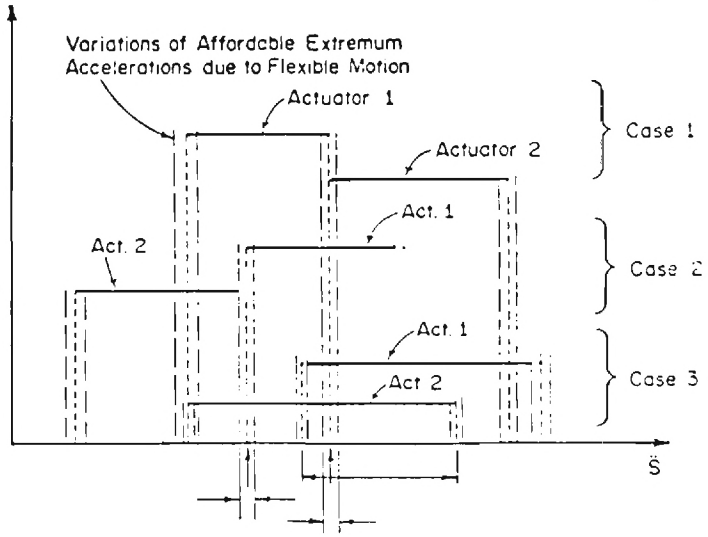

Fig. 3.b Different possible cases during a task.

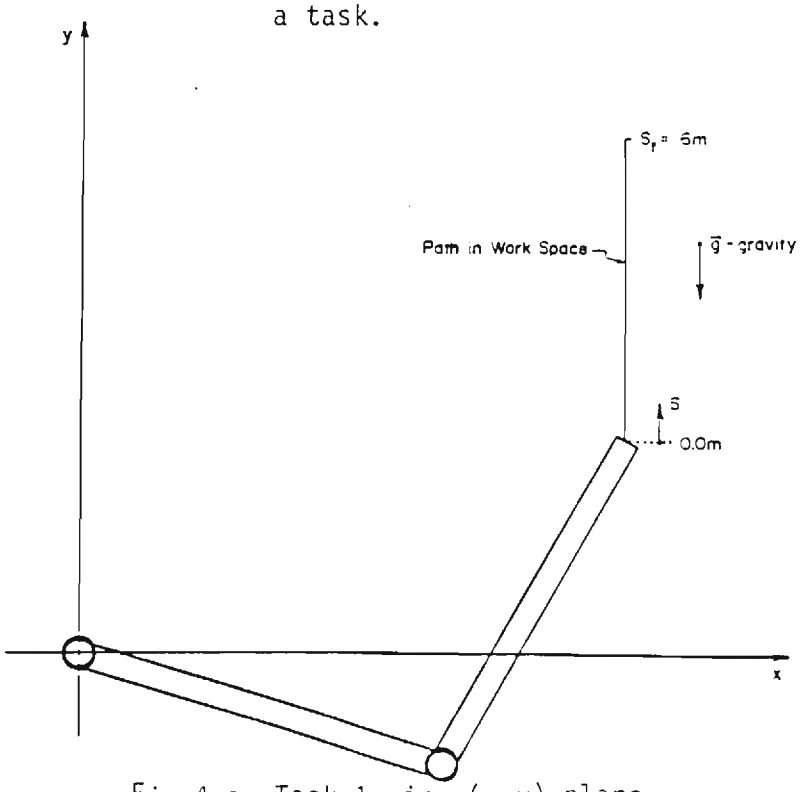

Fig.4.a Task 1 in (x,y) plane.

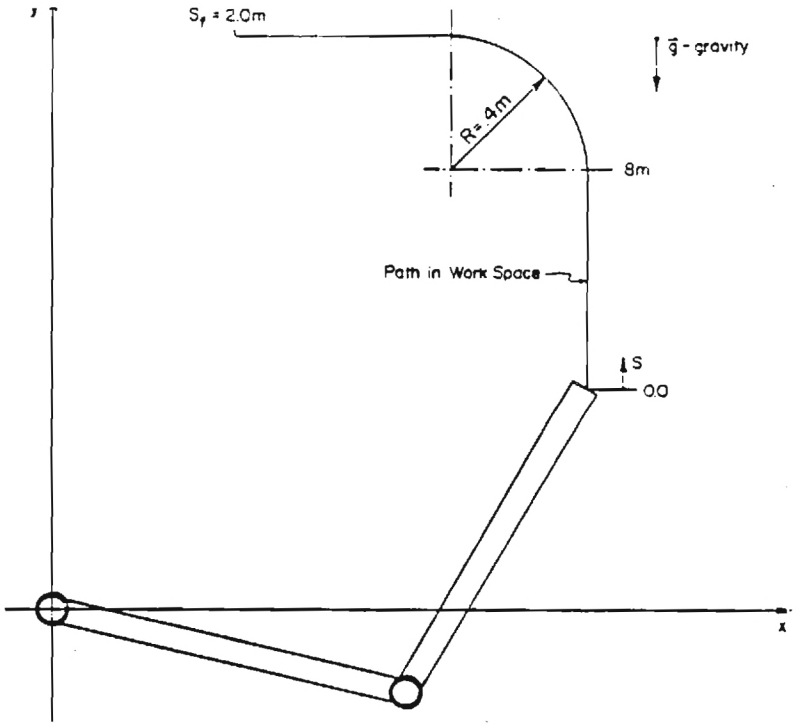

Fig. 4b Task 2 in (x,y) plane.

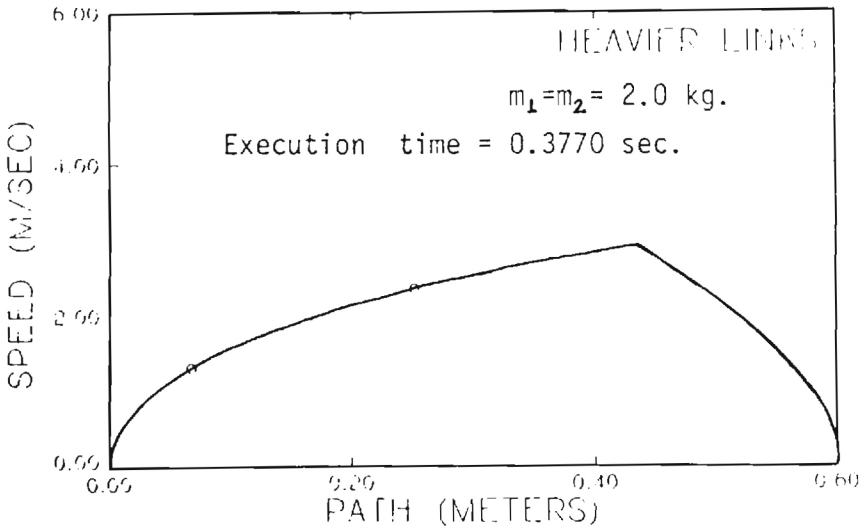

Fig. 5.a Trajectory for Path 1 of heavy links.

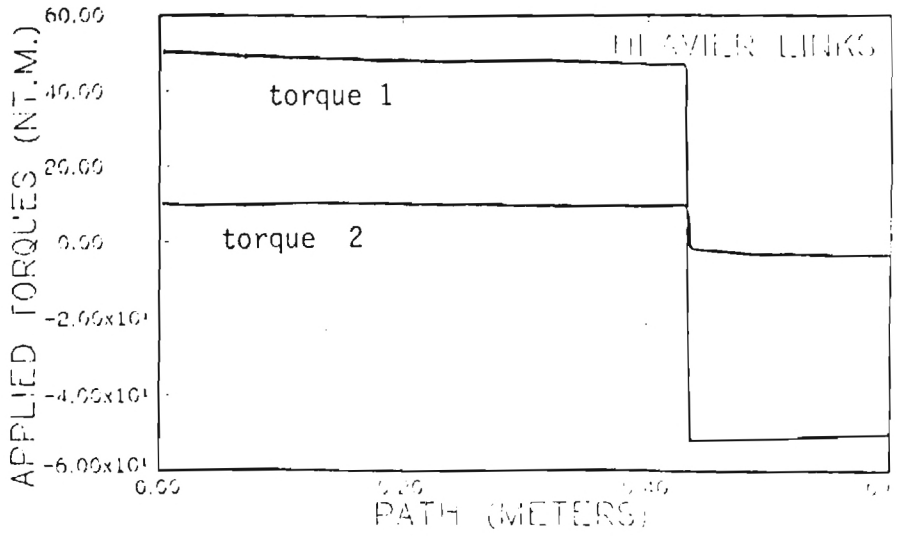

Fig. 5.b Torque histories for path 1.

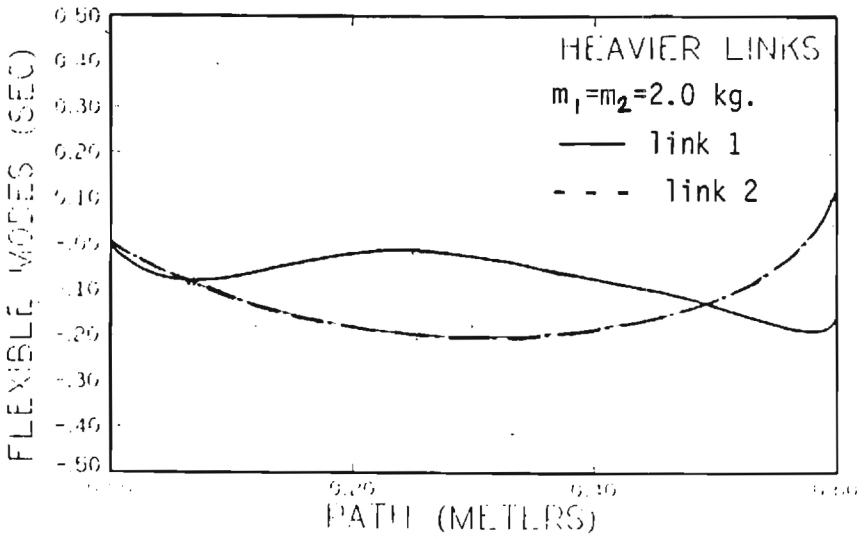

Fig. 5.c Flexible modes time variables

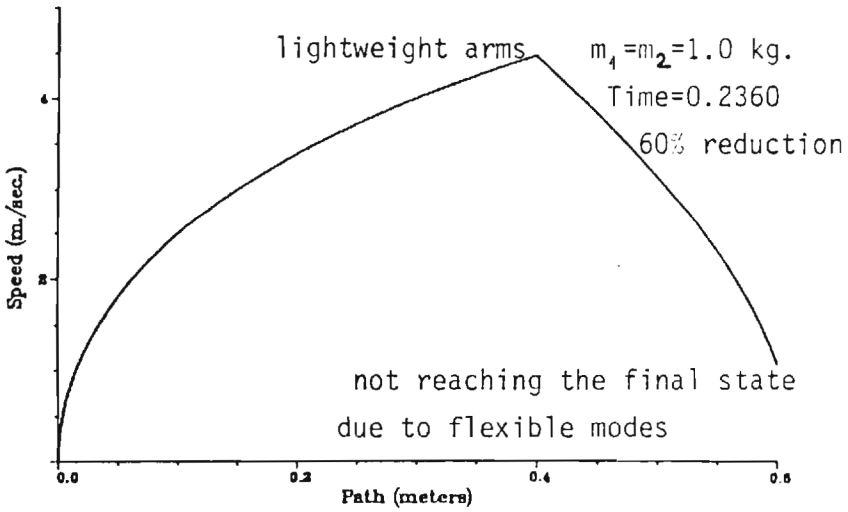

Fig. 6.a Trajectory of lightweight arms.

Find Switch P.

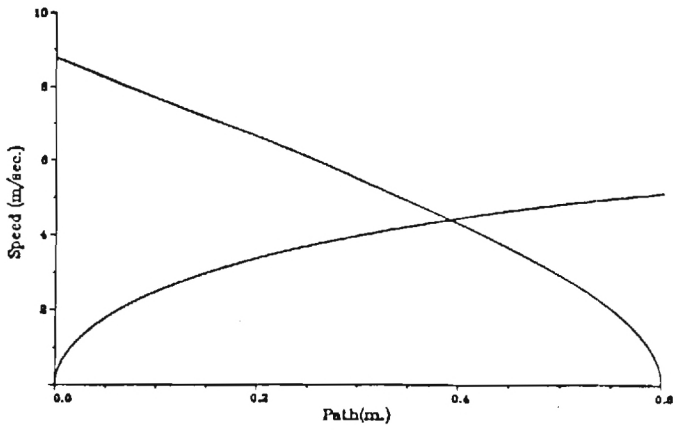

Fig. 6.b Finding the switching point

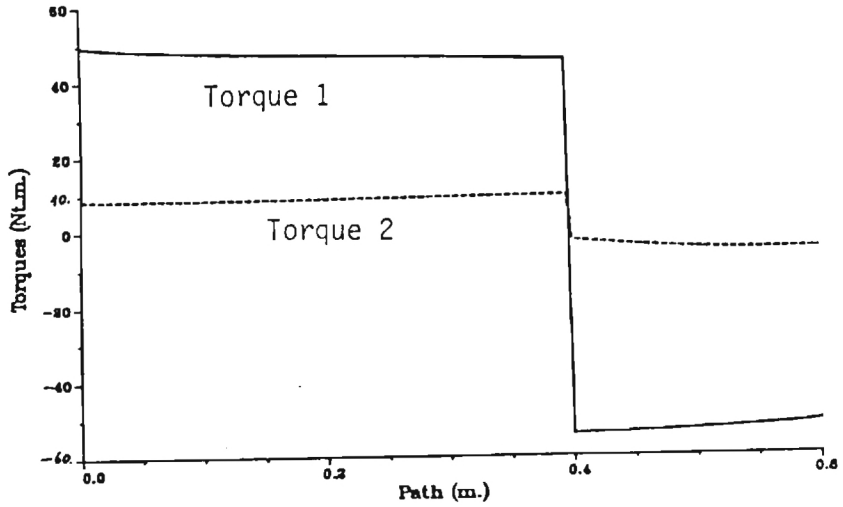

Fig. 6.c Torque histories of lightweight arms along path 1.

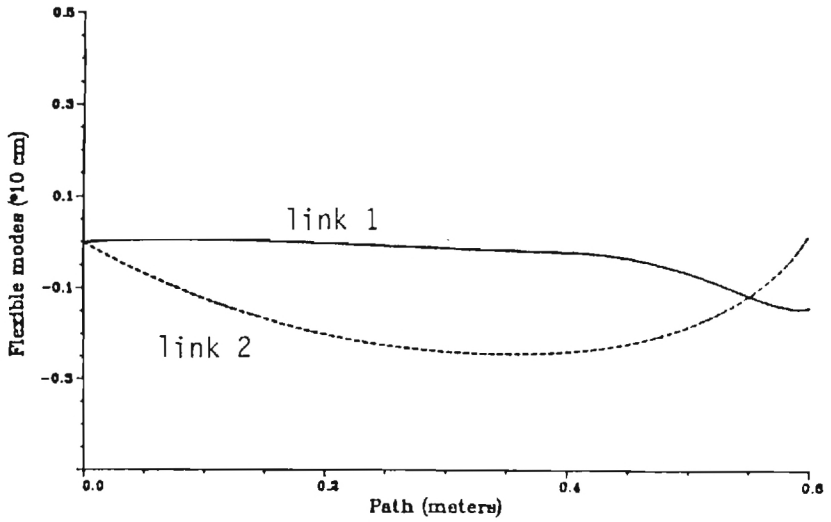

Fig. 6d. Flexible modes along path 1.

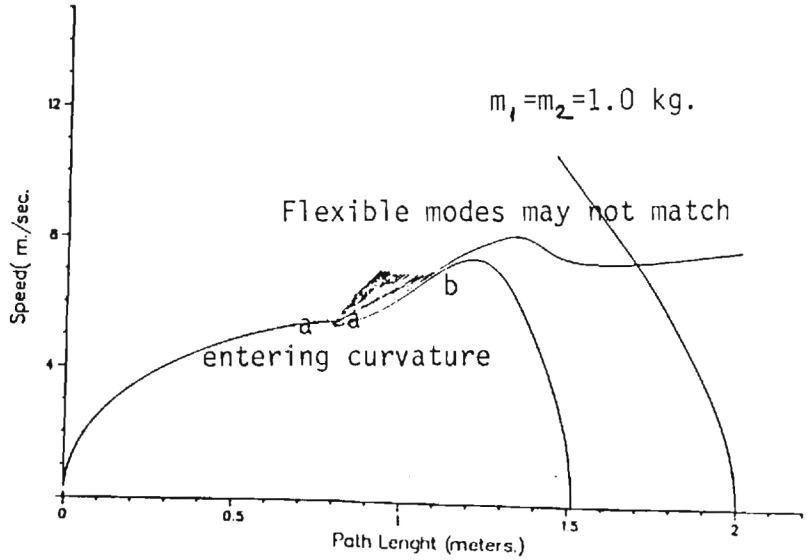

Fig. 7.a Finding the switching points for path 2.

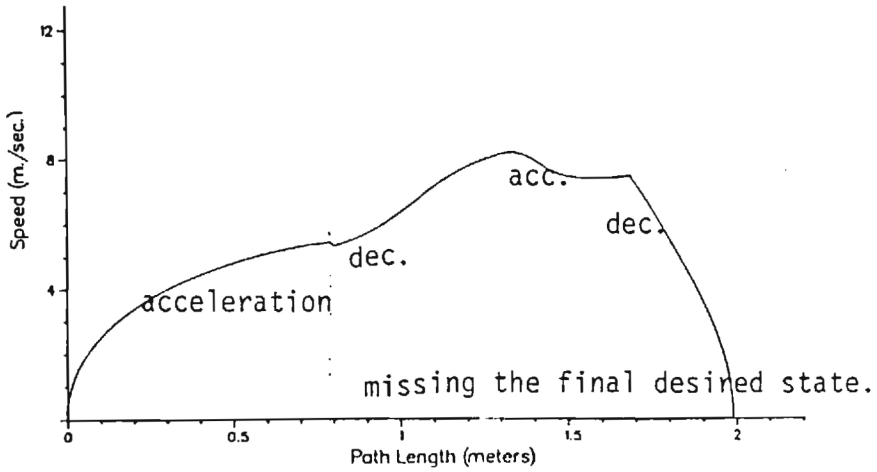

Fig. 7b. Trajectory for path 2.

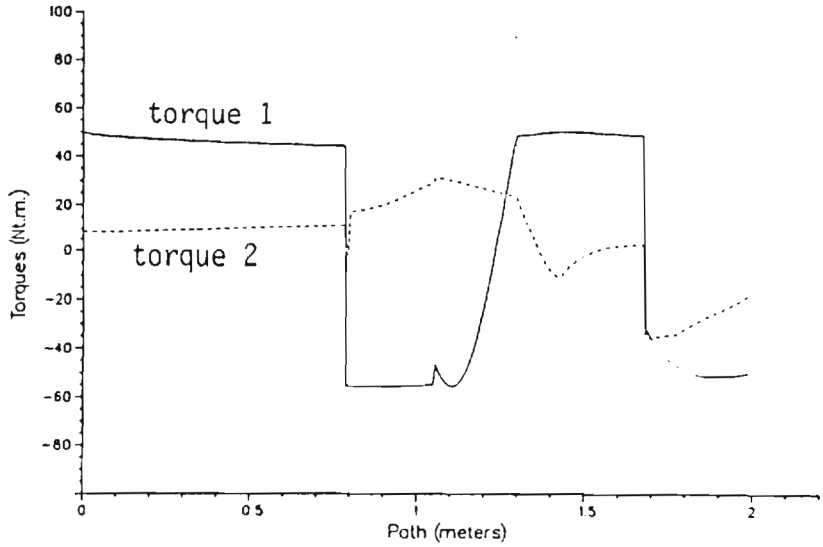

Fig. 7c . Torque histories along path 2

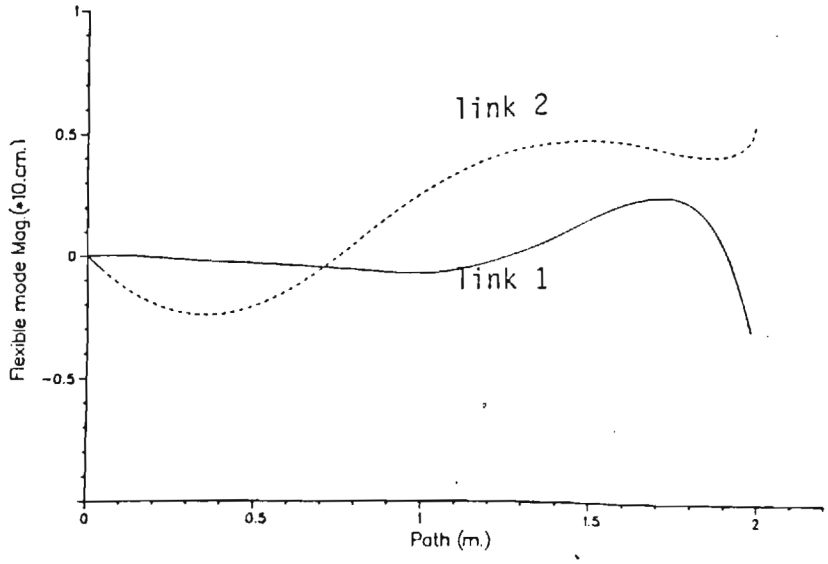

Fig. 7.d Flexible modes along path2.

"from Proceedings of ROBOTS9 Conference June 2-6, 1985 Detroit MI"

Experiments in the Control of a Flexible Robot Arm

Gordon G. Hastings
Georgia Institute of Technology
Atlanta, Georgia

Wayne J. Book
Georgia Institute of Technology

Abstract

Control of flexible manipulator arms offers high performance, light weight, and low cost over conventional rigid members. Presented is an experimental system for evaluating control systems. A dynamic modeling procedure is outlined and an optimal control system is discussed. Reconstruction of flexible modes is accomplished using strain gage data. Velocity of flexible modes is estimated with a reduced order observer. Experimental data is presented to verify dynamic modeling and modal reconstruction. Initial results using a deterministic optimal controller are presented.

INTRODUCTION

Long term success in the competitive race for factory automation depends on the developement of high performance, reliable, low cost automation. Research in the control of flexible structures may offer long term solutions to factory automation problems. Current research in the control of flexible arms appears to offer promise in applications where high performance, long reach, or mobility is required. This paper describes an experimental set-up, dynamic modeling, developement of a controller, and initial results in the optimal control of a flexible arm. The control system design, and dynamic modeling follow the work of Sangveraphunsiri[1].

EXPERIMENTAL SETUP

The setup is a complete laboratory for examining the control of flexible arms with frequencies as high as 100 Hz. The system consists of a flexible arm with payload, DC torque motor with servo-amp, A/D and D/A conversion for measurement sampling, signal conditioning, and 16 bit computer system for implementation of control algorithms. The physical configuration of the flexible arm, torque motor, and sensors is represented in figure 1. A simplified block diagram of the entire system is shown in figure 2. The desired end point position can be input from an external analog signal generator, or from internal trajectory generation software.

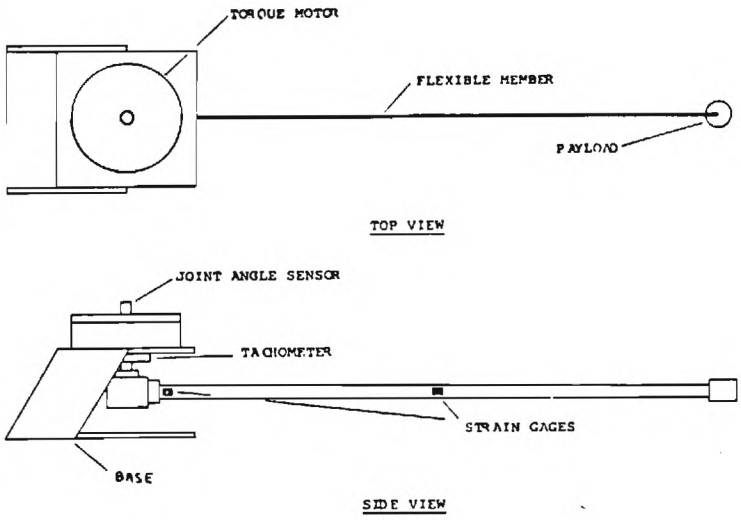

Flexible Beam Apparatus

FIGURE 1

The beam used in initial experiments is a four foot long aluminum beam. The physical characteristics are summarized in table 1. The beam was found to have natural frequencies of 7.3, 17.5, and 42 Hz in the first three modes when mounted in the experimental apparatus with payload. The control computer is an IBM series one system complete with floating point hardware, 64 megabyte hard disk storage, 24 channels of A/D conversion, and 2 channels of D/A conversion. The floating point hardware can accomodate either 32 ,or 64 bit manipulations. A typical value for 32 bit floating point multiplication is 17 microseconds. The characteristics of the A/D, D/A, and the signal conditioning equipment is summarized in table 1.

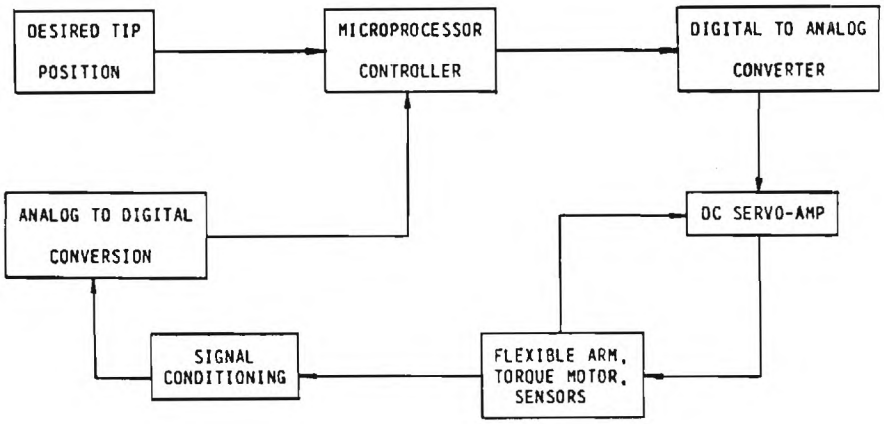

Experimental System Block Diagram

FIGURE 2

The state-space model developed for the system considers the torque motor to be an ideal torque source introducing no frequency attenuation, or phase terms to the input. The torque motor is a brush type DC torque motor, driven by a large servo-amp. The servo-amp has an internal gain of 35,000 and is configured to maintain the motor current proportional to the commanded torque from the D/A on its input. The characteristics of the torque motor and amp are summarized in table 1, and a connection diagram is given in figure 3. Tests of the amp/motor combination demonstrated good frequency response over the range of interest. Brush noise has not been significant in tests to date.

Flexible Beam Characteristics

Material	- Aluminum 6061-T6
Form	- Rectangular 3/4 in. x 3/16 in.
Length	- 48 in.
Moment of Inertia	- 4.12E-4 in.
EI Product	- 4120 lb/in.

Motor and Servo-Amp Characteristics

Motor Manufacturer	- Inland Motor
Torque Constant Kt	- 5.28 in-lb/amp
Back EMF Constant Ke	- 0.60 volts-sec/rad
Max. Rated Torque	- 84 in-lb at 15 amp

Amplifier Manufacturer	- Kepco Inc.
Large Signal Response	- 25 kHz
Slew Rate	- 2 volts/microsec
Max. Rated Current	- +/- 20 amps

Signal Conditioning and Sampling Capabilities

Filtering	- 11Channels,Low/HighPass,4Pole
Straingage Bridges	- 4 Channels,4 Active Gages per Channel
A/D Conversion	- 16 Channels,9600 Samples/sec,12 bits
A/D Conversion	- 8 Channels,20 Samples/sec,12 bits
D/A Conversion	- 2 Channels,+/- 10 volts,20μsec

TABLE 1

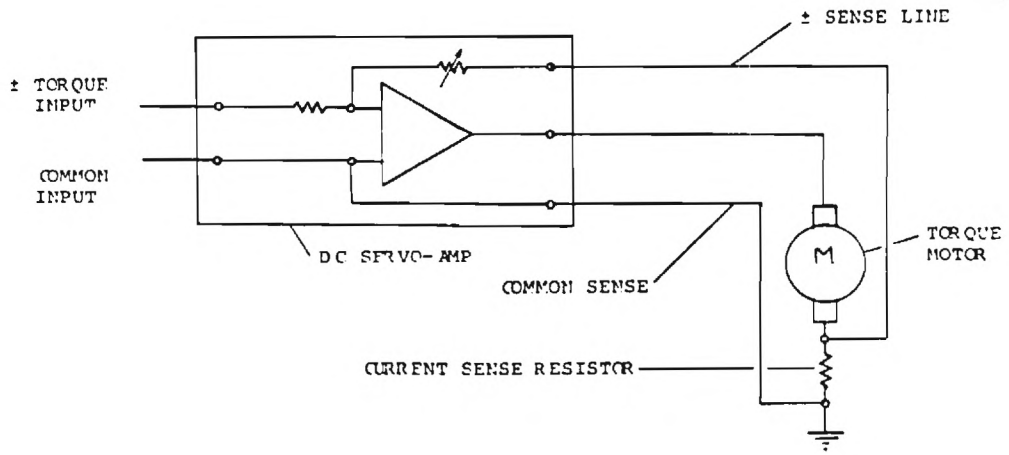

Servo-Amp/Motor Connection Diagram

FIGURE 3

DYNAMIC MODELING

The first step in the design of a controller is to construct an analytical model of the physical system. The model must include the major features of the real system, yet still lend itself to available analysis tools. The model selected represents the system as a truncated series of assumed modes, the first mode

being a rigid body rotation. Two additional flexible modes corresponding to clamped-free beam vibrations are included in the series. Figure 4 graphically depicts the results of a computer program modeling the two flexible modes.

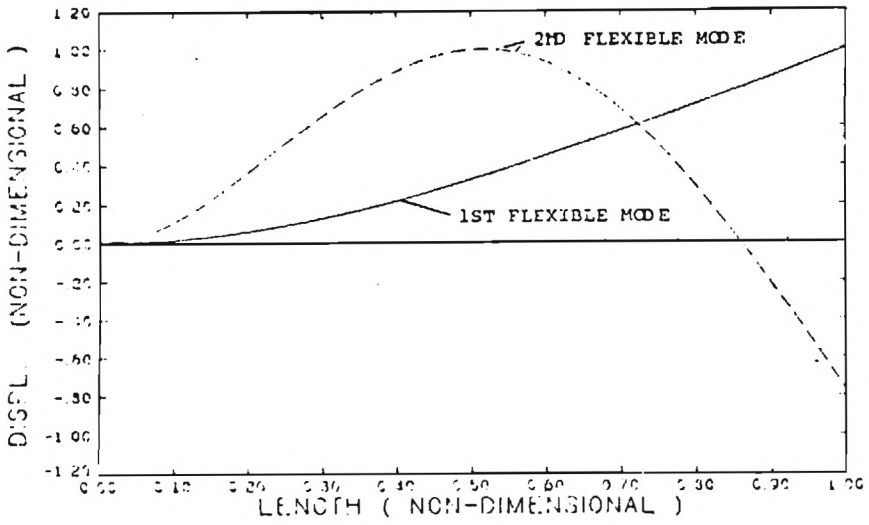

Computed Flexible Mode Shapes

FIGURE 4

The following sentences give a terse outline of the procedure utilized to generate the dynamic equations for the system. A detailed description of the procedure may be found in [1],[2]. LaGrange's equations are formulated for the three mode series after normalizing the modes. The equations are then linearized by assuming small motions, and neglecting terms of higher order than one. The equations can then be organized into a sixth order state-space model of the following form:

$$\begin{bmatrix} \dot{\tilde{x}} \\ \dot{\tilde{z}} \end{bmatrix} = \begin{bmatrix} \Phi_{aa} & \Phi_{ab} \\ \Phi_{ba} & \Phi_{bb} \end{bmatrix} \begin{bmatrix} \tilde{x} \\ \tilde{z} \end{bmatrix} + \begin{bmatrix} \tilde{\Gamma}_a \\ \Gamma_b \end{bmatrix} u \qquad 1.$$

$$\tilde{x} = \begin{bmatrix} \theta \\ q_1 \\ q_2 \\ \dot{\theta} \end{bmatrix} \qquad \tilde{z} = \begin{bmatrix} q_1 \\ q_2 \end{bmatrix} \qquad 2.$$

$\tilde{x}$ - measured state vector

$\tilde{z}$ - unmeasured state vector

$\tilde{\Gamma}$ - input vector

q - flexible mode

θ - joint angle

$\bullet$ - denotes time derivative

u - control torque

The system of equations is partitioned into the measured states x , and the unmeasured states z . An important experimental step in analyzing the controls for flexible aircraft was the verification of the analytical model. The servo-arm was excited with random noise and the transfer function of the open loop system was recorded. Figure 5 graphically compares the transfer function determined from experiment with the transfer function computed from the state-space model. The results agree reasonably well, and the measured modal frequencies were within 3.5 % of the modeled frequencies.

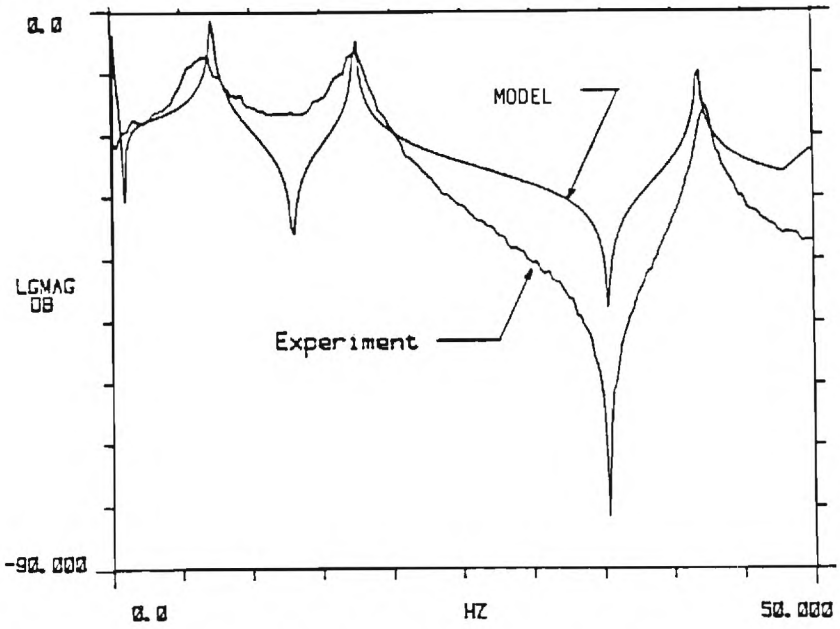

Comparison of Analytic to Experimental Transfer Functic

FIGURE 5

MODAL RECONSTRUCTION

The modern control system employed requires the entire state vector be identified for the control law. Direct measurement of the modal quantities is not possible, only measurement of variables which are functions of linear combinations of modal quantities. Two types of measurement are currently receiving attention, optical measurement of deflections, and strain measurement. The measurement selected for the initial experiments is strain, as this provides a simple, low cost method of collecting the necessary data. Strain measurement systems are compatible with corrupt industrial environments containing process sprays of oils, and dispersed solids as well as processes producing heavy vapors that would obstuct optical paths. The basic approach can be readily adapted to optical measurement of deflection, and future experiments are planned to compare the methods.

The information obtained from the strain gages does not provide direct information about the amplitude of the modal quantities. Equation 3 presents the basic relationship between the flexible modes and the strain. Since we are interested in reconstructing two separate modes, two strain measurements are made, one from the base of the beam and one from the mid-point. Four active gages are used in a full bridge at each measuring point. This implementation compensates for torsional,axial, and transverse strains that would otherwise reduce disturbance rejection. Equation 4 presents the form of the reconstruction relation used to obtain the modal amplitudes from the strain measurements.

$$\begin{bmatrix} \varepsilon(y_1) \\ \\ \varepsilon(y_2) \end{bmatrix} = \begin{bmatrix} c_{11}\dfrac{\partial^2 \phi_1(y_1)}{\partial y^2} & c_{12}\dfrac{\partial^2 \phi_{2}(y_1)}{\partial y^2} \\ \\ c_{21}\dfrac{\partial^2 \phi_1(y_2)}{\partial y^2} & c_{22}\dfrac{\partial^2 \phi_{2}(y_2)}{\partial y^2} \end{bmatrix} \begin{bmatrix} \xi_1(t) \\ \\ \xi_2(t) \end{bmatrix} \qquad 3.$$

$$\tilde{\xi} = A^{-1}\,\tilde{\varepsilon} \qquad 4.$$

$\varepsilon(y)$ - indicates strain at axial distance y

$\phi(y)$ - spatial mode functions

$\xi(y)$ - time dependent modal amplitud-

The coefficients for the reconstruction can be determined by inserting the assumed mode functions into equation 4. Figures 6, and 7 present experimental data used to determine the reconstruction coefficients. The beam was harmonically excited at the frequency of the mode being considered with a unit tip deflection amplitude, and the strain responses monitored. The experiments agreed well with analytical modeling, resulting in a nearly orthogonal relationship between the modes providing 6 to 8 decibels of rejection between the reconstructed modes.

CONTROL SYSTEM DESIGN

The state-space model of the flexible arm is a useful mathematical tool which contains an embedded description of the undesireable plant dynamics introduced by the flexible modes. The problem now is to specify a control law which yields satisfactory dynamic characteristics in the closed loop system. The objective of fast response of the flexible arms payload to commanded positions, is in opposition to minimizing excitation of the flexible modes. The first requires high rates and torques, while the latter favors smooth application of smaller torques. This problem is an excellent candidate for optimal control, which can seek to reach a solution with a relative weighting on the various

states. Deterministic and stochastic controllers have been designed for the experimental system, but the initial results and following discussion will deal only with a deterministic controller.

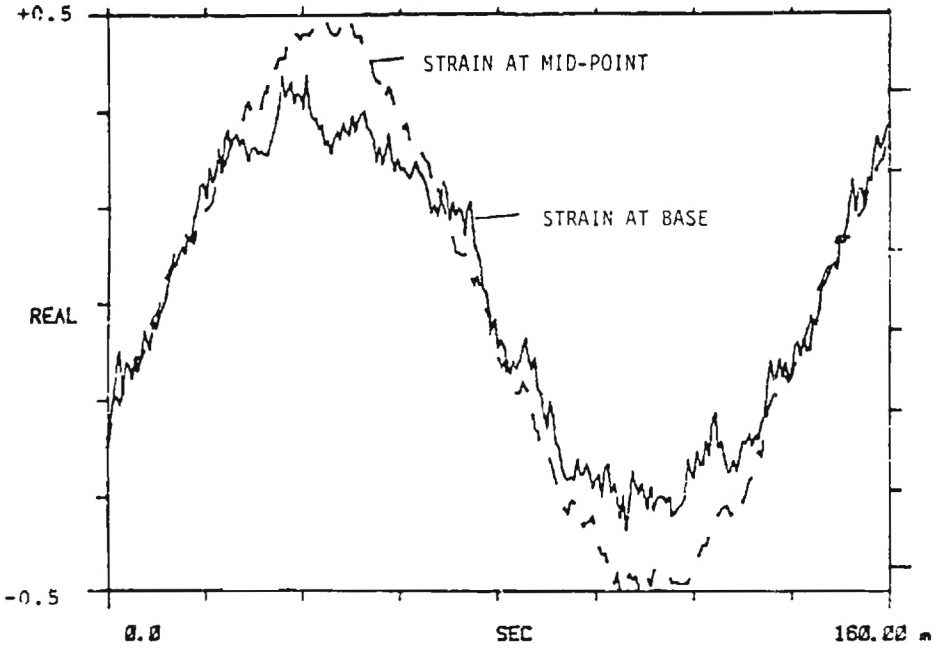

Normalized Strain Response to 7.5 Hz Harmonic Excitation

FIGURE 6

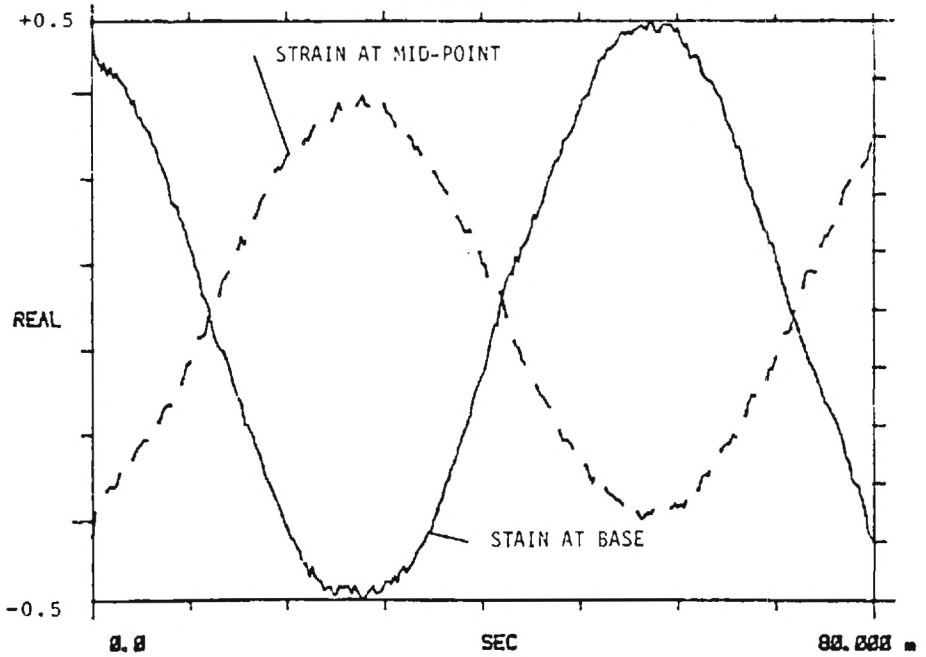

Normalized Strain Response to 17.5 Hz Harmonic Excitation

FIGURE 7

Equation 5 presents a standard formulation of a linear quadratic continuous transient regulator problem where x is the entire state vector. The steady state solution of the control law was computed using subroutines in the ORACLS [5] software package. The basic problem was modified [3] so that the closed loop poles of the system could be specified with an arbitrary degree of stability.

$$P = \int (\tilde{x}^T Q \tilde{x} + Ru)dt \qquad 5.$$

$$u = \tilde{K}^T \tilde{x}$$

Q,R - weighting matricies for the states and control

$\tilde{K}^T$ - control law

The selection of the elements of the weighting matricies remains to a large degree trial and error. In this system it is noted that the second flexible mode is very energetic and large penalties on the second modes velocity, or states highly coupled to the second mode result in high gains on the second state. These high gains result in excessive control action. Additionally the second mode is not a static deflection mode and high state gain causes problems due to measurement errors. The control objective in the second mode is therefore damping, and not steady state error reduction.

STATE ESTIMATION AND REDUCED ORDER-OBSEREVERS

The experiment does not provide for measurement of the entire state vector needed for the selected control law. Estimation of the state from the measured states is accomplished; further, since four of the six states are available from measurement it is only necessary to design a reduced order observer to estimate the two unmeasured modal velocities. Equation 6 presents a well known transformation from the original system to an estimator with error dynamics specified by equation 7[4],[5]. The design of this estimator, and the transformation is straight foward when the number of measured states is equal to the number of estimated states. Specification of the error dynamics completely specifies the transformation.

$$T = \begin{bmatrix} I & 0 \\ \hline -L & I \end{bmatrix} \qquad 6.$$

$$\dot{\tilde{z}}' = (\Phi_{bb} - L\Phi_{ab})\,\tilde{z}' \qquad 7.$$

$\tilde{z}'$ - estimate of the unmeasured states

This system measures four states, and only estimates two. Specification of the estimator error dynamics does not completely specify the transformation, and several arbitrary terms remain. The separation theorem allows for the introduction of the estimator poles on the overall system. During start up of the apparatus it is useful to start the computer before the torque motor. At this time the separation theorem is not applicable. The computed control torque is fed into the estimator instead of the applied torque since it is more readily available. These factors make it desirable to consider the effect of the feedback law on the estimator alone. Equation 8 identifies the estimators dependence on the torque and control law. Equation 8 results in a two element vector for this system. Therefore the "closed loop" estimator poles cannot be completely specified.

$$(\Gamma_b - L\Gamma_a)\, u \qquad 8.$$

$$\dot{\tilde{z}}' = F\tilde{z}' + Gx + Bu \qquad 9.$$

The form of the complete estimator equation is presented in equation 9. In the initial experiments the estimators dependence on input torque was specified to be zero by proper selection of hte transformation L. The torque was not a measured quantity and this specification increases the estimators response to the measured states. The remaining independence in the transformation was resolved by searching the system of equations for the independent terms. Values for the remaining arbitrary terms in the transformation were selected by examining the results of system simulations. Figure 8 depicts a block diagram of the control system and reduced order estimator.

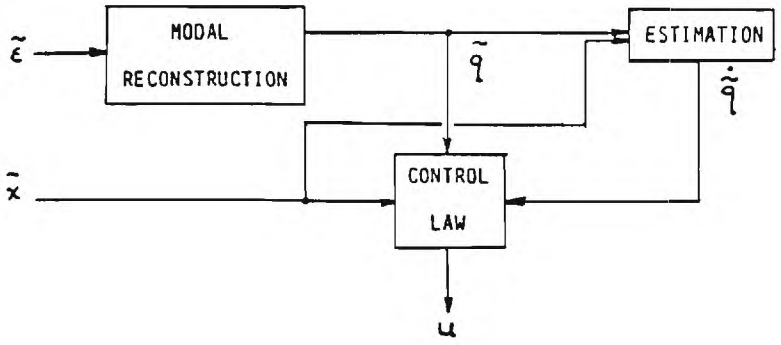

Control System Block Diagram

FIGURE 8

INITIAL RESULTS

The deterministic controller was implemented in assembly language on the IBM control processor and the entire system activated. The closed loop properties of the control system are compared to the open loop in figure 9. It is apparent from the graph that the undesirable modal resonances in the open loop transfer function have been eliminated by the control system. The third flexible mode at 42 Hz which was truncated in the model remained basically unaltered. This initial result is obtained from a first rough cut at the control system, and while it demonstrates the control of the flexible modes it does not appear to be the most appropriate selection.

The weighting matricies used in the optimal design, the degree of stability, and the estimator dynamics were chosen relatively arbitrarily. Considerable data must be gathered to draw relationships between the design parameters and the systems performance. The most revealing performance criteria for the flexible arm control system will be settling time and response bandwidth.

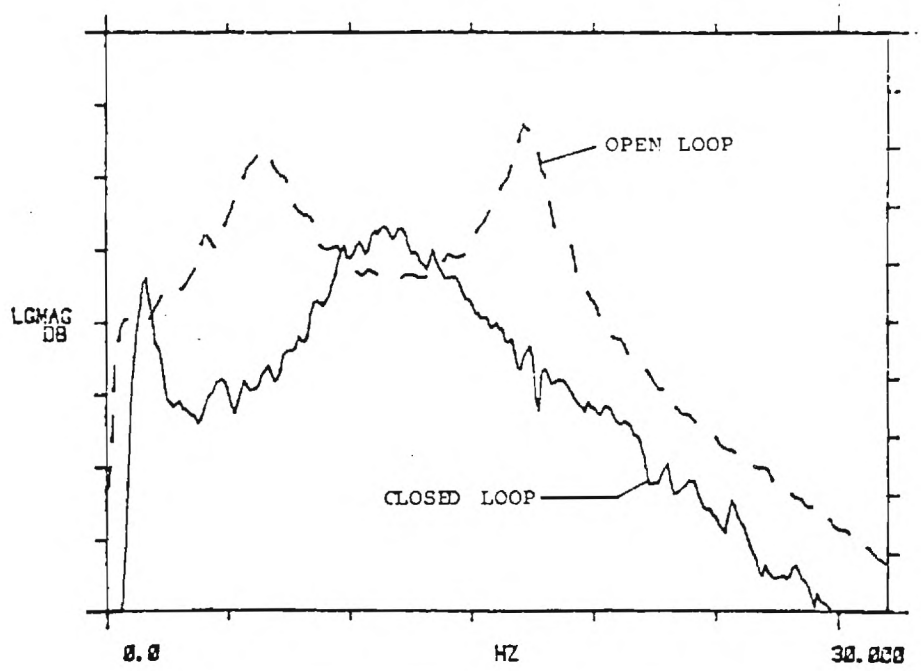

Comparison of Open Loop and Closed Loop Transfer Functions

FIGURE 9

CONCLUSIONS AND FUTURE WORK

An experimental setup for evaluating flexible arm control systems has been constructed and verified. The reconstruction of flexible mode amplitudes from strain gage data for use in control of a flexible arm has been demonstrated. An optimal controller for a flexible arm was implemented and shown to control the flexible modes.

Significant data must be gathered on each control system considered to properly identify the interrelation between the parameters. This data can often be collected via simulation, but experimental verification is often required for developing confidence in the critical assumptions. Many control systems have been proposed for flexible arms[1],[6],[7] and this system provides an opportunity for relative comparisons. Experiments are planned to combine active control of the flexible modes with high performance passive damping treatments[2].

Finally for applications demanding the manipulator apply significant force at the tip schemes must be investigated and implemented which utilize the elements of the work cell itself to gain rigidity[9]

from the Proceedings of the 1985 American Control Conference, Boston, MA
June, 1985, pp 728-729.

EXPERIMENTS IN OPTIMAL CONTOL OF A FLEXIBLE ARM

Gordon G. Hastings, and Wayne J. Book
Department of Mechanical Engineering
Georgia Institute of Engineering, Atlanta, Ga. 30308

INTRODUCTION

Research in the control of flexible arms may offer long term solutions to factory automation problems in applications where high performance, long reach, or mobility is required. This paper discusses the reconstruction of modal quantities from strain gage measurements, and the sensitivity of an optimal controller to variations in payload mass based on analytical models and experiment for a single-link arm.

EXPERIMENTAL SETUP

The setup is a complete laboratory for examining the control of flexible arms with frequencies as high as 100 Hz. The system consists of a flexible arm with payload, DC torque motor with servo-amp, A/D and D/A conversion for measurement sampling, signal conditioning, and 16 bit computer system for implementation of control algorithms. The control computer is equipped with floating point hardware, 64 megabyte hard storage, 24 channels of A/D conversion, and 2 channels of D/A conversion. A typical value for 32 bit floating point multiplication is 17 microseconds. The physical configuration of the flexible arm, torque motor, and sensors is represented in figure no. 1. Figure no. 2 is a block diagram of the system components.

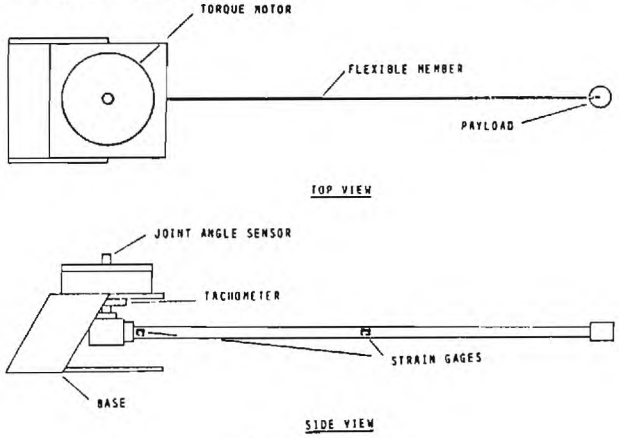

Figure no. 1

The arm is a four foot long rectangular aluminum beam, the first two clamped-free vibration modes were found to be 2.0,and 13.5 hz when mounted in the experimental apparatus with payload.

DYNAMIC MODELING

The first step in the design of controllers for a flexible arm is to construct an analytical model of the physical system. The model must include the major features of the real system, yet still lend itself to available analysis tools. A truncated series of assumed modes was selected, with the first mode being a rigid body rotation. Two additional flexible modes corresponding to clamped-free beam vibrations complete the series.

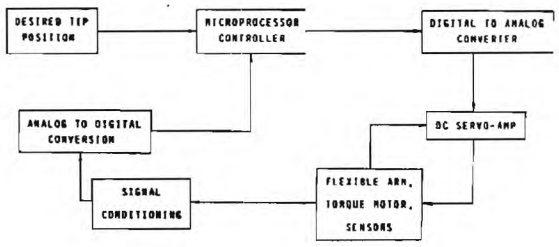

System Block Diagram

Figure no. 2

LaGrange's equations are formulated for the three mode series after normalizing the flexible modes. The resulting dynamic equations are then linearized by assuming small motions, and neglecting terms of higher order than one. The equations can then be organized into a sixth order state space model of the following form:

$$\begin{bmatrix} \dot{\tilde{x}} \\ \dot{\tilde{z}} \end{bmatrix} = \begin{bmatrix} \Phi_{aa} & \Phi_{ab} \\ \Phi_{ba} & \Phi_{bb} \end{bmatrix} \begin{bmatrix} \tilde{x} \\ \tilde{z} \end{bmatrix} + \begin{bmatrix} \tilde{\Gamma}_a \\ \tilde{\Gamma}_b \end{bmatrix} u \qquad 1.$$

$$\tilde{x} = \begin{bmatrix} \theta \\ q_1 \\ q_2 \\ \dot{\theta} \end{bmatrix} \qquad \tilde{z} = \begin{bmatrix} q_1 \\ q_2 \end{bmatrix} \qquad 2.$$

$\tilde{x}$ - measured state vector
$\tilde{z}$ - unmeasured state vector
$\tilde{\Gamma}$ - input vector
q - flexible mode
θ - joint angle
$\cdot$ - time derivative
u - control torque

A detailed description of the modeling procedure may be found in [1],[2].

CONTROL SYSTEM DESIGN

Rapid response of the flexible arms payload to commanded positions requires high rates and torques which tend to excite the flexible modes. The design of a controller must compensate for the flexibility, or accept limited performance. Combining the state-space model with modern control techniques provides a method for specifiying control laws which optimize functions of the systems states. Deterministic and stochastic controllers have been designed for the experimental system, but the initial experiments implemented a deterministic controller.

A control law was selected which satisfied a standard formulation of a linear quadratic continuous transient regulator problem. The steady state solution was computed using subroutines in the ORACLS [3] software package. The basic problem was modified so that the closed loop poles of the system could be specified with an arbitrary degree of stability.

MODAL RECONSTRUCTION

The modern control system employed requires the entire state vector be identified for the control law. Direct measurement of the modal quantities is not possible, only measurement of variables which are functions of linear combinations of modal quantities. Two types of measurement are currently recieving attention, optical measurement of deflections, and strain measurement. The measurement selected for the initial experiments is strain, as this provides a simple, low cost method of collecting the necessary data. The basic approach can be readily adapted to optical measurement of deflection, and future experiments are planned to compare the methods.

Equation 3 presents the basic relationship between the flexible modes and the measured strain data. Since we are interested in reconstructing two separate modes, two strain measurements are made, one from the base of the beam and one from the mid-point. Four active gages are used in a full bridge at each measuring point. This implementation compensates for torsional, axial, and tranverse strains that would otherwise reduce disturbance rejection.

$$\begin{bmatrix} \varepsilon(y_1) \\ \varepsilon(y_2) \end{bmatrix} = \begin{bmatrix} c_{11}\frac{\partial^2 \phi_1}{\partial y^2}(y_1) & c_{12}\frac{\partial^2 \phi_2}{\partial y^2}(y_1) \\ c_{21}\frac{\partial^2 \phi_1}{\partial y^2}(y_2) & c_{22}\frac{\partial^2 \phi_2}{\partial y^2}(y_2) \end{bmatrix} \begin{bmatrix} \xi_1(t) \\ \xi_2(t) \end{bmatrix} \qquad 3.1$$

$$\bar{\xi} = A^{-1}\bar{\varepsilon} \qquad 3.2$$

$\varepsilon(y)$ - indicates strain at axial distance y

$\phi(y)$ - spatial mode functions

$\xi(t)$ - time dependent modal amplitude

The coefficients for the reconstruction can be determined by inserting the asumed mode functions into equation 3. The beam was harmonically excited at the frequency of the mode being considered with a unit tip deflection amplitude, and the strain responses monitored. The experiments agreeded well with analytical modeling, resulting in a nearly orthogonal relationship between the modes providing 6 to 8 decibels of rejection between the reconstructed modes.

MASS SENSITIVITY

The model used for developing the control law was based on a set of assumed modes, manipulators often transport payloads of different masses, therefore, the effect of varying the payload was investigated. The sensitivity of the closed loop poles to variations in payload mass is depicted in figure 3. The locus was determined from a linear model. The mass was varied from the design value, then the dynamic and input matrix was recalculated for each mass point. The optimal gains determined for the design condition were retained, and the closed loop poles determined. The measured time response of the system is shown in figure 4 for no payload, design payload, and four times the design payload using the same optimal gains.

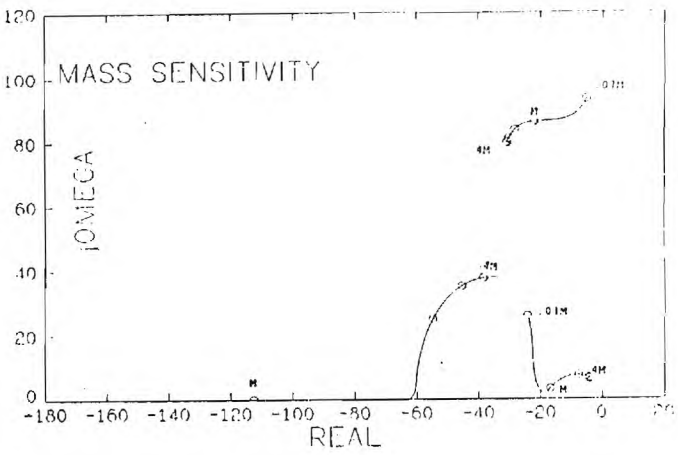

Figure no. 3

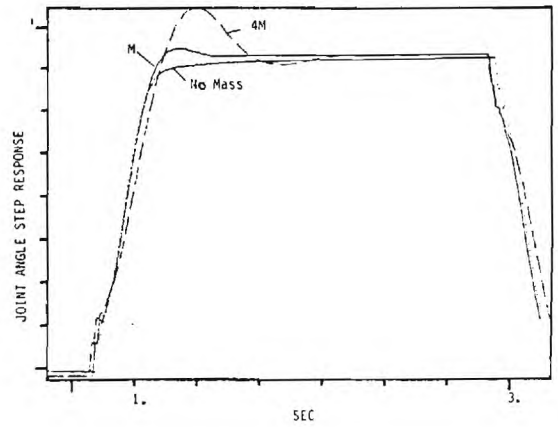

Figure no. 4

CONCLUSIONS

The initial experiments have successfully demonstrated the use of strain measurements to reconstruct flexible modes. Although it is difficult to correlate the root locus with the time response plots both depict moderate sensitivity to large variations in payload mass without sudden transitions to instability.

BIBLIOGRAPHY

[1] V. Sangveraphunsiri, "The Optimal Control and Design of a Flexible Manipulator Arm", PhD Disertation, Dept. of Mech. Eng., Georgia Institute of Technology, Atlanta, Ga.

[2] T. Alberts, S. Dickerson, W. J. Book, "Modeling and Control of Flexible Manipulators", to be published.

[3] E. S. Armstrong, "ORACLS-A System for Linear-Quadratic-Gaussian Control Law Design", NASA TP-1106, April 1978.

VPI&SU/AIAA SYMPOSIUM ON DYNAMICS AND CONTROL OF LARGE FLEXIBLE STRUCTURES

Blacksburg Va. June 1985

EXPERIMENTS IN OPTIMAL CONTROL OF A FLEXIBLE ARM WITH PASSIVE DAMPING

by

Thomas E. Alberts, Ph.D Candidate

Gordon G. Hastings, Ph.D Candidate

Wanye J. Book, Professor

and

Stephen L. Dickerson, Professor

Department of Mechanical Engineering
Georgia Institute of Technology
Atlanta, Georgia 30332

Abstract

This paper presents a hybrid active and passive control scheme for controlling the motion of a lightweight flexible arm. A straightforward developement of LaGrange's equations using a series expansion of assumed flexible modes provides a time domain model for controller design. The active controller design was approached as a steady state linear quadratic continuous regulator. A constrained viscoelastic layer treatment was employed to achieve passive damping. The passive damping treatment serves to enhance the system's stability while providing sound justification for the use of a highly truncated dynamic model and reduced order controller. Initial experimental results comparing controller performance with and without passive damping demonstrate the merit of the proposed combined active/passive approach.

Introduction

Recently a considerable volume of literature has been devoted to the problem of controlling the motions of structures having flexible structural members. While much of this research is performed in the interest of controlling large spacecraft, several investigators [1-6] have considered applying similar principles to the control of industrial

manipulators in the interest of improving manipulator performance and relaxing the structural stiffness requirement imposed by the more conventional rigid body control techniques. Such is the motivation for the work presented in this paper.

Although manipulators are somewhat complicated structures having several flexible links and joints that move independently, many problems associated with controlling such devices can be approached, without loss of generality, by considering a simple single link, single axis configuration. The present investigation concentrates on a single link arm which rotates in the horizontal plane about a pinned end. The authors apply established methods for developing a time domain dynamic model and active controller. Active control is applied to only the first two flexible modes and the rigid body mode. In order to reduce the effect of the ignored flexible modes a constrained viscoelastic layer damping treatment is applied to the surface of the flexible beam. This approach involves sandwiching a thin layer of viscoelastic material between the flexible member's surface and a stiff elastic constraining layer. When elastic deformation of the structure occurs, shear induced plastic deformation imposed in the viscoelastic layer provides the desired mechanical damping effect. Lane [7] has shown, analytically, that the incorporation of the prescribed passive damping treatment can result in faster settling times and considerable improvements in system stability. This paper presents the results of initial experiments performed with the aim of verifying this assertion.

Experimental Facility

The experimental facility is a complete laboratory for examining the control of flexible arms with frequencies as high as 100 Hz. The system consists of a flexible arm with payload, DC torque motor with servo-amp, A/D and D/A conversion for measurement sampling, signal conditioning and 16 bit computer system for implementation of control algorithms. The control computer is equipped with floating point hardware, 64 megabyte hard storage, 24 channels of A/D conversion and 2 channels of D/A conversion. A typical value for 32 bit floating point multiplication is 17 microseconds. The physical configuration of the flexible arm, torque motor and sensors is illustrated in figure 1. Figure 2 is a block diagram of the system components. The arm is a four foot long rectangular aluminum beam with cross sectional dimensions of 3/4 x 3/16 inches. With the active feedback controller operating, the first two natural frequencies of the beam approach its clamped-free modes, accordingly these are the modes assumed in modeling the arm's dynamics. The clamped-free frequencies of the arm with the payload in place are 2.0 and 13.5 Hz.

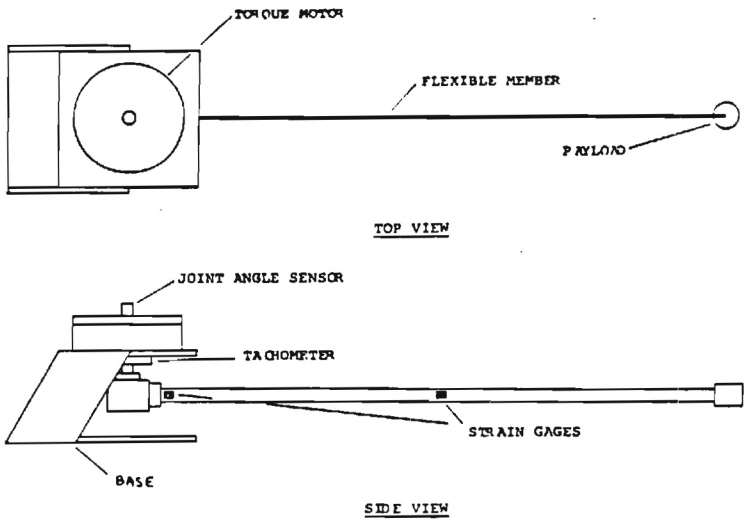

Figure 1. Experimental Arm

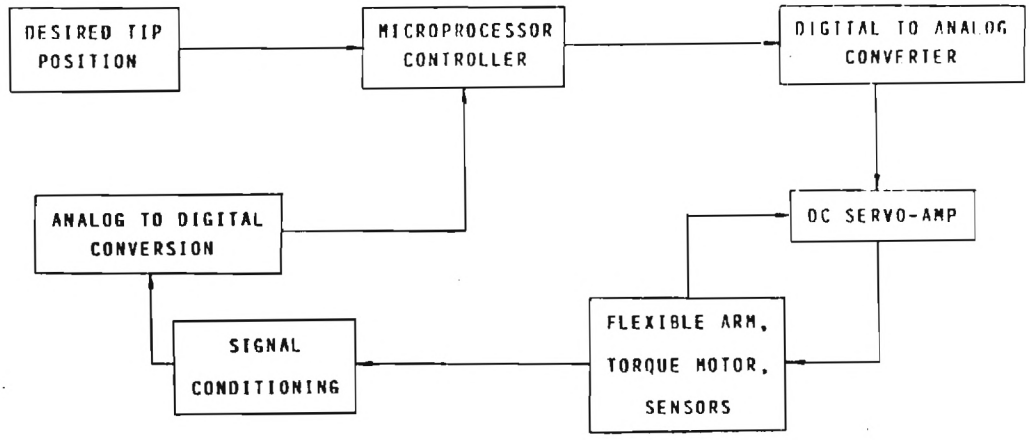

Figure 2. System Block Diagram

Dynamic Modeling

The first step in controller design is to construct an analytical model of the physical system. The model must include the major features of the real system, yet still lend itself to available analysis tools. A truncated series of assumed modes was selected, with the first mode being a rigid body rotation. Two additional flexible modes corresponding to clamped-free beam vibrations complete the series. LaGrange's

equations are formulated for the three mode series after normalizing the flexible modes. The resulting dynamic equations are then linearized by assuming small motions and neglecting terms of higher order than one. The equations can then be organized into a sixth order state space model of the following form:

$$\begin{bmatrix} \dot{\tilde{x}} \\ \dot{\tilde{z}} \end{bmatrix} = \begin{bmatrix} \Phi_{aa} & \Phi_{ab} \\ \Phi_{ba} & \Phi_{bb} \end{bmatrix} \begin{bmatrix} \tilde{x} \\ \tilde{z} \end{bmatrix} + \begin{bmatrix} \tilde{\Gamma}_a \\ \Gamma_b \end{bmatrix} u \qquad (1)$$

$$\tilde{x} = \begin{bmatrix} \theta \\ q_1 \\ q_2 \\ \dot{\theta} \end{bmatrix} \qquad \tilde{z} = \begin{bmatrix} \dot{q}_1 \\ \dot{q}_2 \end{bmatrix} \qquad (2)$$

$\tilde{x}$ - measured state vector

$\tilde{z}$ - unmeasured state vector

$\tilde{\Gamma}$ - input vector

q - flexible mode

θ - joint angle

$\bullet$ - time derivative

u - control torque

A detailed description of the modeling procedure may be found in [8,9].

Modal Reconstruction

The control system employed requires the entire state vector be identified for the control law. Direct measurement of the modal quantities is not possible, however, modal displacements can be calculated as linear combinations of strain measurements. Equation 3 is the basic relationship between the flexible modes and the strain. Since we are interested in reconstructing two separate modes, two strain measurements are made, one from the base of the beam and one from the midpoint. Four active gages are used in a full bridge at each measuring point. This implementation compensates for torsional, axial and transverse strains that would otherwise reduce disturbance rejection. Equation 4 is the form of the reconstruction relation used to obtain the modal amplitudes from the strain measurements.

The coefficients for the reconstruction can be determined by inserting the assumed mode functions into equation 4. Experiments agreed well with the analytical model, resulting in a nearly orthogonal relationship between the modes providing 6 to 8 decibels of rejection between the recon-

structed modes. A reduced order luenberger observer was employed to estimate the modal velocities from the modal amplitudes.

$$\begin{bmatrix} \varepsilon(y_1) \\ \\ \varepsilon(y_2) \end{bmatrix} = \begin{bmatrix} c_{11}\frac{\partial^2}{\partial y^2}\phi_1(y_1) & c_{12}\frac{\partial^2}{\partial y^2}\phi_2(y_1) \\ \\ c_{21}\frac{\partial^2}{\partial y^2}\phi_1(y_2) & c_{22}\frac{\partial^2}{\partial y^2}\phi_2(y_2) \end{bmatrix} \begin{bmatrix} q_1(t) \\ \\ q_2(t) \end{bmatrix} \tag{3}$$

$$\tilde{\xi} = A^{-1}\,\tilde{\varepsilon} \tag{4}$$

$\varepsilon(y)$ - indicates strain at position y

$\phi(y)$ - spatial mode functions

$q(t)$ - time dependent modal amplitude

Control System Design

The objective of fast response of the flexible arm's payload to commanded positions, is in opposition to minimizing excitation of the flexible modes. The first requires high rates and torques, while the latter favors smooth application of smaller torques. This problem is an excellent candidate for optimal control, which provides a solution with relative weighting on the various states.

Equation 5 is the standard formulation of a linear quadratic continuous transient regulator problem where **X** is the full state vector. The steady state solution of the control law was computed using subroutines in the ORACLS [10] software package. The basic problem was modified [11] so that the closed loop poles of the system could be specified with an arbitrary degree of stability.

$$P = \int (X^T Q X + R u^2)\,dt \tag{5}$$

$$u = K^T X$$

where

Q, R = weighting matrices

and K^T = control law

The selection of the elements of the weighting matrices remains to a large degree trial and error. In this system it is noted that the second flexible mode is very energetic and large penalties on the second mode velocity or states coupled to the second mode result in high gains on the second state. These high gains result in excessive control action. Additionally the second mode is not a static deflection mode and high state gain causes problems due to measurement errors. The control objective in the second mode is therefore damping rather than steady state error reduction.

Passive Damping

Lane [7] introduced the concept of controlling a flexible manipulator arm using a hybrid active/passive control strategy. Passive control involves moving the flexible system's poles to the left by physically adding mechanical damping to the system. This has the effect of improving stability and response of the overall system while reducing the detrimental effects of both control and observation spillover. The application of constrained viscoelastic damping layers was proposed as a passive control measure. The approach involves sandwiching a thin film of viscoelastic material between the flexible member's surface and an elastic constraining layer. Materials having high elastic moduli provide the most effective elastic constraining layers. When elastic deflection of the structure occurs, shear induced plastic deformation is imposed in the viscoelastic layer. The energy dissipation associated with the plastic deformation provides the desired mechanical damping. This concept is illustrated in Figure 3. For further details regarding the

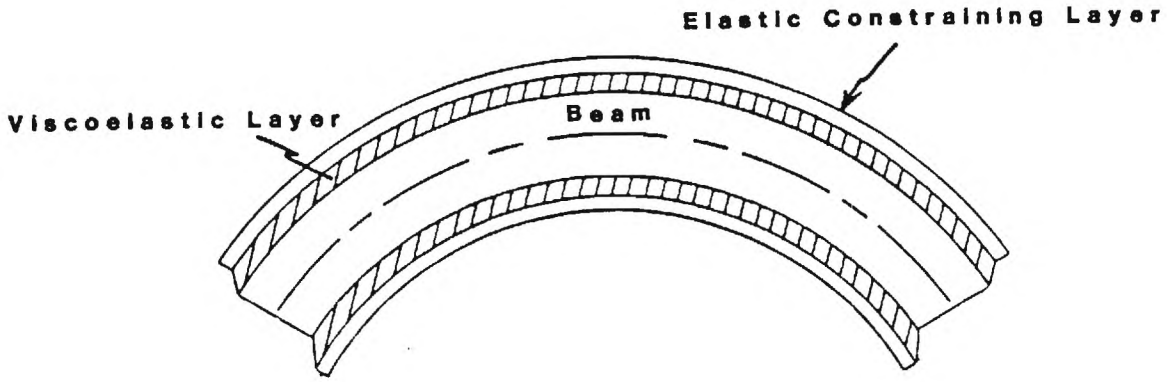

Figure 3. Treated Beam Element Under Flexure

theory associated with constrained viscoelastic layer damping the reader is referred to references [12-15].

Plunkett and Lee [12] have observed that a relationship exsists between the length of the elastic constraining layer and the damping ratio. For example, if the constraining layer is very long, relatively little shear is induced in the viscoelastic layer at locations remote to the endpoints. Conversly, if the constraining layer is very short, a more uniform shear distribution results, however the plastic deformation is of small magnitude, even at the endpoints. This suggests the existence of some optimal length, to which constraining layer sections could be cut to provide the optimal damping for a given configuration. Plunkett and Lee have developed a method for calculating this optimal section length. The damping obtained through application of constrained viscoelastic layers is frequency dependent and accordingly section length optimization is performed with respect to a prescribed frequency. With regard to the present application the section length has been selected so as to optimize the damping in the vicinity of the lowest frequency uncontrolled modes. It is important to note that when the constraining layer is not sectioned, the damping is optimal for very low frequencies and consequently, non-sectioned treatments generally will not enhance the control of flexible structures significantly. Figure 4 compares theoretically calculated damping ratios for sectioned and non-sectioned treatments. The data represents the aluminum beam discussed above, with a .002 inch viscoelastic layer and .010 inch thick steel constraining layer partitioned into 1.72 inch sections. The treatment is applied to both sides of the beam. It is evident from these curves that the damping for the frequency range of interest is substantially increased by simply cutting the constraining layer into sections. Figure 4 also includes the experimentally measured damping ratios for the treated beam described above. Figure 5 presents a comparison between the frequency response for an untreated beam and one incorporating the sectioned constrained layer treatment.

Upon examination of the sectioned constraining layer data presented in figure 4, one finds that while the shapes of the experimental and theoretical curves are in reasonable agreement, the damping ratios are significantly overestimated by Plunkett and Lee's method. The authors find that for very thin constraining (.0015 inch steel) layers the experimental and theoretical values agree within about 10%, however when the constraining layer thickness is increased, in the interest of increasing the damping provided, the agreement tends to be poor. The authors believe that this trend may be attributed to a number of simplifying assumptions made by Plunkett and Lee, which provide adequate results for thin constraining layers, but may be violated as constraining layer thickness

is increased. Probably foremost among these is the assumption that the constraining layer experiences only axial stress that is uniform throughout its thickness. Alberts is presently investigating the extension of Plunkett and Lee's model to accommodate thicker constraining layers.

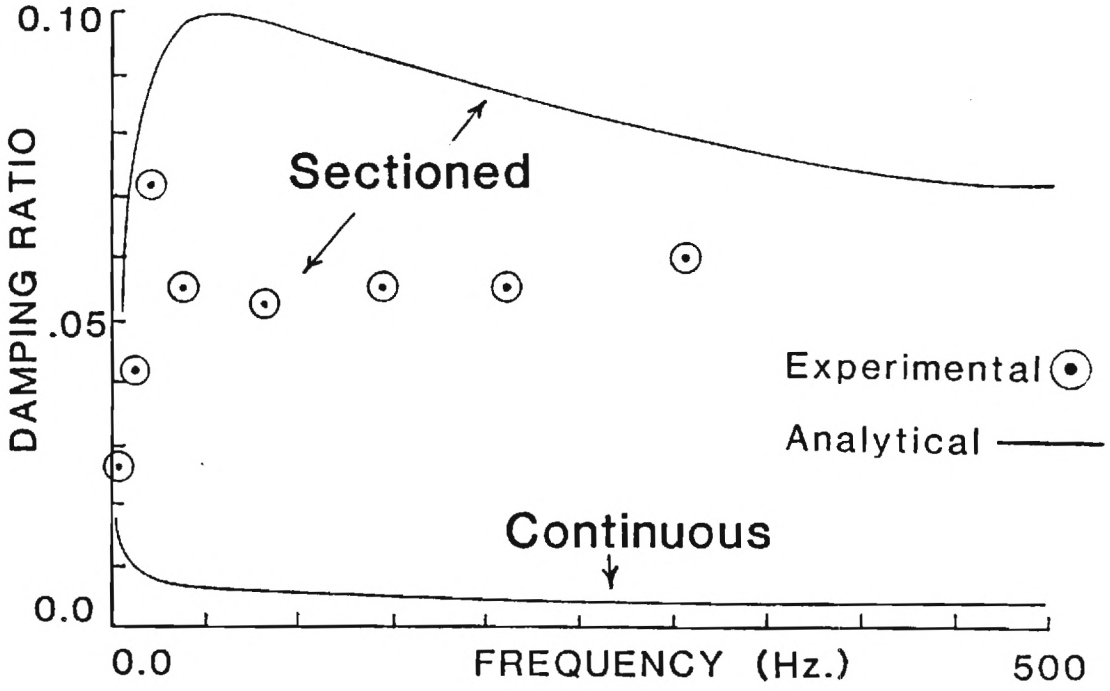

Figure 4. Damping Ratio "vs" Frequency

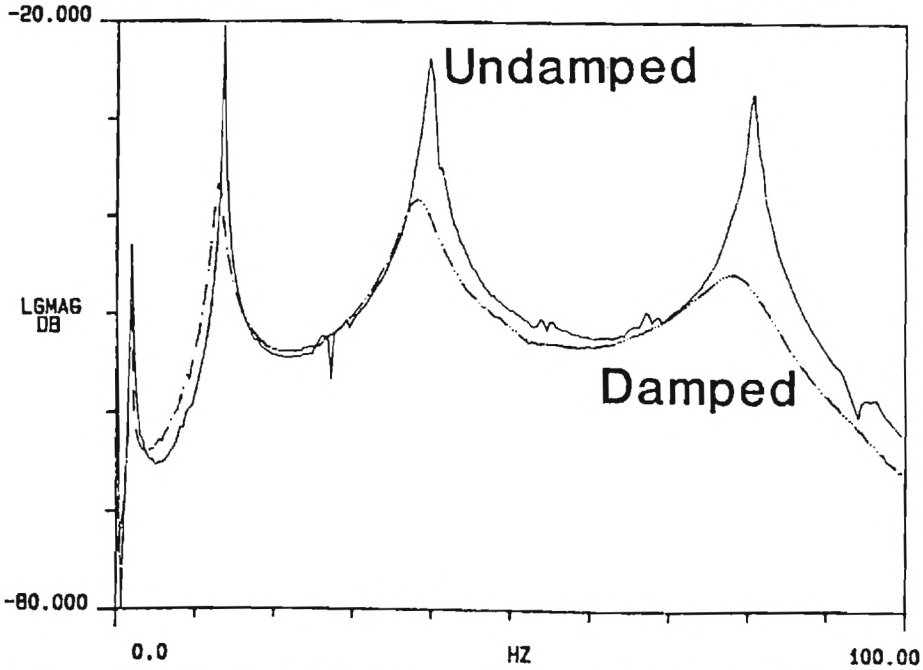

Figure 5. Frequency Response of Damped and Undamped Beams

Although the performance of the damping treatment falls short of the theoretical predictions, the constrained layer damping technique remains a lightweight, unobstructive, inexpensive and highly effective means of reducing the vibrations of the higher modes. The treatment described adds approximately 0.024 inches to the thickness of the beam and 0.42 pounds per square foot of treated surface to its weight. In applications where very light weight is desired, treatments utilizing carbon fiber composites as the constraining layer material provide performance similar to steel but weigh only 0.094 lbs. per square foot of treated surface.

Experimental Results

The results of employing the active controller described in previous sections in connection with controlling a beam with no passive damping treatment are represented by the time response curves of figure 6. From these results the effectiveness of the modal feedback for settling the first mode of vibration is readily apparent. The second flexible mode's amplitude is too small to view in this plot however the effect of the active controller on this mode is evident from frequency response curves (figure 9). It was observed that

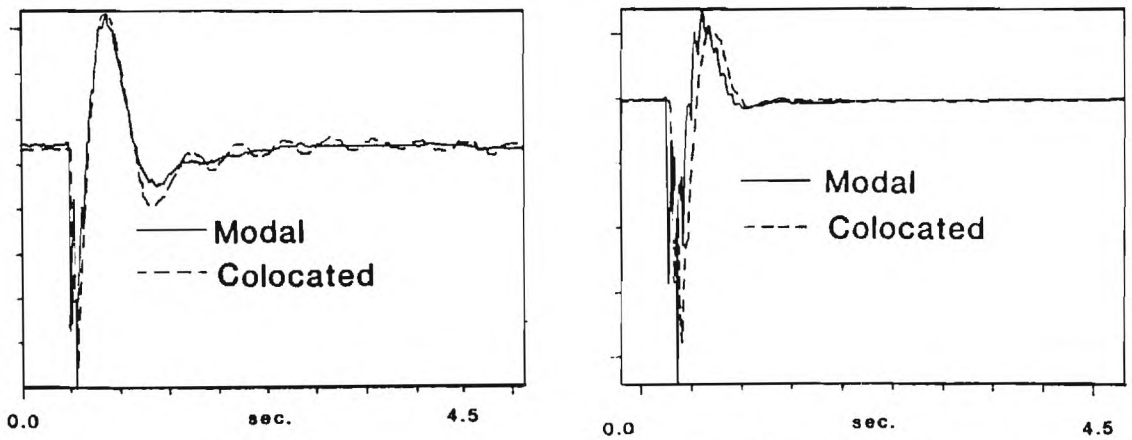

a)strain b)control torque

Figure 6. Time Response of Stable System Without Passive Damping

by increasing the gain on the rigid body mode, instability could be induced in the uncontrolled modes. This proved to be a good opportunity to demonstrate the stabilizing effect of the proposed passive damping method. Starting with the gain matrix used to generate the results of figure 6, the rigid body gains were progressively increased until instability was induced in the lower uncontrolled modes. In this condition the arm was initially quiescent, but the application of a step position command resulted in growing oscillations in the

uncontrolled flexible modes. Figure 7a represents the response of the untreated beam with rigid body position and rate feedback only. In this case instability occurs at about 22 Hz. which apparently corresponds to the system's third closed loop pole as shown in figure 9. When modal feedback is included (figure 7b) the instability occurs at 41 Hz. which corresponds with the fourth closed loop pole.

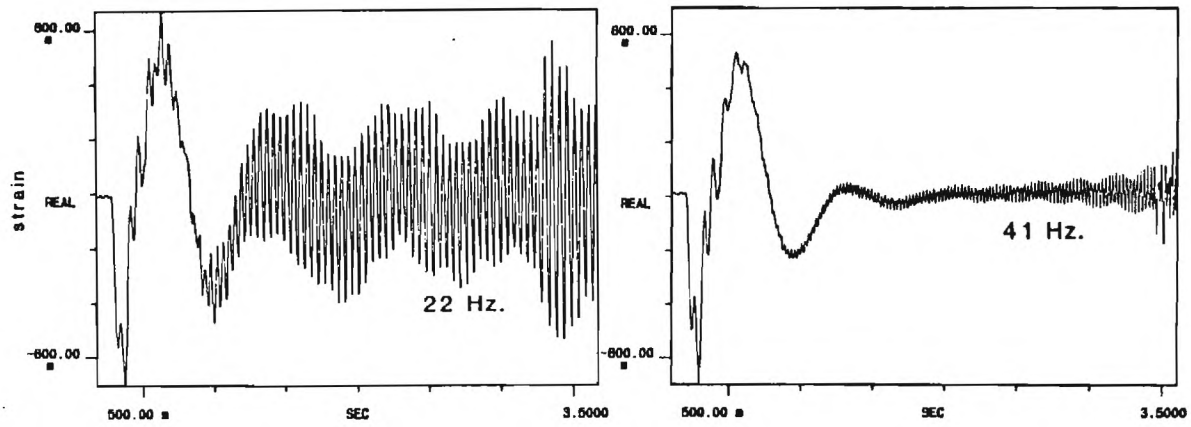

a)colocated feedback only b)full modal feedback

Figure 7. Time Response of the Unstable System Without Passive Damping

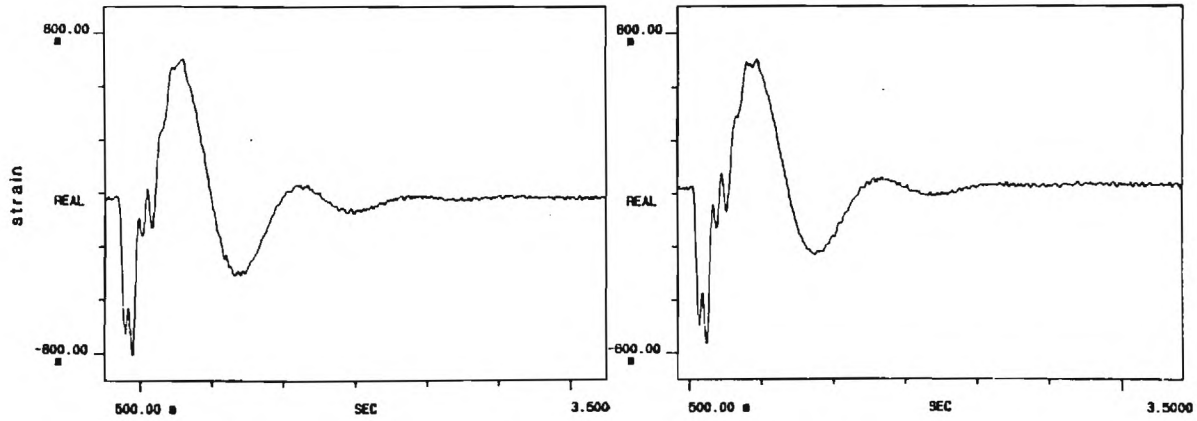

a)colocated feedback only b)full modal feedback

Figure 8. Time Response of the Same System (figure 7) Stabilized with Passive Damping

Without changing the gain matrix, the arm in the experimental system was replaced by an identical arm incorporating the constrained layer damping treatment. As shown in figures 8a and 8b the treatment has eliminated the instability. Figure 9 represents the transfer functions between input torque and payload acceleration for the open-loop system and

the colocated rate and position feedback system, both with passive damping. The frequency response of this system with full modal feedback is very similar to the colocated feedback case with the lower frequency poles slightly attenuated and broadened, as might be expected.

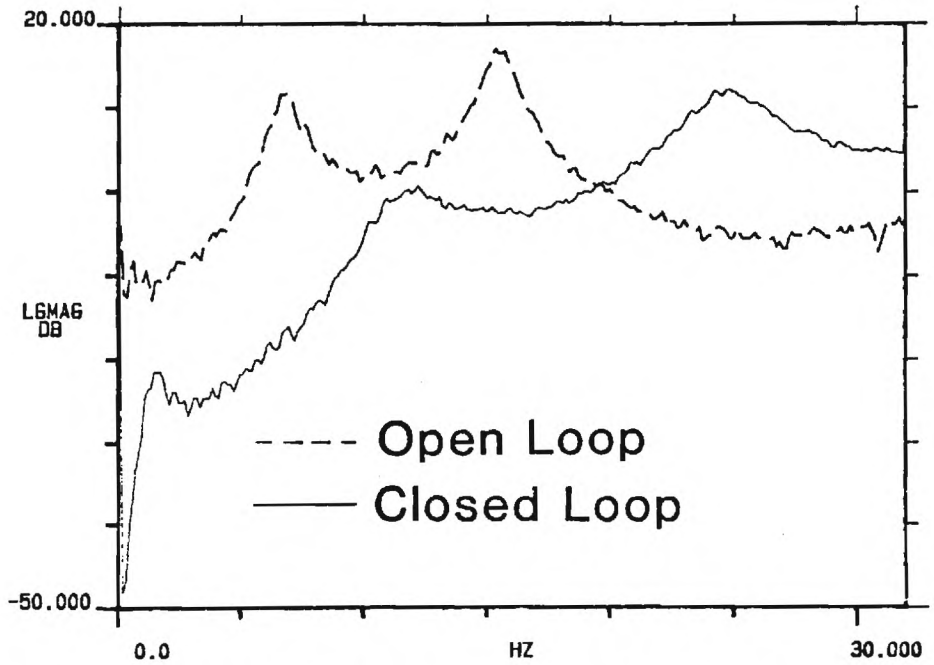

Figure 9. Frequency Response of Open Loop System and Closed Loop, Colocated Feedback System With Passive Damping

Conclusions

The control of the rigid body mode and the first two flexible modes of a lightweight arm has been demonstrated using a standard steady state linear quadratic regulator. Increasing the rigid body mode feedback gains was found to lead to instability in the low frequency uncontrolled modes. A constrained viscoelastic layer damping treatment, incorporating the notion of length optimized, sectioned constraining layers has been shown to provide an easy to apply and inexpensive method of stabilizing these uncontrolled modes.

In obtaining the initial results presented, the weighting matrices, degree of stability and the estimator dynamics were chosen rather arbitrarily. The authors acknowledge that the values selected for the initial tests may not be the most appropriate selections. The authors are presently working towards "tightening up" the control loop such that the full performance capabilities of the system may be realized.

Finally, it may be appropriate to note that utilizing the proposed hybrid control scheme in space may pose some problems not experienced in earthly applications insofar as the physical properties of viscoelastic materials are somewhat dependent upon temperature and apparently certain visco elastic materials are subject to degradation and outgassing [16] when exposed to the space environment. Nonetheless, the application of viscoelastics to damping problems in space is an area being actively pursued. Trudell, et.al. [16] suggest that the adoption of passive damping measures will play a crucial role in the successful solution of in large space structure vibration control problems.

Acknowledgments

This research partially funded by Georgia Tech's Material Handling Research Center (MHRC) and through NSF grant number MEA 8303539.

References

1. Book, W.J., "Analysis of Massless Elastic Chains With Servo Controlled Joints", Journal of Dynamic Systems, Measurement and Control, Vol.101, September 1979, pp.187-192

2. Book, W.J., "Recursive Lagrangian Dynamics of Flexible Manipulator Arms Via Transformation Matrices",Carnegie-Mellon University Robotics Institute Technical Report,CMU-RI-TR-8323, Dec. 1983

3. Truckenbrodt, A., "Modelling and Control of Flexible Manipulator Structures", 4th CISM-IFToMM Symp., Warszawa, 1981

4. Cannon, R.H. and Schmitz, E., "Initial Experiments on the End-Point Control of a Flexible One Link Robot", International Journal for Robotics Research, MIT Press, Cambridge Mass., Vol.3, No.3, Fall 1984

5. Cannon, R.H. and Schmitz, E., "Further Experiments on the End-Point Control of a Flexible One Link Robot", submitted for publication in Journal of Dynamic Systems, Measurement and Control, 1984

6. Sangveraphunsiri, V., The Optimal Control and Design of a Flexible Manipulator Arm, Ph.D Dissertation, Dept. of Mech. Eng., Georgia Inst. of Tech., 1984

7. Lane, J.S., Design and Control Principles for Flexible Arms Using Active and Passive Control, M.S. Thesis, Dept. of Mech. Eng., Georgia Inst. of Tech., Mar. 1984

8. V. Sangveraphunsiri, "The Optimal Control and Design of a Flexible Manipulator Arm", PhD Dissertation, Dept. of Mech. Eng., Georgia Institute of Technology, Atlanta, Ga.

9. T. Alberts, S. Dickerson, W. J. Book, "Modeling and Control of a Flexible Manipulator Arm: Volume I", MHRC-TR-85-06, Georgia Tech., Feb. 1985, Release Date July 1985

10. E. S. Armstrong, "ORACLS-A System for Linear-Quadratic-Gaussian Control Law Design", NASA TP-1106, April 1978.

11. Anderson, B. O. D., and Moore, J. B.: "Linear System Optimization With Prescribed Degree of Stability", Proc. IEEE, Vol. 116, No. 12, December 1969

12. Plunkett, R. and Lee, C.T., "Length Optimization for Constrained Viscoelastic Layer Damping", J. Accoust. Soc.of Amer., Vol.48, No.1, 1970, pp.150-161

13. Kerwin, E.M. Jr.,"Damping of Flexural Waves by a Constrained Viscoelastic Layer", J. Acoust. Soc. Amer., Vol.31, No.7, July 1959, pp.952-962

14. Nashif, A.D. and Nicholas, T.,"Vibration Control by Multiple-Layered Damping Treatment", Shock and Vib. Bull., No.41, Part 2, Dec. 1970, pp.121-131

15. Torvik, P., "The Analysis and Design of Constrained Layer Damping Treatments", Damping Applications for Vibration Control, Ed. by P. Torvik, ASME, N.Y., 1980

16. Trudell, R.W., Curley, R.C. and Rogers, L.C., Passive Damping in Large Space Structures, AIAA-80-0677, 13 pgs.

Published in Robotics and Manufacturing Automation
ASME, M. Donath & M. Leu, ed. 1985 pp 97-107

COMBINED APPROACHES TO LIGHTWEIGHT ARM UTILIZATION

Wayne J. Book, Stephen L. Dickerson
Gordon Hastings, Sabri Cetinkunt, and Thomas Alberts

School of Mechanical Engineering
Georgia Institute of Technology
Atlanta, GA 30332

ABSTRACT

In order to use lightweight arms the combination of a number of new approaches in arm design and control may be necessary. This paper describes four complimentary research efforts and how their results will work together. The bracing strategy is proposed first as one scenario of arm usage. It braces the arm against a passive structure to increase rigidity during fine motions of the end effector. Large motions of the arm require path and trajectory planning. Research on minimum time motions that avoid unnecessarily exciting vibrations is described next. The damping of those vibrations that are excited can be accomplished through a combination of active modal feedback control and passive damping. The enhancement of the damping characteristics of arm structures is described. This is important for stable feedback control with actuators and controllers with limited bandwidth. Analytical and experimental results for constrained layer damping are described in the context of the control problem. An active modal control has been implimented on a simple one link beam. As higher bandwidth is sought from this physical system deviations from the predicted results were observed. A refinement of the model to include anti-aliasing filter, sample-data, and amplifier effects explains the behavior as explained.

INTRODUCTION

The performance of manipulator arms must be defined in the context of the task the arm. Speed, accuracy, dexterity, weight, complexity, and reliability are some of the dimensions of the performance measure. One fundamental issue in the design of arms is the arm rigidity and the interaction of the control system with the dynamics of the arm its actuators and sensors. The limitations on controlling a flexible motion system certainly limit the performance of robot arms designed today. Research to understand and overcome these limitations is an important component of extending overall robot performance in several of the dimensions mentioned above.

This material is based in part on work supported by the National Science Foundation under grant MEA-8303539 and by the Georgia Tech Material Handling Research Center.

In an effort to make lighter robot arms feasible, an hence determine their desirability, severa complimentary approaches can be taken together. Thi paper describes research underway investigating thes approaches separately and in combination. The separat approaches are:

1. Feedback control of flexible state variables.

2. Enhanced passive damping of flexible modes.

3. Path and trajectory planning to constrain excitement of the flexible modes.

4. The bracing strategy to rigidize the base of th "wrist" for subsequent fine motions.

Notably absent from consideration are studies of mor rigid arm configurations and materials. It appear that the consequences of these approaches to designin lighter arms are better understood and somewha decoupled from the issues under study here. They coul be incorporated with the approaches under study in commercial design.

The present paper will briefly describe all fou approaches listed and the interactive roll they play The references listed will provide more detail on th individual approaches.

THE BRACING STRATEGY

The small, high bandwidth motions often required fo precision manipulation tasks are called fine motions The high bandwidth and accuracy needed for fine motions are principal reasons arm rigidity has been sought i existing designs. While more complex controls ca theoretically provide this behavior even in lightweigh arms, practical problems of disturbance rejection an plant uncertainty encourage us to seek alternatives The bracing strategy [1] achieves large configuratio changes (gross motion) with the lightweight arm followed by bracing the arm near its end against a passive bracing structure. This structure may b provided explicitly for that purpose or it may consis of the work piece itself. The rigidity of th lightweight arm is now supplemented with the rigidity of the bracing structure. Subsequent fine motions tak place at additional degrees of freedom past the bracing point. They have the benefit of a fairly rigid base and typically a shorter chain of links. The control o the fine motions might ignore the effects o flexibility for this reason.

The fine motions of the braced end effector are not the subject of this paper. Suffice it to say that the bracing action may compromise the accuracy of the end effector location relative to the arm base. Control of the fine motion based on sensing the end effector's position and perhaps force relative to the work piece becomes even more important with the bracing strategy.

In order to apply the bracing strategy one must obtain certain capabilities. First, the light weight arm must be moved rapidly over a large configuration change. Secondly, the arm must be brought into a controlled collision with the bracing structure which positions the end effector accurately enough and does not damage the arm or work piece. Finally, a bracing action must occur. This action may be the application of force normal to the bracing surface to achieve adequate friction to avoid slipping. Alternatively, it could be actuation of a suction or magnetic attachment.

Integration Of Design And Control Approaches

Using the bracing strategy as the scenario of arm operation, the role of the remaining three approaches first listed will now be established.

During a rapid configuration change the precise position of the arm is not usually of concern until the end of the path. As the end of the path is approached it is important to avoid collisions and to facilitate the second phase: the docking with the bracing structure. Both needs are served if the configuration change is completed with minimal excitation of the flexible degrees of freedom, though this must be completed in minimum time. The path of the arm in the work space must avoid obstacles which may dictate the general nature of the path. If we assume the arm deflection is small relative to the clearance allowed in the path, the joint histories alone are sufficient to guarantee no collisions. Our minimum time control research first assumes that the joint angles are prescribed as a function of an independent path variable, s. One is only allowed to alter the velocity along the path, ds/dt, to improve the arm performance. The second phase is to modify the joint histories to improve the performance at critical points in the motion.

At the end of a configuration change additional small arm motions are needed to accomplish bracing. It may be preferable not to use bracing in some applications, in which case these motions constitute the fine motions of the task. The system is not changing configuration so a linear controller is a good candidate for this application. It must have a relatively high bandwidth and must act to damp out the flexible modes. A linear optimal regulator has been studied analytically and experimentally for this purpose. Its behavior is enhanced if a passive damping treatment is applied to the arm structure. This is important in light of the practical limitations on the bandwidth of actuators and the speed of computers to actively control the high frequency modes of the flexible arm. The regulator and damping treatment are both described further in the

Force must be applied by the end of the flexible arm to achieve bracing with friction. The current regulator is not so sensitive that the application of force with the end of the arm degrades the behavior. Force control is important to maintain the braced condition, however, and will be the subject of future research.

TRAJECTORY PLANNING FOR FLEXIBLE MANIPULATORS

Today, most trajectory planning algorithms do not consider the dynamics of manipulators, rather constant and/or piece wise constant accelerations for the overall task are used and an overall maximum allowable speed is set. [2,3,4]. However, robotic manipulators are highly nonlinear dynamic systems, so it is expected that affordable accelerations and decelerations and maximum speeds will vary as a function of states. For the traditional schemes to work, the trajectory must be planned for the worst possible case. The capabilities of the system will be used only a small part of the time. Bobrow et.al. [5] first reported that for every point on the path there is an associated maximum allowable speed and maximum affordable acceleration and deceleration, and these values can drastically vary from one state to another. Incorporating the manipulator dynamics into the trajectory planning, the minimum time trajectories were found for different manipulator models [5,6] with limited actuator capabilities moving along pre-defined paths. Shin and McKay [7] solved the same problem independently.

Light-weight manipulators with the same actuator capabilities will be faster. The main problem associated with the light-weight structures is the flexible vibrations. Fig. 1 conceptually shows the performance improvement in terms of increased speed.

In this section we show the performance improvements due to

1. Use of light-weight arms

2. Incorporating the manipulator dynamics into trajectory planning level.

Flexible Manipulator Dynamic Model In Joint And Path Variables

A general dynamic modelling technique for flexible robotic manipulators was developed by Book using a recursive Lagrangian-assumed modes method. Homogeneous transformation matrices are used for kinematic relations of the system [8]. A two link flexible robotic manipulator is modelled using that technique. In the model no actuator dynamics are considered, rather the net torque input to the links is considered as the input variable. No friction at joints nor in the structural vibrations is considered. Flexibility of each link is approximated with one assumed mode for each link. The dynamic model of the manipulator may be expressed in general terms as:

$$[J]_{4\times 4}\ \underline{\ddot{q}} = \underline{f}(\underline{q},\underline{\dot{q}}) + \underline{Q} \qquad (1)$$

where

$\underline{q}^T$: $[\theta_1, \theta_2, \delta_1, \delta_2]$ Angles and modes

$\underline{Q}^T$: $[T_1, T_2, 0, 0]$ Net input torques

$[J]_{4x4}$: Generalized Inertia Matrix

$\underline{f}^T$: $[f_1, f_2, f_3, f_4]$ Nonlinear dynamic terms

The problem is to find the minimum time trajectories for a given manipulator with limited actuator capabilities moving along a fixed path, with state constraints (bounded flexible vibration constraint). Once the path to be moved along is specified

$$S=S(x,y) \qquad (2)$$

From inverse kinematic formulation, the corresponding joint angles can be found as

$$\underline{\theta}=\underline{\theta}(s) \quad , \quad \underline{\theta}^T=[\theta_1, \theta_2] \qquad (3)$$

Similarly, once the speed along the path is known $\dot{S}(S)$

$$\dot{\underline{\theta}}=\dot{\underline{\theta}}(s,\dot{s}) \qquad (4)$$

and

$$\ddot{\underline{\theta}}=\ddot{\underline{\theta}}(s,\dot{s},\ddot{s}) \qquad (5)$$

Knowing the relations (3),(4),(5) in analytical or numerical form, the manipulator dynamics in part can be expressed in path variables.

$$\begin{bmatrix} C_{11}(s,\underline{\delta}) \\ C_{12}(s,\underline{\delta}) \end{bmatrix}_{2x1} \ddot{s} = \begin{bmatrix} T_1 \\ T_2 \end{bmatrix} - \begin{bmatrix} C_{21}(s,\dot{s},\underline{\delta},\dot{\underline{\delta}},\vec{e}_t,\vec{e}_n,\rho) \\ C_{22}(s,\dot{s},\underline{\delta},\dot{\underline{\delta}},\vec{e}_t,\vec{e}_n,\rho) \end{bmatrix}_{-1} \qquad (6.a)$$

$$\begin{bmatrix} \ddot{\delta}_1 \\ \ddot{\delta}_2 \end{bmatrix} = \begin{bmatrix} J_{33} & J_{34} \\ J_{43} & J_{44} \end{bmatrix} \begin{bmatrix} f_3-g_3+h_1(s,\dot{s},\vec{e}_t) \\ f_4-g_4+h_2(s,\dot{s},\vec{e}_t) \end{bmatrix} \qquad (6.b)$$

$$f_i=f_i(s,\dot{s},\underline{\delta},\dot{\underline{\delta}}) \qquad (7)$$

$$g_i=g_i(s,\dot{s},\vec{e}_t,\vec{e}_n,\rho) \qquad (8)$$

$$J_{ij}=J_{ij}(s,\underline{\delta}) \qquad (9)$$

$\vec{e}_t, \vec{e}_n$: Unit Tangetial and normal Vectors along the path

ρ : Curvature of the path at any point.

Notice that flexible modes also affect the position of the end effector, but are not included in the definition of the path. This is mainly due to the fact that we do not have a "direct" control on the flexible vibrations and would like to keep them as small as possible in general.

Formulation Of The Near Minimum Time Trajectory Proble

Using the classical variational calculus principles the optimum control/programming problem may be formulated as following:

Minimize $$J = \int_0^{t_f} dt = \int_{so}^{s_f} \frac{ds}{\dot{s}}$$

$$\dot{s}(So) = \dot{So}$$

$$\dot{s}(s_f) = \dot{s}_f \text{ Initial and final states in path variables.}$$

Subject to :

System dynamics, Equations (6a) and (6b).

Actuator constraints

$$T_{i_{min}}(\underline{\theta},\dot{\underline{\theta}}) \le T_i \le T_{i_{max}}(\underline{\theta},\dot{\underline{\theta}}) \qquad i = 1,2 \qquad (2)$$

Dynamic inequality constraints on flexible modes

$$a_i(t) \le \delta_i(t) \le b_i(t) \qquad i=1,2 \qquad (3)$$

The constraints (3) naturally arise in flexible structures. If such a constraint is not imposed there is no guarantee on the accuracy of the end point along the path. At first the problem will be solved without considering these constraints. This solution will be used as a nominal solution for the trajectory modification step so that (3) are satisfied.

The solution method we use closely follows Bobrow et.al.'s method with some modifications for flexible manipulators. The solution of the above stated optimization problem follows: for any path S(x,y) with given $\dot{S}_o(S_o)$, $\dot{S}_f(S_f)$ to minimize J, $\dot{S}$ should be as large as possible while satisfying the system dynamics and actuator constraints. In order to do so at any state on the path one should use maximum acceleration or deceleration. Then, the problem is reduced to finding the maximum accelerations and decelerations associated with each state of interest. It can be seen from equation (6a) that for each $(S,\dot{S})$

$$\ddot{s}_d \le \ddot{s} \le \ddot{s}_a \qquad (4)$$

$$\ddot{s}_a = \min\left\{\ddot{s}_{ai}\right\} \qquad (5)$$

$$\ddot{s}_d = \max\left\{\ddot{s}_{di}\right\} \qquad (6)$$

Obviously, there may be some range of speeds associated with every point on the path that the system can no longer afford to satisfy all conditions (the $\dot{S}$ range that above inequality is violated.) Collection of these ranges defines the forbidden region on $(S,\dot{S})$ plane. The boundary between allowed and forbidden regions is constant for a given rigid manipulator for a given task. In the case of flexible manipulators, due to the coupling between equations (6.a) and (6.b) this

boundary

is also a function of flexible modes, not only $(S,\dot{S})$. So, depending on the time history of flexible modes and unpredictable disturbances the boundary will vary. This is not true in the rigid case where the true extremum can be found. At this point the problem is to find when to use maximum accelerations and maximum decelerations (i.e. to find the switching point(s)).

Finding switching points for flexible manipulators:

1. Integrate $\ddot{S}=\ddot{S}(x,y)$ from final state backward in time until it crosses the boundary into forbidden region or initial position, using maximum deceleration.

2. Integrate $\ddot{S}(x,y)$ Forward in time with maximum acceleration until the boundary is reached or the two curves crossed each other. If the two curve crossed each other before they enter forbidden region, then find that point. This is the last switching point and terminate the search. If not, then

3. Backup on the forward integrated curve and integrate forward with maximum deceleration until a the trajectory passes tangent to the boundary.

4. Then using the point as new starting point go to step two.

Notice that the last switching point is not the exact switching point because the flexible modes will not match at this point. That will cause one to miss the final state somewhat. Also, when searching for the switching points one has to move in a continuous manner in order to keep track of the flexible mode histories accurately. In that sense, the algorithm given at [5] has been modified for flexible robotic manipulators.

Simulation Results And Discussion

The two-link flexible manipulator model for task one (shown in Fig. 2a) was simulated for the two different cases in order to show the performance improvement achieved due to a light-weight system. In both cases actuators have same capabilities. It is found that weight reduction by a factor of 2 results in approximately a 60 % time improvement. This improvement, of course, slightly varies depending on the task. Joint actuator histories are shown in Fig. 4b and flexible mode responses are shown in Fig. 3b and 4c.

Task 2 (Shown in Fig. 2b) simulated for light-weight manipulator and results are shown Fig 5 a-c. The final trajectory is shown in heavy lines. One interesting point in this simulation is the fact that as soon as the manipulator end point enters the curvature the system must accelerate along the path in order to obey the constraints. In Fig. 5a the curve ab shows that right before the curvature the system is able to afford deceleration (aa' curve), but as end point enters the curvature, then the sudden appearance of a normal acceleration term in the dynamics of the system makes the difference.

ROLE OF PASSIVE DAMPING IN CONTROL OF FLEXIBL
MANIPULATORS

The central problem in achieving high-performanc
control of a flexible manipulator is the ability t
"damp" the oscillations of the structure. This is mad
difficult by the presence in the structural elements o
many (infinite) "modes" of vibration which ar
inherently lightly damped. Attempts to increase th
characteristic speed of motion must deal with thes
lightly damped structural modes. The greater th
characteristic speed desired the more modes that ar
significant. The modes become significant in two ways
1. the oscillations themselves prolong the settlin
time or equivalently give greater dynamic errors and 2
attempts to actively control some modes result i
instability of other modes, generally of hig
frequency.

Both of these phenomena are alleviated by increase
structural damping which can be achieved by usin
"lossy" materials or by applying a surface treatment t
the structural elements. Both have the effect o
increasing the damping ratio associated with th
various eigenvalues (or modes). It is interesting t
note that for a manipulator with a payload that i
heavy with respect to the weight of the manipulato
only the first structural modal frequency i
significantly changed by changes in payload weight
the higher frequency eigenvalues are essentially thos
of a beam that is pinned (for a point mass payload) a
the payload end. Attempts to stiffen the manipulato
by thickening the link walls do raise the frequency o
the first structural mode but do relatively little t
increase the frequency of higher modes. Thus if th
higher modes are significant in the sense described i
the preceeding paragraph, beefing up the structure ma
do little good. Thus one is left with either activel
controlling these higher frequency modes or increasin
the structural damping.

The following discussion deals with: first the amoun
of damping available from constrained, singlelayer
passive-damping treatments; second, the theoretica
effect of passive damping on the location of the close
loop eigenvalues; and third, some experimental result
of an attempt to control a beam with and without a
constrained layer passive damping treatment.

Characteristics of Constrained Layer Passive Damping

Constrained layer passive damping is achieved b
sandwiching a thin layer of viscoelastic materia
between the surface of the structure and a stiff (bu
naturally elastic) constraining layer. When th
structure deforms, shear induced plastic deformation i
imposed in the viscoelastic layer which provides th
desired mechanical damping effect. Kane [9] and others
[10,11,12,13] have shown that the constraining layer i
sectioned as shown in Figure 6 to achieve the greates
damping. The optimal section length does depend upo
the frequency of oscillation that is being damped
Fortunately, the damping effect is rather broad band
shown in Fig. 7 and can be optimized to maximize th
damping of those modes which are most troublesome i

the combined active/passive system; generally, the modes with frequencies just above the actively controlled mode(s). The amount of damping available can be increased by using a stiffer, hence heavier, constraining layer, but does not depend upon the thickness of the viscoelastic layer. Usually a very thin constraining layer would be used as dictated by fabrication requirements.

Effect of Passive Damping on the Location of Closed-Loop Eigenvalues

Lane[9] also studied the thoretical effect of passive damping on the location of closed-loop eigenvalues for a simple pinned-free beam that was actively controlled. In this control system, the torque at the driven end (pinned) was taken as a linear combination of four quantities, the angular velocity and position at the driven end and the linear velocity and position at the payload end. He considered the first 5 structural frequencies, i.e. twelfth order, in his beam model. Using root locus techniques the best he was able to do for the undamped case was for the dominant poles to be at -5./+/-5.2j with a gain margin, for closed-loop poles at -6.8+/-588j, of 0.6 db. Using passive damping the comparable result was dominant poles at -12.23+/-1.725j with gain margin for poles at -61.17+/-585j of 8.9 db. Thus passive damping allowed faster, less oscillatory motion with gain margins that insured system stability.

The particular beam analyzed was 6 feet long, of aluminum, weighing 3.3 pounds, and with a payload of 100 pounds. The passive damping treatment, assumed to use a graphite fiber composite and a 3M brand viscoelastic material, added 0.3 pounds.

Experimental Results With Passive Damping

Alberts and Hastings [14] conducted an experiment with a flexible beam with modal control of the rigid body plus the first two structural modes. Angular position and rate at the driven end plus the output of two strain gages along the length were used with a Luenberger observer to attempt to reconstruct six states of this system. Gains were adjusted to maximize performance, guided in part by a linear quadratic optimization analysis. As higher performance was sought, unmodelled dynamics resulted in the behavior shown in Figure 8b for the untreated beam. When the same beam with the damping treatment was used the results of Figure 9(b) were obtained, illustrating the substantial effect of the damping in the case of model inaccuracy. These Figures are plots of strain for a step response in position. The beam is four feet long, with a 3/4 inch by 3/16 inch cross-section. The first two clamped-free frequencies with the payload in place are 2.0 and 13.5 Hz. The setup is described further below.

EXPERIMENTS IN REAL TIME CONTROL OF A FLEXIBLE MANIPULATOR

Current investigation of the control of flexible arms has progressed to the experimental phase. Initial results concerning the performance of an LQR optimal controller has been reported in other publications [15],[16]. Continuing investigations striving to achieve faster, tighter control differ significantly from the results anticipated by the analytical work. Diagnosis of the causes of the discrepancies have been carried out on simpler collocated control experiments, and will be discussed in this section. The following section describes the apparatus utilized in carrying outcurrentexperiments.

Experimental Apparatus

The setup is a complete laboratory for examining the control of flexible arms with frequencies as high as 100 Hz. The system consists of a flexible arm with payload, DC torque motor with servo-amp, A/D and D/A conversion for measurement sampling, signal conditioning, and 16 bit computer system for implementation of control algorithms. The physical configuration of the flexible arm, torque motor, and sensors is represented in Fig.10. The desired end point position can be input from an external analog signal generator, or from internal trajectory generation software.

The beam is a four foot long aluminum beam with a 3/4" by 3/16" cross section oriented for preferred bending in the horizontal plane. The beam was found to have natural frequencies of 7.3, 17.5, and 42 Hz in the first three modes when mounted in the experimental apparatus with payload. The control computer is an IBM series one system complete with floating point hardware, 64 megabyte hard storage, 24 channels of A/D conversion, and 2 channels of D/A conversion. The floating point hardware can accommodate either 32 or 64 bit manipulations. A typical value for 32 bit floating point multiplication is 17 microseconds.

The state-space model developed for the system considers the torque motor to be an ideal torque source introducing no attenuation or phase to the input. The torque motor is a brush type, permanent magnet, DC torque motor, driven by a large servo-amp. The servo-amp has an internal gain of 35,000 and is configured to maintain the motor current at a constant proportion of the commanded torque from the D/A on its input. Commutation of the armature has not introduced significant noise in tests to date.

Analysis Of Experimental Discrepancies

Experimental observations have indicated significantly lower damping ratios, and generally less stability than predicted by analytical models. Collocated control is being utilized as a tool for resolving the discrepancies, initial investigations have been aimed at identifying physical phenomena, which were not included in the model. Collocated controllers have

been investigated [17],[18],[9] more than the complex optimal controllers, and provide a better basis for identifying phenomena residing in the experimental apparatus.

Figure 8a is a time record of the strain measured at the base of the flexible arm with joint angle and angular velocity gains that result in slowly growing amplitudes of oscillations. Fig. 9a records the strain for the same gains; however, passive damping has been added to the arm. Past analysis of collocated feedback controllers utilizing joint angle and joint angular velocity have not predicted this result, and instead predict stable results for all gain combinations with velocity feedback. Fig. 11 depicts a closed loop root locus based on this type of analysis for increasing gains. The velocity gain is adjusted to be .2 of the angle feedback gain.

This reduction in stability from prediction has also been observed in optimal regulators applied to the same system [14]. Although many directions could be pursued in resolving the discrepancies, the investigation focused on three major facets of the physical hardware that were not contained in earlier models:

1. Servo-amp, motor combination as a torque source.

2. Sampleand hold behavior of digital to analog converter.

3. Signal conditioning applied to tachometer to remove commutation noise.

These factors were investigated separately and cumulatively for their impact on the stability of the closed loop system via root locus analysis. A block diagram of the open loop transfer function from commanded torque to joint angular velocity is presented in Fig. 12a. Collocated feedback is depicted in the block diagram shown in Fig. 12b after reduction of the diagram in Fig. 12a to a transfer function bT(s).

The transfer function from torque applied at the base of the flexible arm to the joint angular velocity can be described as a sum of clamped-free flexible modes over a sum of pinned-free flexible modes plus a rigid body mode with an appropriate scaling factor. The zeros which are measurement dependent, input relationships are adequately described by clamped-free modes, for a system employing collocated feedback. The transfer function includes one additional flexible mode in both the numerator and denominator of the transfer function than were plotted out. A four-pole filter was employed on the tachometer for reduction of commutation noise, and a suitable transfer function was developed for Kv(s). A zero order hold was included on the input to the T(s) transfer function to account for the digital conversion hardware.

The resultant closed loop transfer function could then be examined by varying the gains, and monitoring the resultant pole variations. The torque behavior of servo-amp/motor combination was the least significant or the most ideal of the factors considered and was included in the development of Fig. 11. Sampling and holding the commanded torque did have a destabilizing effect; however, over the range of sampling periods effected in the experiment it alone did not explain the observed trends. The filter utilized on the tachometer was the most destabilizing influence as it drastically alters the departure angle from the open loop poles. The frequency of the filter poles are approximately 30 times higher than the flexible frequencies of interest, yet suprisingly still strongly affect the stability. The proximity of the flexible poles to the imaginary axis makes this extremely important in accurately describing the behavior.

Optimal controllers implemented to date have increased the gain margin [16], but design approaches have not attempted to account for the impact of the hardware used in implementing the controllers.

Fig. 13 shows the results of including both the sample/hold and signal conditioning in the transfer function. Rigid body modes are omitted for clarity. The cross over frequency for the case without passive damping is roughly 122 rad/sec which agrees very well with the observed instability depicted in Fig. 8a. Modal damping ratios without the addition of passive damping have been measured to fall between .005 and measured damping ratios to approximately .06. The dashed line is in accordance with the difference in stability observed in Fig. 9a, and adds credence to the analytical results.

CONCLUSIONS

The various approaches described above are complimentary but may not in all cases to be used together. Analytical and experimental approaches are both essential to progress on the control of lightweight arms. More complete experiments on multi-link, multi-joint arms are under development. The greatest advantage to the suite of techniques seems to be for lange arms where the motion sought naturally separates into gross and fine motions with high bandwidth. Hardware consistent with this situation is under design.

REFERENCES

1. Book, Wayne, "The Bracing Strategy for Robot Operation," Joint IFToMM-CISM Symposium on the Theory of Robots and Manipulators, Udine, Italy, June, 1984.

2. Kahn, M.E. and B. Roth, "The Near-Minimum Time Control of Open-Loop Articulated Kinematic Chains," Journal of Dynamic Systems, Measurement, and Control, ASME Trans., Vol.93, No.3, Sept 1971, pp 141-171.

3. Luh, J.Y.S. and C.S. Lin, "Optimum Path Planning For Mechanical Manipulators," Journal of Dyn. Syst. Measurement and Control, ASME Trans., Vol. 102, No. 2, June, 1981, pp142-151.

4. Luh, J.Y.S. and M.W. Walker, "Minimum-time Along the Path for a Mechanical Manipulator," Proc. of IEEE Conf. on Decision and Control, Dec. 1977 New Orleans,LA, pp 755-759.

5. Bobrow, J.E., S. Dubowsky, and J.S.Gibson, "On the Optimal Control of Robotic Manipulators with Actuator Constraints," Proc.of 1983 ACC, San Fransisco, CA June, 1983,pp 782-787.

6.Dubowsky, S., Z. Shiller, "Optimal Dynamic Trajectories For Robotic Manipulators," Fifth CISMIFToMM Symposium On The Theory And Practice Of Robotic Manipulators, June 26-29, 1984, Udine, Italy, pp96-103.

7. Shin, K.G. and M.D. McKay "Minimum-Time Control Of Robotic Manipulators With Geometric Path Constraints," IEEE Trans. on Automatic Control, Vol AC-30 No.6, June 1985, pp 531-541.

8. Book, W.J. "Recursive Lagrangian Dynamics of Flexible Manipulators," The International Journal of Robotics Research, MIT Press, v.3 n.3, pp. 87-101, Fall, 1984.

9. Lane, J.S., "Design and Control Principles for Flexible Arms Using Active and Passive Control," M.S. Thesis, Dept. of Mechanical Engr., Georgia Institute of Technology, 1984.

10. Plunket, R. and C.T. Lee, "Length Optimization for constrained Viscoelastic Layer Damping," J. Accoust. Soc. of Amer., Vol. 48, No. 1, 1970, pp 150-161.

11. Kerwin, E.M. Jr., "Damping of Flexural Waves by a Constrained Viscoelastic Layer," J. Accoust. Soc. Amer., V. 31, N. 7, July, 1959, pp. 952-962.

12. Nashif, A.D. and T. Nicholas, "Vibration Control by Multiple-Layered Damping Treatment," Shock and Vib. Bull., N. 41, Part 2, Dec. 1970, pp 121-131.

13. Torvik, P., "The Analysis and Design of Constrained Layer Damping Treatments,"Damping Applications for Vibration Control, P. Torvik, Ed., ASME, NY, 1980.

14. Alberts, Thomas, G. Hastings, W. Book, and S. Dickerson, "Experiments in Optimal Control of a Flexible Arm with Passive Damping," Fifth VPI&SU/AIAA Symposium on Dynamics & Control of Large Structures, Blacksburg, VA, June 12, 1985.

15. G. Hastings and W. Book, "Experiments in the Control of a Flexible Robot Arm," ROBOTS 9 Exposition & Conference, Detroit, MI, June 2, 1985.

16. G. Hastings and W. Book, "Experiments in the Optimal Control of a Flexible Manipulator," Proceedings of the 1985 American Control Conference, July, 1985.

17. W. Book, "Modelling, Design and Control of Flexible Manipulator Arms," Ph.D. Dissertation, Dept. of M.E., M.I.T., April, 1974.

18. G. Martin, "On the Control of Flexible Mechanical Systems," Ph.D. Thesis, Stanford U., 1978.

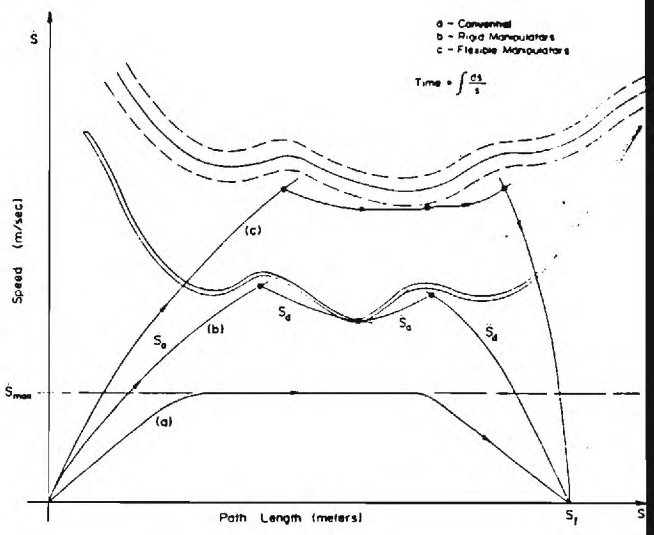

Fig. 1 Three different trajectory plans.

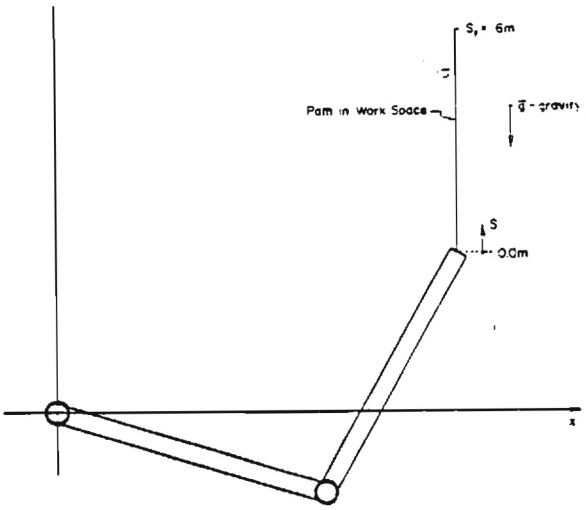

Fig. 2a Task 1 in (x,y) plane.

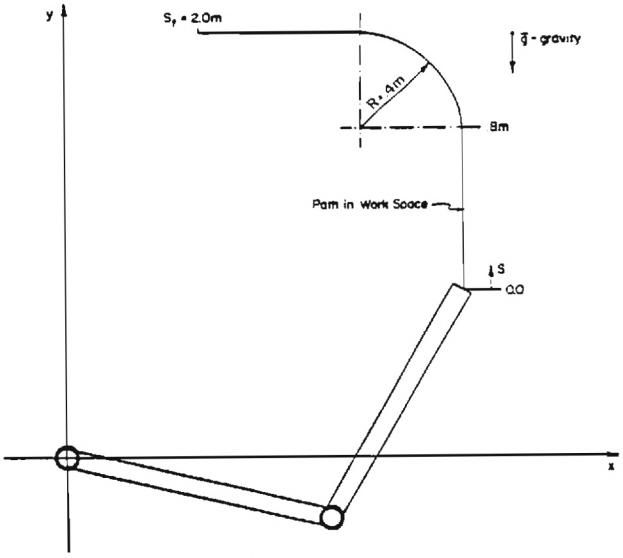

Fig. 2b Task 2 in (x,y) plane.

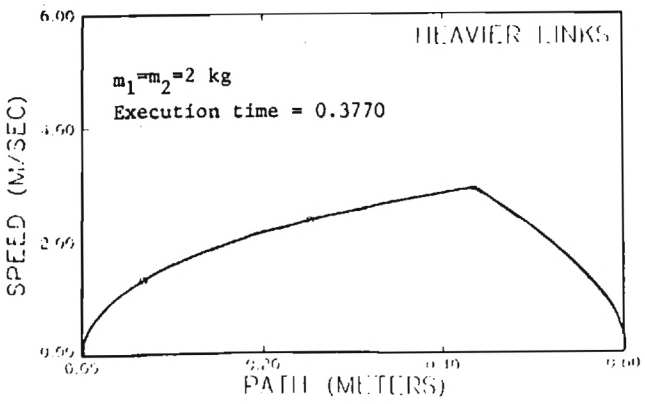

Fig. 3a Trajectory in (s,s) plane for Task 1 (heavy links).

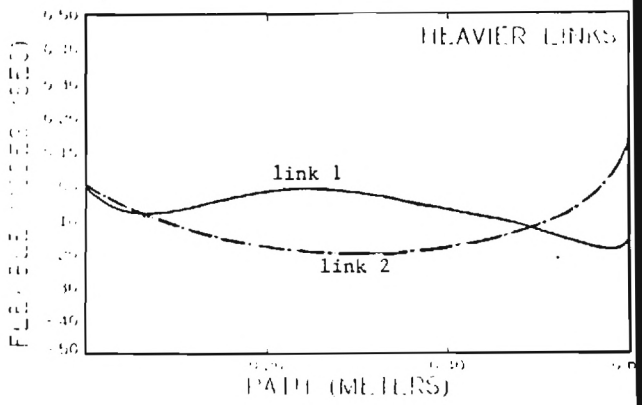

Fig. 3b Flexible modes for Task 1.

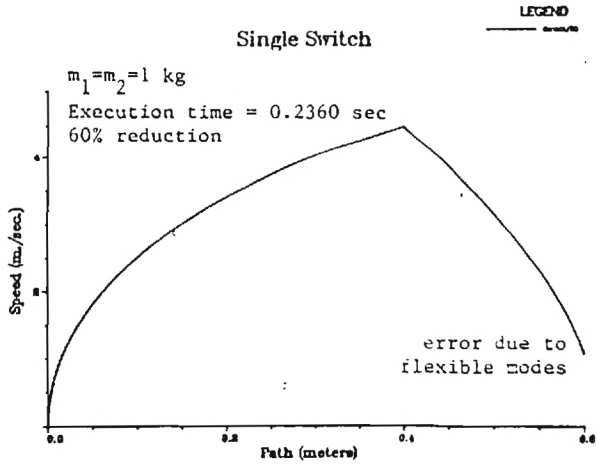

Fig. 4a Trajectory in (s,s) plane for Task 1 (light links)

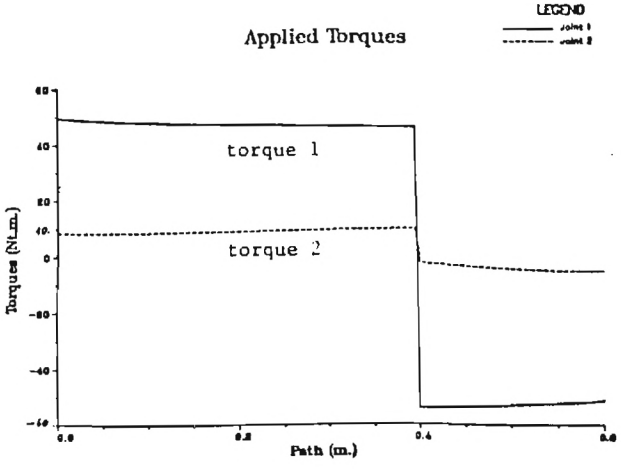

Fig. 4b Actuator torque histories for Task 1.

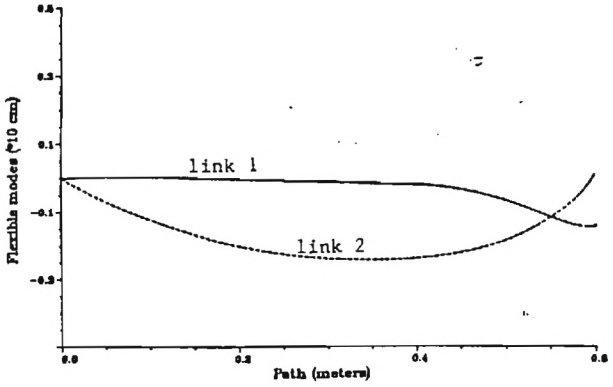

Fig. 4c Flexible modes for Task 1 (light links).

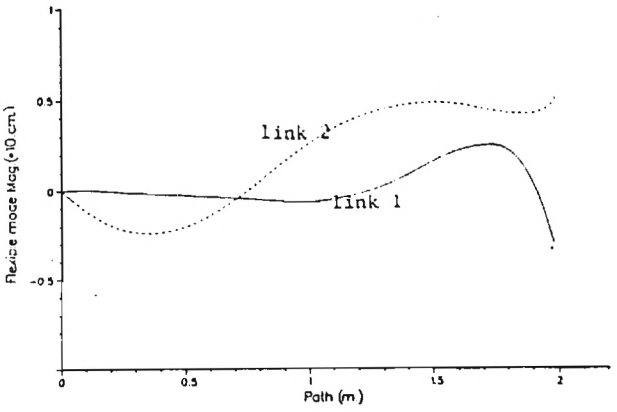

Fig. 5c Flexible modes for Task 2.

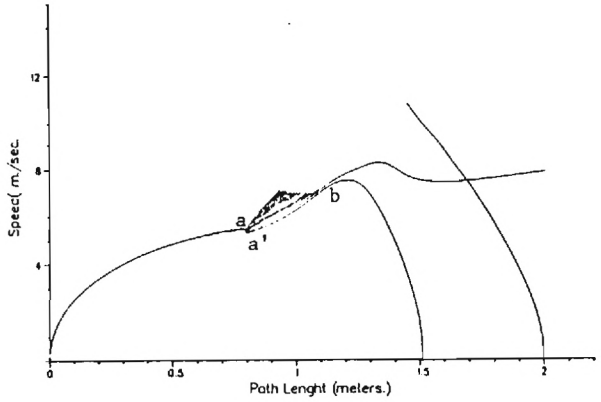

Fig. 5a Finding the switching points for Task 2.

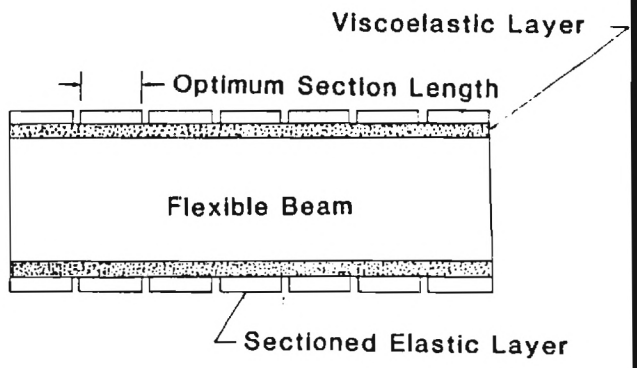

Fig. 6 Length optimized constraining layer.

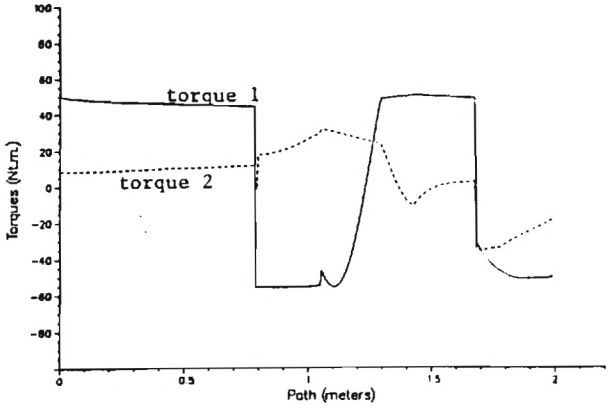

Fig. 5b Torque histories for Task 2.

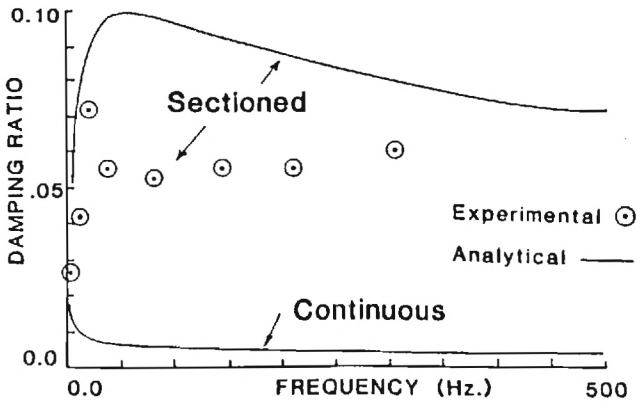

Fig. 7 Comparison of sectioned and continuous constraining layer treatments.

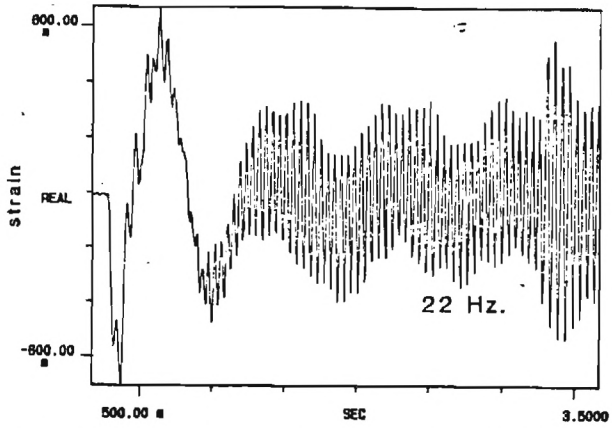

Fig. 8a Unstable system with colocated feedback only without passive damping.

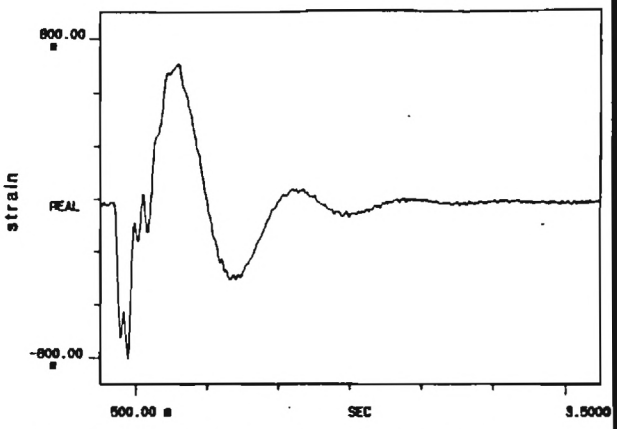

Fig. 9a System stabilized by addition of passive damping, colocated feedback only.

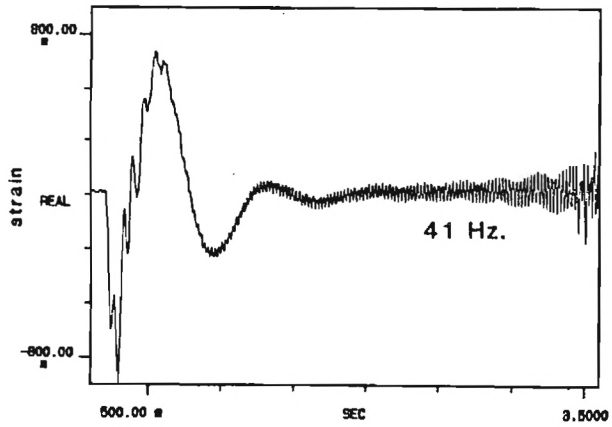

Fig. 8b Unstable system with modal feedback without passive damping.

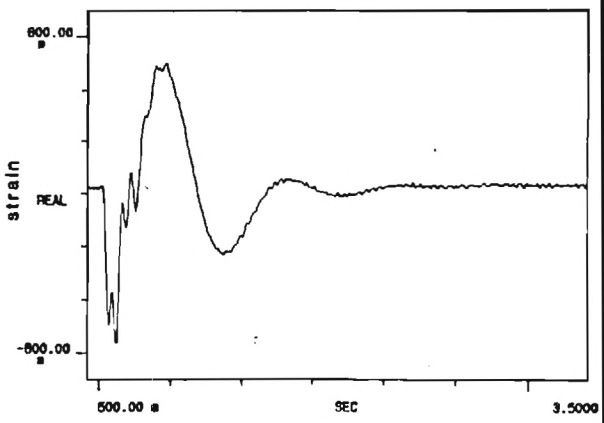

Fig. 9b System stabilized by addition of passive damping with modal feedback.

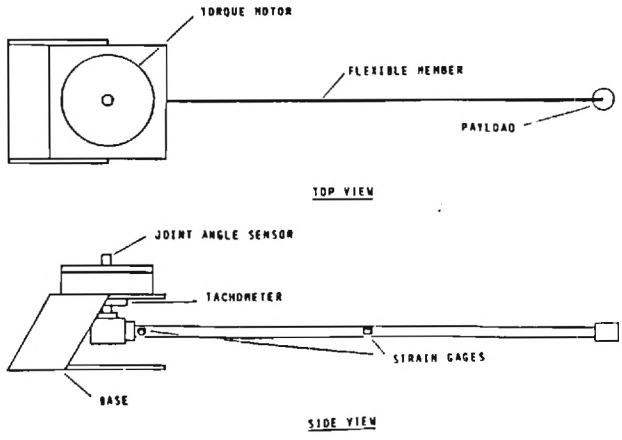

Fig. 10 Experimental one link arm.

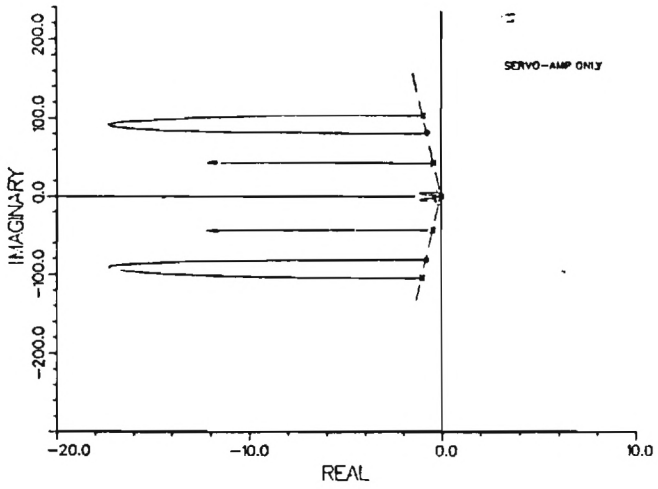

Fig. 11 Root locus for transfer function with servo-amp only.

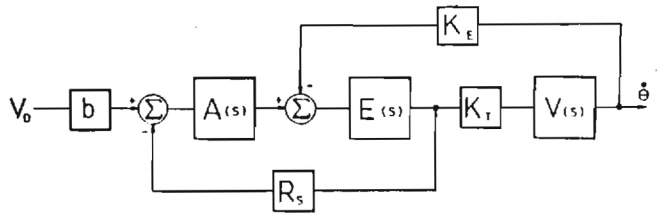

Fig. 12a Open loop block diagram. Symbols are:

A(s)	Amplifier transfer function, 35,000/s, v/v
E(s)	Motor electrical transfer function, 1/(Ls+R), amp/volt
V(s)	Torque to joint velocity transfer function, rad/sec-in-lb
K_e	Motor back emf constant, volt-sec/rad
K_t	Motor torque constant, in-lb/amp
$K_v(s)$	Velocity feedback transfer function, v-sec/rad
K_p	Joint angle feedback gain, volt/rad
b	Input gain, volt/volt
V_d	Desired torque voltage
R_s	Current sense resistor
T(s)	Open loop transfer function

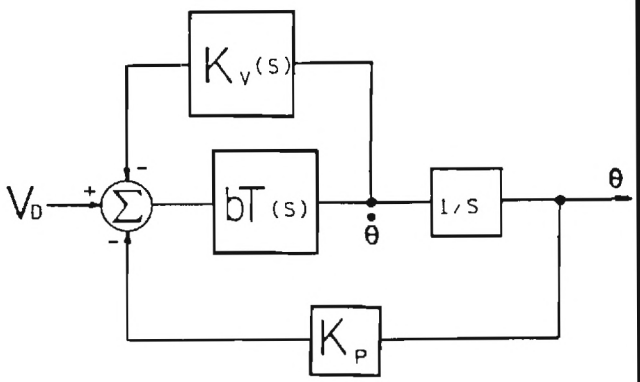

Fig. 12b Block diagram, colocated feedback.

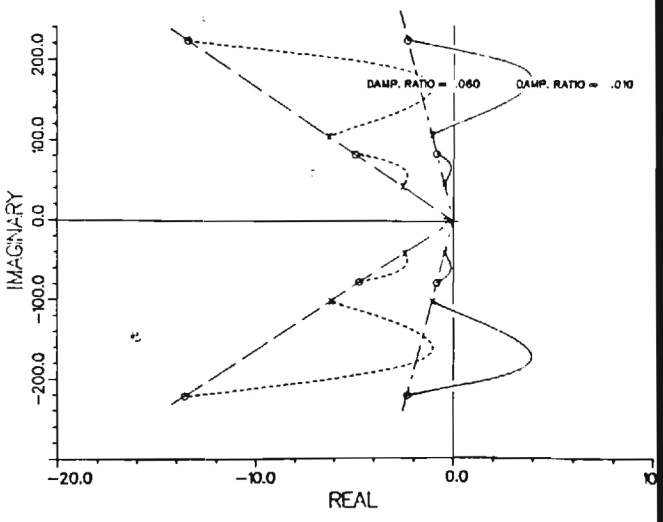

Fig. 13 Root locus for transfer function with filter, sampling, and servo-amp.

(Presented at the 1985 IEEE Conference on Decision and Control
Fort Lauderdale, FL.
December 11-13, 1985)

NEAR OPTIMUM CONTROL OF FLEXIBLE ROBOT ARMS ON FIXED PATHS

Wayne J. Book
Sabri Cetinkunt

George W. Woodruff
School of Mechanical Engineering
Georgia Institute of Technology
Atlanta, GA 30332

ABSTRACT

This paper presents the analysis and modification of near optimum trajectories for robotic manipulators moving along pre-defined paths. Modifications of trajectories are done such that the vibrations due to flexibility of arms and other components of the manipulator are minimized. Ultimately, the productivity of robotic manipulators depends on the speed of the task execution. Higher productivity requires higher speed of operation and in turn better control and trajectory generation algorithms. Today trajectory generation algorithms do not consider the dynamic characteristics of the manipulators. In order to utilize the available capability in the optimum manner the trajectory generation algorithms need to consider the dynamics of the manipulator, actuator constraints, nature of the task, and flexibility of arms and compliance of the joint connections.

In the search for an optimal trajectory that will meet all of the above requirements while optimizing some criterion, some simplifying assumptions have to be made and/or some of the requirements have to be kept out of the formulation so that the defined problem can be solved or some feasible solutions obtained. Once the simplified problem is solved, one may consider modifying the original solution in such a way that the excluded requirements are also satisfied to some extent.

In this paper the minimum time control solution of a two link flexible arm with actuator constraints is presented. We solved the minimum time problem with no constraints on the flexible modes and show the time improvement due to the use of light-weight arms. The objective is to modify the trajectory, such that flexible vibrations are bounded while changing the solution from the previous one as little as possible. Practical ways of trajectory modifications for flexible arms are discussed.

I. INTRODUCTION

Today, most trajectory planning algorithms do not consider the dynamics of the manipulators, rather constant and/or piece wise constant accelerations for the overall task are used and an overall maximum allowable speed is set [5,6,7]. However, robotic manipulators are highly nonlinear dynamic systems, so it is expected that affordable accelerations and maximum speeds will vary as a function of states. For the traditional schemes to work, the trajectory must be planned for the worst possible case. The capabilities of the system will be used only a small part of the time. Bobrow et.al. [1] first reported that for every point on any path, there is an associated maximum allowable speed and maximum affordable acceleration and deceleration for every speed in the affordable range, and these values can drastically vary from one state to another. Incorporating the manipulator dynamics into the trajectory planning level, they found the minimum time trajectories for different manipulator models [1,2] with limited actuator capabilities moving along pre-defined paths. Shin and McKay [3] solved the same problem independently.

Light-weight manipulators with the same actuator capabilities will be faster. The main problem associated with the light-weight structures is the flexible vibrations. Fig. 1 conceptually shows the performance improvement in terms of increased speed and faster task executions.

In this paper we show the performance improvements due to:

1. use of light-weight arms
2. incorporating the manipulator dynamics into the trajectory planning level
3. discuss flexible vibrations during a near minimum time trajectory execution and considerations of path modifications such that flexible vibrations will be bounded. This problem is similar in nature to the one raised by Hollerbach [8] and Kiriazov et. al [9].

II. FLEXIBLE MANIPULATOR DYNAMIC MODEL IN JOINT AND PATH VARIABLES

A general dynamic modelling technique for flexible robotic manipulators was developed by Book using a recursive Lagrangian-assumed modes method. Homogeneous transformation matrices are used for kinematic relations of the system [4]. A two link flexible robotic manipulator is modelled using that technique (Fig. 2). In the model no actuator dynamics is considered, rather the net torque input to the links is considered as the input variable. No friction at joints nor in the structural vibrations are explicitly considered. Flexibility of each link is approximated with one assumed mode for each link. The dynamic model of the manipulator may be expressed in general terms as :

$$[J]_{4x4}\ \underline{\ddot{q}} = \underline{f}(\underline{q},\underline{\dot{q}}) + \underline{Q} \qquad (2\text{-}1)$$

where

$\underline{q}^T$: $[\theta_1, \theta_2, \delta_1, \delta_2]$ Joint angles and flexible mode time variables

$\underline{Q}^T$: $[T_1, T_2, 0, 0]$ Net input torques

This material is based in part on work supported by the National Science Foundation under grant MEA-8303539

$[J]_{4x4}$: Generalized Inertia Matrix symmetric, pos. definite.

$\underline{f}^T: [f_1, f_2, f_3, f_4]$ Nonlinear dynamic terms including centrifugal, gravitational, effective spring and Coriolis forces.

The problem is to find the minimum time trajectories for a given manipulator with limited actuator capabilities moving along a fixed path, with state constraints (bounded flexible vibration constraints). Once the path to be moved along is specified as a combination of Cartesian variables (x and y for the 2 d.o.f. case), distance along the path S can be specified as

$$S=S(x,y) \quad . \tag{2-2}$$

From the inverse kinematic formulation, the corresponding joint angles for a rigid arm of the same dimensions can be found as

$$\underline{\theta}=\underline{\theta}(s) \quad , \quad \underline{\theta}^T=[\theta_1,\theta_2] \tag{2-3}$$

Similarly, once the speed $\dot{S}(S)$ along the path is known

$$\dot{\underline{\theta}}=\dot{\underline{\theta}}(s,\dot{s}) \tag{2-4}$$

and

$$\ddot{\underline{\theta}}=\ddot{\underline{\theta}}(s,\dot{s},\ddot{s}) \tag{2-5}$$

Knowing the relations (2-3)-(2-5) in analytical or numerical form, the manipulator dynamics in part can be expressed in path variables under the assumption that somehow the joint relationships specified in (2-3)-(2-5) will be maintained. These joint variables specify the torques and flexible states as follows

$$\begin{bmatrix} C_{11}(s,\underline{\delta}) \\ C_{12}(s,\underline{\delta}) \end{bmatrix}_{2x1} \ddot{s} = \begin{bmatrix} T_1 \\ T_2 \end{bmatrix} - \begin{bmatrix} C_{21}(s,\dot{s},\underline{\delta},\dot{\underline{\delta}},\vec{e}_t,\vec{e}_n,\rho) \\ C_{22}(s,\dot{s},\underline{\delta},\dot{\underline{\delta}},\vec{e}_t,\vec{e}_n,\rho) \end{bmatrix} \text{a)}$$

$$\begin{bmatrix} \ddot{\delta}_1 \\ \ddot{\delta}_2 \end{bmatrix} = \begin{bmatrix} J_{33} & J_{34} \\ J_{43} & J_{44} \end{bmatrix}^{-1} \begin{bmatrix} f_3-g_3+h_1(s,\dot{s},\ddot{e}_t) \\ f_4-g_4+h_2(s,\dot{s},\ddot{e}_t) \end{bmatrix} \tag{2-6b}$$

where

$$f_i=f_i(s,\dot{s},\underline{\delta},\dot{\underline{\delta}}) \tag{2-7}$$

$$J_{ij}=J_{ij}(s,\underline{\delta}) \tag{2-8}$$

$$g_i=g_i(s,\dot{s},\vec{e}_t,\vec{e}_n,\rho) \tag{2-9}$$

$\vec{e}_t, \vec{e}_n$: Unit tangent and normal vectors along the path.

ρ : Curvature of the path at a point.

Note that once the path to be followed has been defined, the degrees of freedom of the rigid manipulator reduces to one, no matter how many joints it has. Then the manipulator dynamics can be expressed as a second order non-linear ordinary differential equation. If the flexiblitiy of links are included in the model but not in the definition of the path, as is the case here, there will be additional flexible dynamics coupled with each other and the rigid dynamics.

III. FORMULATION OF THE NEAR MINIMUM TIME TRAJECTORY PROBLEM FOR FLEXIBLE MANIPULATORS

Recall that

$$\frac{d..}{dt} \equiv \frac{d..}{ds}\cdot\frac{ds}{dt} = \dot{S}\,\frac{d..}{ds} = Z\,\frac{d..}{ds}$$

where $\dot{S}$ is the speed along the path can be varied as a function of S. That suggests that every variable can be expressed as function of independent variable S, distance along the path. Let $S(S)=Z(S)$ in all the following. Initial and final states along the path would normally be given, $Z_o(S_o)$ and $Z_f(S_f)$. The optimum trajectory problem may be stated, using the path variable S as the independent variable rather than time, as follows:

Optimality criterion:

$$\text{Minimize} \quad J = \int_0^{t_f} dt = \int_{so}^{s_f} \frac{ds}{\dot{s}} \tag{3-1}$$

Subject to initial and final states of the path variables:

$$Z(S_o)=Z_o \qquad Z(S_f)=Z_f$$

System dynamics, expressed in path variables:

$$C_{1i}(s,\underline{\delta}).Z.Z' = T_i(s,Z) - C_{2i}(s,Z,\underline{\delta}) \quad i=1,2$$

$$Z^2\begin{bmatrix} \delta_1'' \\ \delta_2'' \end{bmatrix} + Z.Z'\begin{bmatrix} \delta_1' \\ \delta_2' \end{bmatrix} = J^{-1}_{2x2}\begin{bmatrix} f_1(s,Z,\underline{\delta}) \\ f_2(s,Z,\underline{\delta}) \end{bmatrix} \tag{3-2}$$

Actuator constraints:

$$T_{i\,min.}(s,Z) \le T_i \le T_{i\,max.}(s,Z) \tag{3-3}$$

Dynamic inequality constraints on flexible modes:

$$a_i(s) \le \ddot{\delta}_i(s) \le b_i(s) \qquad i=1,2 \tag{3-4}$$

The constraints (3-4) naturally arise in flexible structures. If such a constraint is not imposed there is no guarantee on the accuracy of the end point along the path. Following the rationale expressed in the introduction, one would solve the problem without the constraint (3-4). The problem reduces to the one solved in [1],[2],[3].

The solution method we use closely follows Bobrow et.al.'s method with some modifications for flexible manipulators. The solution of the above stated optimization problem follows: for any path S(x,y,z) with given $Z(S_o), Z(S_f)$ to minimize J, Z should be as large as possible while satisfying the system dynamics and actuator constraints. In order to do so at any state on the path one should use maximum acceleration or deceleration. Then, the problem is reduced to finding the maximum accelerations and decelerations associated with each state of interest. It can be seen from equation (2-6a) that for each (S_i,Z_i)

$$\ddot{s}_d \le \ddot{s} \le \ddot{s}_a$$

$$\ddot{S}_a = \min \left\{ \ddot{S}_{ai} \right\} \qquad (3\text{-}5)$$

$$\ddot{S}_d = \max \left\{ \ddot{S}_{di} \right\}$$

There may be some range of speeds associated with every point on the path that system can no longer satisfy all conditions (the $\dot{Z}$ range that above inequality is violated). The collection of these ranges defines the forbidden region on (S,$\dot{Z}$) plane. The boundary between allowed and forbidden regions is constant for a given rigid manipulator for a given task. In the case of flexible manipulators, due to the coupling between equations (2-6a) and (2-6b) this boundary is also a function of flexible modes, not only (S, $\dot{Z}$). So, depending on the time history of the flexible modes and unpredictable disturbances the boundary will vary. This is not true in the rigid case where the true extreme can be found. At this point the problem is to find when to use maximum accelerations and when maximum decelerations (i.e. to find the switching point(s)).See Fig. 3a-3b.

Finding switching points for near optimal performance of flexible manipulators then proceeds as follows:

1. Integrate $\dot{S}=\dot{S}(x,y)$ from the final state backward in time until it crosses forbidden region or initial position, using maximum deceleration.

2. Integrate $\ddot{S}(x,y)$ forward in time from initial conditions $(S_0,\dot{Z}_0)$ with maximum acceleration until the boundary is reached or the two curves cross each other. If the two curves cross each other before they enter forbidden region, then find that point. This is the last switching point and terminates the search. If not, then

3. Backup on the last forward integrated curve and integrate forward with maximum deceleration until the trajectory intersects:

   a. the boundary of the forbidden region. If the intersection is not tangent within some tolerance, repeat 3.

   b. or the line $\dot{Z} = 0$. In this case the distance backed up in 3 was too great. Reduce the amount of backup and repeat 3.

4. Then using the tangent point as new starting point go to step two.

Notice that the last switching point is not the exact switching point, because the flexible modes will not match at this point. That will cause one to miss the final state somewhat. Also, when searching for the switching points one has to move in a continuous manner in order to keep track of the flexible mode histories accurately. In that sense, the algorithm given in [1] has been modified for flexible robotic manipulators.

IV. TRAJECTORY MODIFICATION AND FLEXIBLE MODES

Once the near optimal trajectory $\dot{Z}(S)$ of the previous problem is found, one may consider modifying the trajectory in such a way that the constraints on the flexible modes are satisfied too. For any modified $\dot{Z}(S)$ which is affordable by actuators the equation (3-2b) can be integrated forward using the initial conditions of flexible modes at the beginning of the task.

$$\underline{\delta}(s_0) = \underline{\delta}_0 \qquad (4\text{-}1)$$

In fact regardless of the affordability of any trajectory in (S,$\dot{Z}$) plane, the flexible mode history along the path can be found by an integration along that trajectory.

A number of practical trajectory modifications using the cubic spline functions have been tried by the authors. Trajectories are modified in a smoothing fashion so that abrupt changes of torques at the switching points are avoided, expecting that the modified trajectory will result in less excited flexible modes. To some extent that is true, but since the dynamics of the flexible modes are highly complicated and nonlinear, not only the torques but also the coupling between states are important, particularly in the case of a minimum time problem. The initial trajectory modifications have not resulted in a favorable dynamic behavior and may not be generalized for all paths, because the shape of the path is also part of the dynamics and this is not explicitly mapped in to (S,$\dot{Z}$) plane. Some simulation results are shown in Fig. 8 - 10.

The trajectory modification problem is currently being formulated as an optimum control problem with dynamic constraints. A generalized quasilinearization algorithm is applied iteratively starting with the unconstrained solution and iteratively approaching to the solution of the problem with dynamic constraints [10],[11],[12].

V. SIMULATION RESULTS AND DISCUSSION

The two-link flexible manipulator model for task one (shown in Fig. 4a) was simulated for the two different cases in order to show the performance improvement achieved due to a light-weight system. In both cases actuators have the same capabilities. It is found that weight reduction by a factor of 2 results in approximately 60 % time reduction (Fig. 5a and 6a). This improvement, of course, varies depending on the task. Joint actuator histories are shown in Fig. 5b-6c and flexible mode responses are shown in Fig. 5c-6d.

Task 2 (Shown in Fig. 4b) was simulated for light-weight manipulator and results are shown Fig 7 a-d. The final trajectory is shown in Fig. 7b. One interesting point in this simulation is the fact that as soon as the manipulator end point enters the curvature the system must accelerate along the path in order to obey the constraints. In Fig. 7a the curve ab shows that immediately before the curvature the system is able to decelerate (aa' curve), but as end point enters the curvature the sudden appearance of a normal acceleration term in the dynamics of the system appears and end of the manipulator has to accelerate in order to stay on the path. This indicates how sensitive a trajectory modification would be in this part of the trajectory. The other point in the case of flexible arms is that at the last switching point flexible modes are not same, since they have different histories. This will cause error in the final state reached. See Fig. 6a, 7a. The last switching point needs to be varied from the original result of the above algorithm.

VI. CONCLUSION AND FURTHER WORK

In this paper we showed ways to improve performance and productivity of Robotic manipulators with flexible arms. One way was to use light-weight structures and the other was to incorporate the dynamics of manipulators in to trajectory planning level and make optimum utilization of given manipulator. Some practical trajectory modifications are presented. The sensitivity of the trajectories on (S,Ż) plane is very high. Any small change in the slope may end up with quite different flexible mode history depending on the path and the speed along the path. The slope of the trajectory at the beginning of the task should be carefully modified if the execution time is of any interest, for small slopes where speed is small will take long execution time. Application of the method requires the manipulator dynamics, geometric path in work space, and actuator capabilities. Obviously as trajectory gets closer to the forbidden region boundary system capabilities are being used to the limits and any disturbance or uncertainty can easily put the system in to forbidden region and end of the manipulator will leave the desired path. This situation is more clear in the case of flexible robotic manipulators. While this analysis is nice in terms of knowing the maximum capabilities, in practice there will be some safety factor that will require to keep the trajectory away from the forbidden region boundary certain amount.

REFERENCES

1. Bobrow,J.E., Dubowsky,S., Gibson,J.S. "On the Optimal Control of Robotic Manipulators with Actuator Constraints" Proc. of 1983 ACC, San Fransisco, CA June 1983, pp 782-787.

2. Dubowsky,S., Shiller,Z. "Optimal Dynamic Trajectories For Robotic Manipulators" Fifth CISM-IFToMM Symposium on the Theory And Practice of Robotic Manipulators Preprints, June 26-29 1984, Udine, Italy ,pp 96-103.

3. Shin, K.G., McKay, M.D. "Minimum-Time Control Of Robotic Manipulators With Geometric Path Constraints" IEEE Trans. on Automatic Control, Vol AC-30 No.6, June 1985 pp 531-541.

4. Book, W.J. "Recursive Lagrangian Dynamics of Flexible Manipulators", The International Journal of Robotic Research, MIT Press, V.3,N.3 pp. 87-101, Fall, 1984.

5. Kahn, M.E., Roth, B. "The Near-Minimum Time Control of Open-loop Articulated Kinematic Chains" Journal of Dynamic Systems, Measurement, and Control. ASME Trans., Vol.93, No.3, Sept. 1971, pp 141-171.

6. Luh, J.Y.S., Lin, C.S. "Optimum Path Planning For Mechanical Manipulators", J. of Dynamic Systems, Measurement, and Control, ASME Trans., Vol.102, No.2, June 1981, pp 142-151.

7. Luh, J.Y.S., Walker, M.W., "Minimum-time Along the Path for a Mechanical Manipulator", Proc.of IEEE Conf. on Decision and Control, Dec. 1977, New Orleans, LA, pp 755-759.

8. Hollerbach, J.M. "Dynamic Scaling of Manipulator Trajectories" Proc. of ACC, June 1983, San Fransisco, CA.

9. Kiriazov, P., Marinov, P., "A Method for Time-Optimal Control of Dynamically Constrained Manipulators", Preprints of Fifth CISM-IFToMM Symposium On the Theory and Practice of Robots and Manipulators, 26-29 June 1984 , Udine, Italy.

10. McGill, R. "Optimal Control,Inequality State Constraints, and the Generalized Newton-Raphson Algorithm", Journal of SIAM, Ser. A, Vol. 3, No. 2, 1965, pp 291-298.

11. Mcgill, R., Kenneth, P. "Solution of Variational Problems by Means of a Generalized Newton-Raphson Operator", AIAA Journal, Vol. 2, No. 10, October 1964, pp 1761-1766.

12. Schley, C.H. Jr., Lee, I. "Optimal Control Computation by the Newton-Raphson Method and the Riccati Transformation", IEEE Transactions on Automatic Control, Vol. AC-12, No. 2, April 1967, pp 139-144.

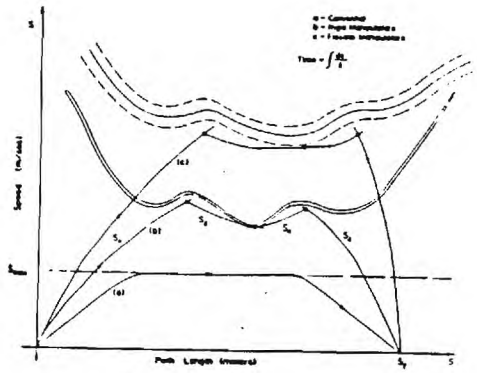

Fig.1 Different trajectory plans.

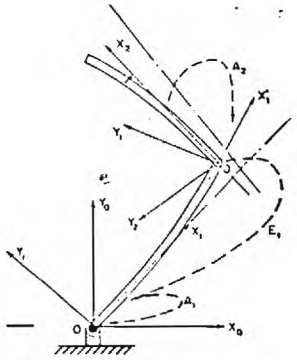

Fig.2 Manipulator Model.

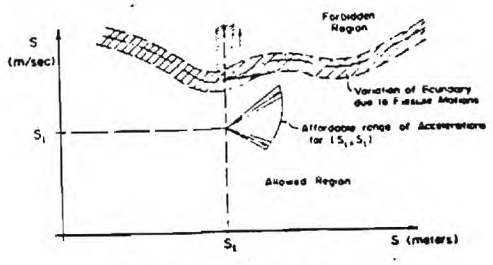

Fig. 3.a (S,Ṡ) Plane

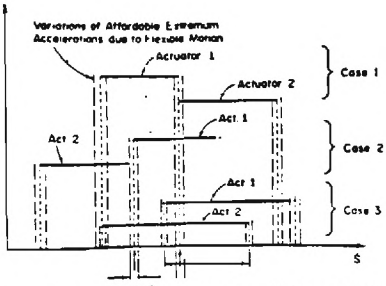

Fig. 3.b Different possible cases during a task.

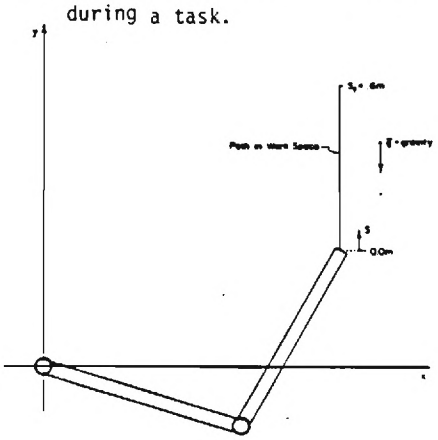

Fig. 4a. Task 1 in (x,y) plane.

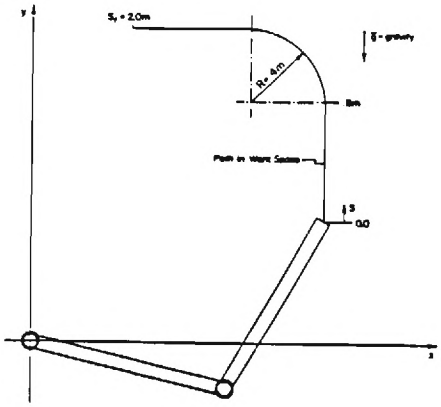

Fig. 4b Task 2 in (x,y) plane.

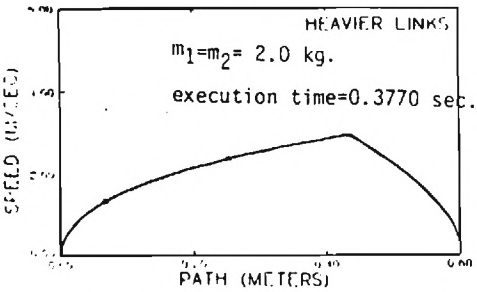

Fig. 5.a Trajectory for Path 1 of heavy links.

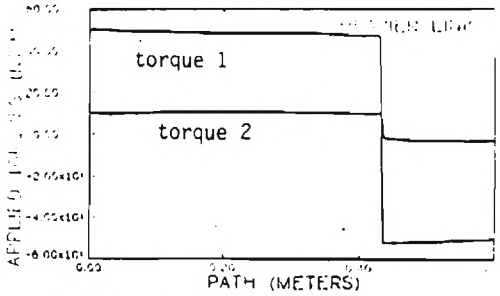

Fig. 5b. Torques along the path 1

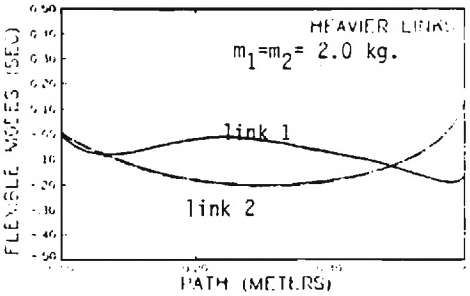

Fig. 5.c Flexible modes time variable

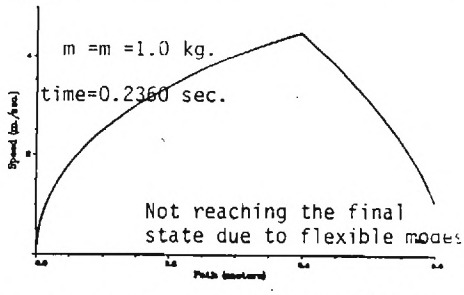

Fig. 6.a Trajectory of lightweight arm

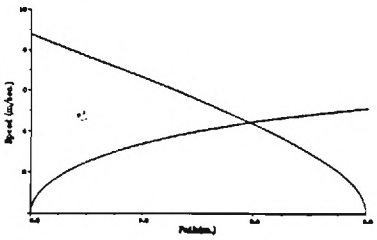

Fig. 6.b Finding the switching poin

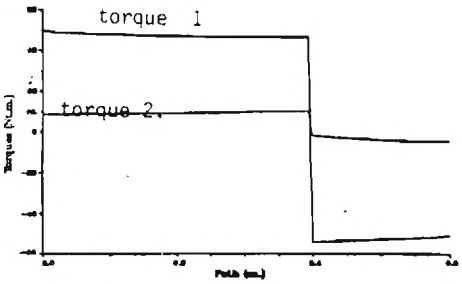

Fig. 6.c Torque histories of lightweig arms along path 1.

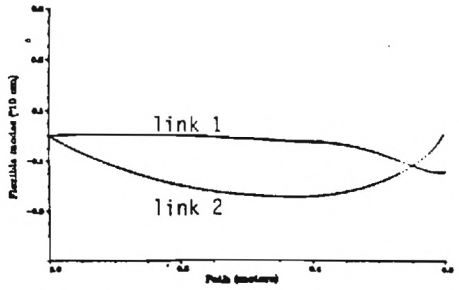

Fig. 6d. Flexible modes along path 1.

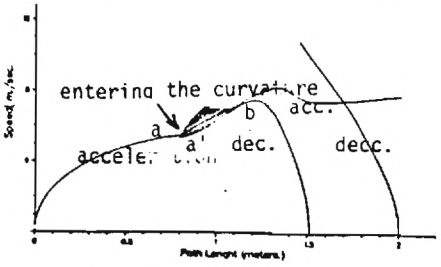

Fig. 7a. Finding the switching points for path 2.

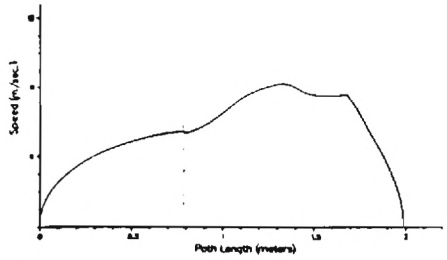

Fig. 7b. Trajectory for path 2.

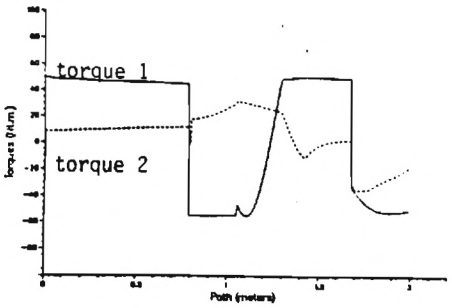

Fig. 7c. Torques along path 2.

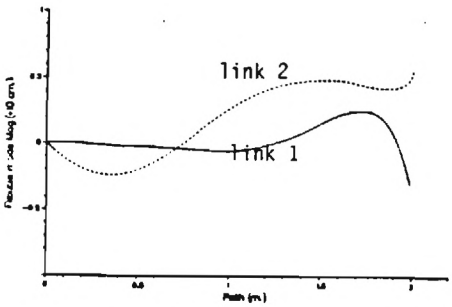

Fig. 7d. Flexible modes along path2.

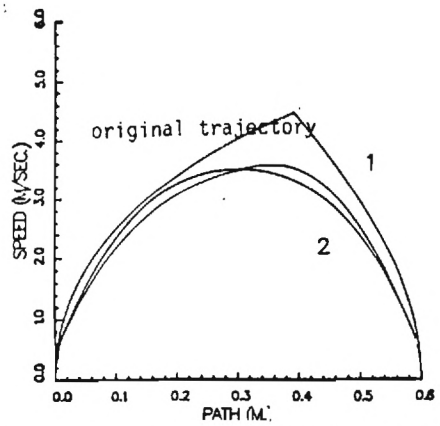

Fig. 8 Original and Modified Trajectories

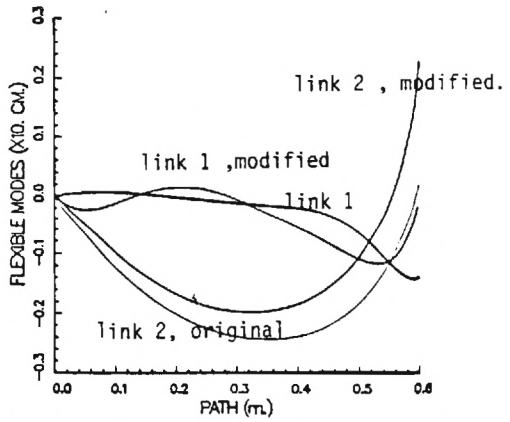

Fig. 9a. Flexible modes along original and modified trajectory 1.

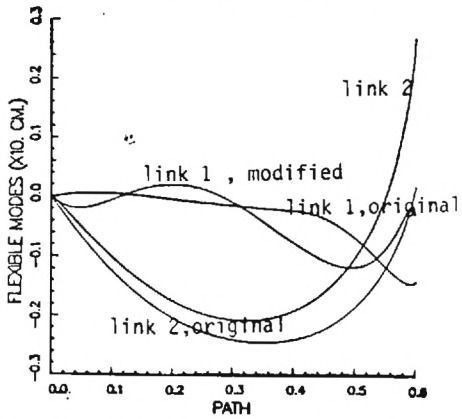

Fig. 9b. Flexible modes along original and modified trajectory 2.

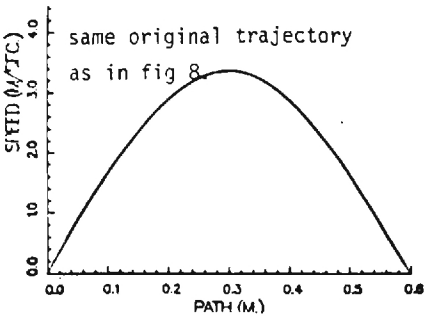

Fig. 10a. Modified trajectory 3.

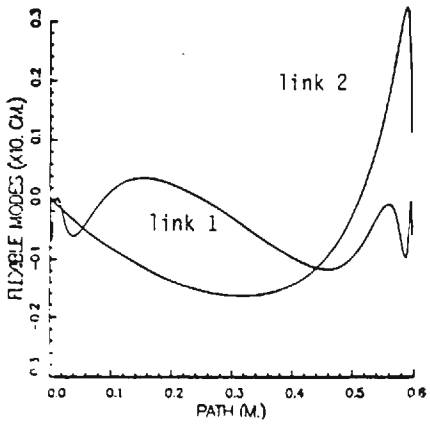

Fig. 10b. Flexible modes along modified trajectory 3.

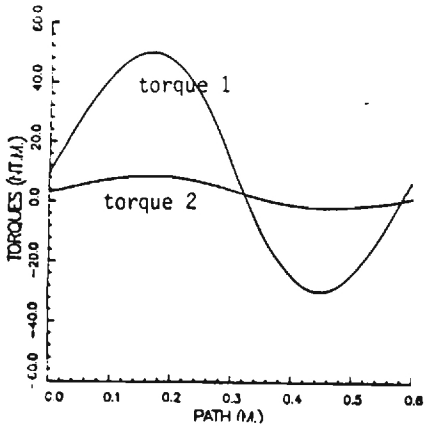

Fig. 10c. Torque histories along modified trajectory 3.

(Presented at the 1985 IEEE Conference on Decision and Control
Fort Lauderdale, FL.
December 11-13, 1985)

NEAR OPTIMUM CONTROL OF FLEXIBLE ROBOT ARMS ON FIXED PATHS

Wayne J. Book
Sabri Cetinkunt

George W. Woodruff
School of Mechanical Engineering
Georgia Institute of Technology
Atlanta, GA 30332

ABSTRACT

This paper presents the analysis and modification of near optimum trajectories for robotic manipulators moving along pre-defined paths. Modifications of trajectories are done such that the vibrations due to flexibility of arms and other components of the manipulator are minimized. Ultimately, the productivity of robotic manipulators depends on the speed of the task execution. Higher productivity requires higher speed of operation and in turn better control and trajectory generation algorithms. Today trajectory generation algorithms do not consider the dynamic characteristics of the manipulators. In order to utilize the available capability in the optimum manner the trajectory generation algorithms need to consider the dynamics of the manipulator, actuator constraints, nature of the task, and flexibility of arms and compliance of the joint connections.

In the search for an optimal trajectory that will meet all of the above requirements while optimizing some criterion, some simplifying assumptions have to be made and/or some of the requirements have to be kept out of the formulation so that the defined problem can be solved or some feasible solutions obtained. Once the simplified problem is solved, one may consider modifying the original solution in such a way that the excluded requirements are also satisfied to some extent.

In this paper the minimum time control solution of a two link flexible arm with actuator constraints is presented. We solved the minimum time problem with no constraints on the flexible modes and show the time improvement due to the use of light-weight arms. The objective is to modify the trajectory, such that flexible vibrations are bounded while changing the solution from the previous one as little as possible. Practical ways of trajectory modifications for flexible arms are discussed.

I. INTRODUCTION

Today, most trajectory planning algorithms do not consider the dynamics of the manipulators, rather constant and/or piece wise constant accelerations for the overall task are used and an overall maximum allowable speed is set [5,6,7]. However, robotic manipulators are highly nonlinear dynamic systems, so it is expected that affordable accelerations and maximum speeds will vary as a function of states. For the traditional schemes to work, the trajectory must be planned for the worst possible case. The capabilities of the system will be used only a small part of the time. Bobrow et.al. [1] first reported that for every point on any path, there is an associated maximum allowable speed and maximum affordable acceleration and deceleration for every speed in the affordable range, and these values can drastically vary from one state to another. Incorporating the manipulator dynamics into the trajectory planning level, they found the minimum time trajectories for different manipulator models [1,2] with limited actuator capabilities moving along pre-defined paths. Shin and McKay [3] solved the same problem independently.

Light-weight manipulators with the same actuator capabilities will be faster. The main problem associated with the light-weight structures is the flexible vibrations. Fig. 1 conceptually shows the performance improvement in terms of increased speed and faster task executions.

In this paper we show the performance improvements due to:

1. use of light-weight arms
2. incorporating the manipulator dynamics into the trajectory planning level
3. discuss flexible vibrations during a near minimum time trajectory execution and considerations of path modifications such that flexible vibrations will be bounded. This problem is similar in nature to the one raised by Hollerbach [8] and Kiriazov et. al [9].

II. FLEXIBLE MANIPULATOR DYNAMIC MODEL IN JOINT AND PATH VARIABLES

A general dynamic modelling technique for flexible robotic manipulators was developed by Book using a recursive Lagrangian-assumed modes method. Homogeneous transformation matrices are used for kinematic relations of the system [4]. A two link flexible robotic manipulator is modelled using that technique (Fig. 2). In the model no actuator dynamics is considered, rather the net torque input to the links is considered as the input variable. No friction at joints nor in the structural vibrations are explicitly considered. Flexibility of each link is approximated with one assumed mode for each link. The dynamic model of the manipulator may be expressed in general terms as :

$$[J]_{4\times 4}\ \underline{\ddot{q}} = \underline{f}(\underline{q},\underline{\dot{q}}) + \underline{Q} \qquad (2\text{-}1)$$

where

$\underline{q}^T$: $[\theta_1, \theta_2, \delta_1, \delta_2]$ Joint angles and flexible mode time variables

$\underline{Q}^T$: $[T_1, T_2, 0, 0]$ Net input torques

This material is based in part on work supported by the National Science Foundation under grant MEA-8303539

$[J]_{4x4}$: Generalized Inertia Matrix symmetric, pos. definite.

$\underline{f}^T$: $[f_1, f_2, f_3, f_4]$ Nonlinear dynamic terms including centrifugal, gravitational, effective spring and Coriolis forces.

The problem is to find the minimum time trajectories for a given manipulator with limited actuator capabilities moving along a fixed path, with state constraints (bounded flexible vibration constraints). Once the path to be moved along is specified as a combination of Cartesian variables (x and y for the 2 d.o.f. case), distance along the path S can be specified as

$$S=S(x,y) \quad . \tag{2-2}$$

From the inverse kinematic formulation, the corresponding joint angles for a rigid arm of the same dimensions can be found as

$$\underline{\theta}=\underline{\theta}(s) \quad , \quad \underline{\theta}^T=[\theta_1,\theta_2] \tag{2-3}$$

Similarly, once the speed $\dot{S}(S)$ along the path is known

$$\dot{\underline{\theta}}=\dot{\underline{\theta}}(s,\dot{s}) \tag{2-4}$$

and

$$\ddot{\underline{\theta}}=\ddot{\underline{\theta}}(s,\dot{s},\ddot{s}) \tag{2-5}$$

Knowing the relations (2-3)-(2-5) in analytical or numerical form, the manipulator dynamics in part can be expressed in path variables under the assumption that somehow the joint relationships specified in (2-3)-(2-5) will be maintained. These joint variables specify the torques and flexible states as follows

$$\begin{bmatrix} C_{11}(s,\underline{\delta}) \\ C_{12}(s,\underline{\delta}) \end{bmatrix}_{2x1} \ddot{s} = \begin{bmatrix} T_1 \\ T_2 \end{bmatrix} - \begin{bmatrix} C_{21}(s,\dot{s},\underline{\delta},\dot{\underline{\delta}},\vec{e}_t,\vec{e}_n,\rho) \\ C_{22}(s,\dot{s},\underline{\delta},\dot{\underline{\delta}},\vec{e}_t,\vec{e}_n,\rho) \end{bmatrix} \tag{2-6a}$$

$$\begin{bmatrix} \ddot{\delta}_1 \\ \ddot{\delta}_2 \end{bmatrix} = \begin{bmatrix} J_{33} & J_{34} \\ J_{43} & J_{44} \end{bmatrix}^{-1} \begin{bmatrix} f_3-g_3+h_1(s,\dot{s},\ddot{e}_t) \\ f_4-g_4+h_2(s,\dot{s},\ddot{e}_t) \end{bmatrix} \tag{2-6b}$$

where

$$f_i=f_i(s,\dot{s},\underline{\delta},\dot{\underline{\delta}}) \tag{2-7}$$

$$J_{ij}=J_{ij}(s,\underline{\delta}) \tag{2-8}$$

$$g_i=g_i(s,\dot{s},\vec{e}_t,\vec{e}_n,\rho) \tag{2-9}$$

$\vec{e}_t, \vec{e}_n$: Unit tangent and normal vectors along the path.

ρ : Curvature of the path at a point.

Note that once the path to be followed has been defined, the degrees of freedom of the rigid manipulator reduces to one, no matter how many joints it has. Then the manipulator dynamics can be expressed as a second order non-linear ordinary differential equation. If the flexiblitiy of links are included in the model but not in the definition of the path, as is the case here, there will be additional flexible dynamics coupled with each other and the rigid dynamics.

III. FORMULATION OF THE NEAR MINIMUM TIME TRAJECTORY PROBLEM FOR FLEXIBLE MANIPULATORS

Recall that

$$\frac{d..}{dt} \equiv \frac{d..}{ds}\frac{ds}{dt} = \dot{S}\frac{d..}{ds} = Z\frac{d..}{ds}$$

where $\dot{S}$ is the speed along the path can be varied as a function of S. That suggests that every variable can be expressed as function of independent variable S, distance along the path. Let $S(S)=Z(S)$ in all the following. Initial and final states along the path would normally be given, $Z_0(S_0)$ and $Z_f(S_f)$. The optimum trajectory problem may be stated, using the path variable S as the independent variable rather than time, as follows:

Optimality criterion:

$$\text{Minimize} \quad J = \int_0^{t_f} dt = \int_{so}^{s_f} \frac{ds}{\dot{s}} \tag{3-1}$$

Subject to initial and final states of the path variables:

$$Z(S_0)=Z_0 \qquad Z(S_f)=Z_f$$

System dynamics, expressed in path variables:

$$C_{1i}(s,\underline{\delta}).Z.Z' = T_i(s,Z) - C_{2i}(s,Z,\underline{\delta}) \quad i=1,2$$

$$Z^2\begin{bmatrix} \delta_1'' \\ \delta_2'' \end{bmatrix} + Z.Z'.\begin{bmatrix} \delta_1' \\ \delta_2' \end{bmatrix} = J^{-1}_{2x2}\begin{bmatrix} f_1(s,Z,\underline{\delta}) \\ f_2(s,Z,\underline{\delta}) \end{bmatrix} \tag{3-2}$$

Actuator constraints:

$$T_{i\,min.}(s,Z) \le T_i \le T_{i\,max.}(s,Z) \tag{3-3}$$

Dynamic inequality constraints on flexible modes:

$$a_i(s) \le \delta_i(s) \le b_i(s) \qquad i=1,2 \tag{3-4}$$

The constraints (3-4) naturally arise in flexible structures. If such a constraint is not imposed there is no guarantee on the accuracy of the end point along the path. Following the rationale expressed in the introduction, one would solve the problem without the constraint (3-4). The problem reduces to the one solved in [1],[2],[3].

The solution method we use closely follows Bobrow et.al.'s method with some modifications for flexible manipulators. The solution of the above stated optimization problem follows: for any path $S(x,y,z)$ with given $Z(S_0),Z(S_f)$ to minimize J, Z should be as large as possible while satisfying the system dynamics and actuator constraints. In order to do so at any state on the path one should use maximum acceleration or deceleration. Then, the problem is reduced to finding the maximum accelerations and decelerations associated with each state of interest. It can be seen from equation (2-6a) that for each (S_i,Z_i)

$$\ddot{S}_d \le \ddot{S} \le \ddot{S}_a$$

$$\ddot{S}_a = \min \left\{ \ddot{S}_{ai} \right\} \qquad (3\text{-}5)$$

$$\ddot{S}_d = \max \left\{ \ddot{S}_{di} \right\}$$

There may be some range of speeds associated with every point on the path that system can no longer satisfy all conditions (the Z range that above inequality is violated). The collection of these ranges defines the forbidden region on (S,Z) plane. The boundary between allowed and forbidden regions is constant for a given rigid manipulator for a given task. In the case of flexible manipulators, due to the coupling between equations (2-6a) and (2-6b) this boundary is also a function of flexible modes, not only (S, Z). So, depending on the time history of the flexible modes and unpredictable disturbances the boundary will vary. This is not true in the rigid case where the true extreme can be found. At this point the problem is to find when to use maximum accelerations and when maximum decelerations (i.e. to find the switching point(s)).See Fig. 3a-3b.

Finding switching points for near optimal performance of flexible manipulators then proceeds as follows:

1. Integrate $\dot{S}=S(x,y)$ from the final state backward in time until it crosses forbidden region or initial position, using maximum deceleration.

2. Integrate $\ddot{S}(x,y)$ forward in time from initial conditions (S_0,Z_0) with maximum acceleration until the boundary is reached or the two curves cross each other. If the two curves cross each other before they enter forbidden region, then find that point. This is the last switching point and terminates the search. If not, then

3. Backup on the last forward integrated curve and integrate forward with maximum deceleration until the trajectory intersects:

   a. the boundary of the forbidden region. If the intersection is not tangent within some tolerance, repeat 3.

   b. or the line Z = 0. In this case the distance backed up in 3 was too great. Reduce the amount of backup and repeat 3.

4. Then using the tangent point as new starting point go to step two.

Notice that the last switching point is not the exact switching point, because the flexible modes will not match at this point. That will cause one to miss the final state somewhat. Also, when searching for the switching points one has to move in a continuous manner in order to keep track of the flexible mode histories accurately. In that sense, the algorithm given in [1] has been modified for flexible robotic manipulators.

IV. TRAJECTORY MODIFICATION AND FLEXIBLE MODES

Once the near optimal trajectory Z(S) of the previous problem is found, one may consider modifying the trajectory in such a way that the constraints on the flexible modes are satisfied too. For any modified Z(S) which is affordable by actuators the equation (3-2b) can be integrated forward using the initial conditions of flexible modes at the beginning of the task.

$$\underline{\delta}(s_0) = \underline{\dot{\delta}}_0 \qquad (4\text{-}1)$$

In fact regardless of the affordability of any trajectory in (S,Z) plane, the flexible mode history along the path can be found by an integration along that trajectory.

A number of practical trajectory modifications using the cubic spline functions have been tried by the authors. Trajectories are modified in a smoothing fashion so that abrupt changes of torques at the switching points are avoided, expecting that the modified trajectory will result in less excited flexible modes. To some extent that is true, but since the dynamics of the flexible modes are highly complicated and nonlinear, not only the torques but also the coupling between states are important, particularly in the case of a minimum time problem. The initial trajectory modifications have not resulted in a favorable dynamic behavior and may not be generalized for all paths, because the shape of the path is also part of the dynamics and this is not explicitly mapped in to (S,Z) plane. Some simulation results are shown in Fig. 8 - 10.

The trajectory modification problem is currently being formulated as an optimum control problem with dynamic constraints. A generalized quasilinearization algorithm is applied iteratively starting with the unconstrained solution and iteratively approaching to the solution of the problem with dynamic constraints [10],[11],[12].

V. SIMULATION RESULTS AND DISCUSSION

The two-link flexible manipulator model for task one (shown in Fig. 4a) was simulated for the two different cases in order to show the performance improvement achieved due to a light-weight system. In both cases actuators have the same capabilities. It is found that weight reduction by a factor of 2 results in approximately 60 % time reduction (Fig. 5a and 6a). This improvement, of course, varies depending on the task. Joint actuator histories are shown in Fig. 5b-6c and flexible mode responses are shown in Fig. 5c-6d.

Task 2 (Shown in Fig. 4b) was simulated for light-weight manipulator and results are shown Fig 7 a-d. The final trajectory is shown in Fig. 7b. One interesting point in this simulation is the fact that as soon as the manipulator end point enters the curvature the system must accelerate along the path in order to obey the constraints. In Fig. 7a the curve ab shows that immediately before the curvature the system is able to decelerate (aa' curve), but as end point enters the curvature the sudden appearance of a normal acceleration term in the dynamics of the system appears and end of the manipulator has to accelerate in order to stay on the path. This indicates how sensitive a trajectory modification would be in this part of the trajectory. The other point in the case of flexible arms is that at the last switching point flexible modes are not same, since they have different histories. This will cause error in the final state reached. See Fig. 6a, 7a. The last switching point needs to be varied from the original result of the above algorithm.

VI. CONCLUSION AND FURTHER WORK

In this paper we showed ways to improve performance and productivity of Robotic manipulators with flexible arms. One way was to use light-weight structures and the other was to incorporate the dynamics of manipulators in to trajectory planning level and make optimum utilization of given manipulator. Some practical trajectory modifications are presented. The sensitivity of the trajectories on (S,Ż) plane is very high. Any small change in the slope may end up with quite different flexible mode history depending on the path and the speed along the path. The slope of the trajectory at the beginning of the task should be carefully modified if the execution time is of any interest, for small slopes where speed is small will take long execution time. Application of the method requires the manipulator dynamics, geometric path in work space, and actuator capabilities. Obviously as trajectory gets closer to the forbidden region boundary system capabilities are being used to the limits and any disturbance or uncertainty can easily put the system in to forbidden region and end of the manipulator will leave the desired path. This situation is more clear in the case of flexible robotic manipulators. While this analysis is nice in terms of knowing the maximum capabilities, in practice there will be some safety factor that will require to keep the trajectory away from the forbidden region boundary certain amount.

REFERENCES

1. Bobrow,J.E., Dubowsky,S., Gibson,J.S. "On the Optimal Control of Robotic Manipulators with Actuator Constraints" Proc. of 1983 ACC, San Fransisco, CA June 1983, pp 782-787.

2. Dubowsky,S., Shiller,Z. "Optimal Dynamic Trajectories For Robotic Manipulators" Fifth CISM-IFToMM Symposium on the Theory And Practice of Robotic Manipulators Preprints, June 26-29 1984, Udine, Italy ,pp 96-103.

3. Shin, K.G., McKay, M.D. "Minimum-Time Control Of Robotic Manipulators With Geometric Path Constraints" IEEE Trans. on Automatic Control, Vol AC-30 No.6, June 1985 pp 531-541.

4. Book, W.J. "Recursive Lagrangian Dynamics of Flexible Manipulators", The International Journal of Robotic Research, MIT Press, V.3,N.3 pp. 87-101, Fall, 1984.

5. Kahn, M.E., Roth, B. "The Near-Minimum Time Control of Open-loop Articulated Kinematic Chains" Journal of Dynamic Systems, Measurement, and Control. ASME Trans., Vol.93, No.3, Sept. 1971, pp 141-171.

6. Luh, J.Y.S., Lin, C.S. "Optimum Path Planning For Mechanical Manipulators", J. of Dynamic Systems, Measurement, and Control, ASME Trans., Vol.102, No.2, June 1981, pp 142-151.

7. Luh, J.Y.S., Walker, M.W., "Minimum-time Along the Path for a Mechanical Manipulator", Proc.of IEEE Conf. on Decision and Control, Dec. 1977, New Orleans, LA, pp 755-759.

8. Hollerbach, J.M. "Dynamic Scaling of Manipulator Trajectories" Proc. of ACC, June 1983, San Fransisco, CA.

9. Kiriazov, P., Marinov, P., "A Method for Time-Optimal Control of Dynamically Constrained Manipulators", Preprints of Fifth CISM-IFToMM Symposium On the Theory and Practice of Robots and Manipulators, 26-29 June 1984 , Udine, Italy.

10. McGill, R. "Optimal Control,Inequality State Constraints, and the Generalized Newton-Raphson Algorithm", Journal of SIAM, Ser. A, Vol. 3, No. 2, 1965, pp 291-298.

11. Mcgill, R., Kenneth, P. "Solution of Variational Problems by Means of a Generalized Newton-Raphson Operator", AIAA Journal, Vol. 2, No. 10, October 1964, pp 1761-1766.

12. Schley, C.H. Jr., Lee, I. "Optimal Control Computation by the Newton-Raphson Method and the Riccati Transformation", IEEE Transactions on Automatic Control, Vol. AC-12, No. 2, April 1967, pp 139-144.

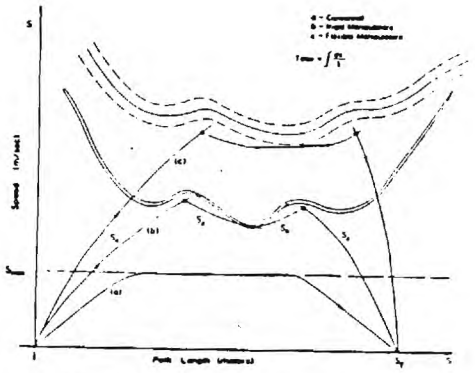

Fig.1 Different trajectory plans.

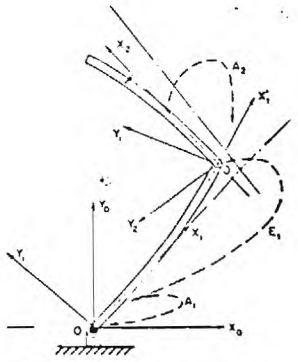

Fig.2 Manipulator Model.

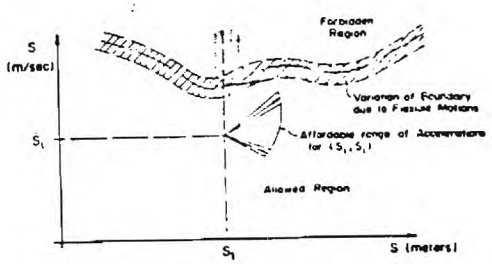

Fig. 3.a $(S,\dot{S})$ Plane

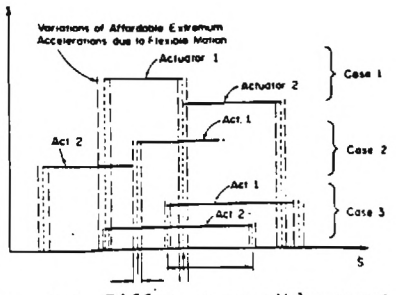

Fig. 3.b Different possible cases during a task.

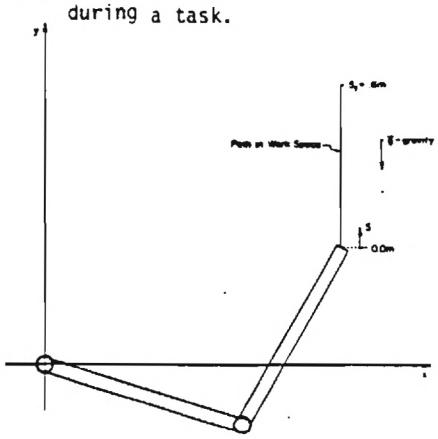

Fig. 4a. Task 1 in (x,y) plane.

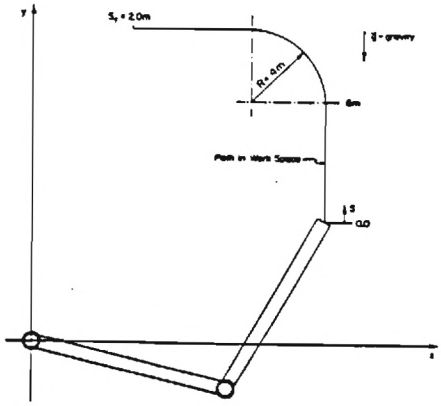

Fig. 4b Task 2 in (x,y) plane.

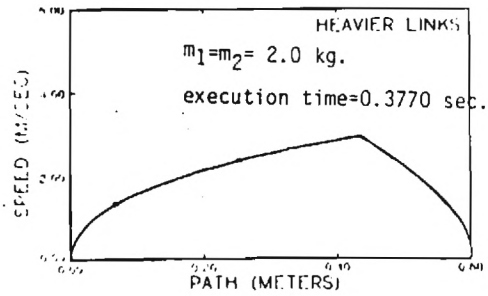

Fig. 5.a Trajectory for Path 1 of heavy links.

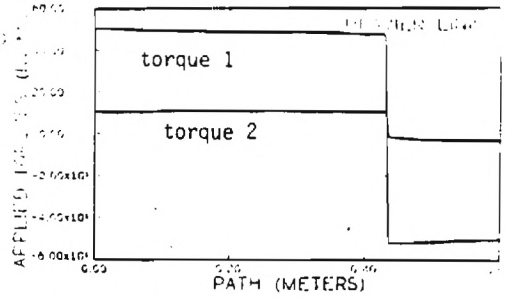

Fig. 5b. Torques along the path 1

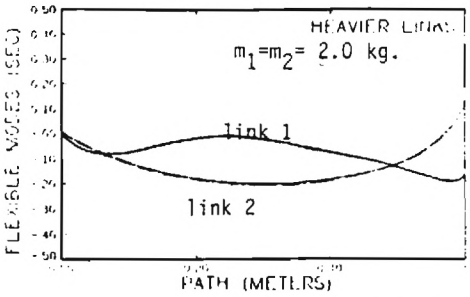

Fig. 5.c Flexible modes time variables

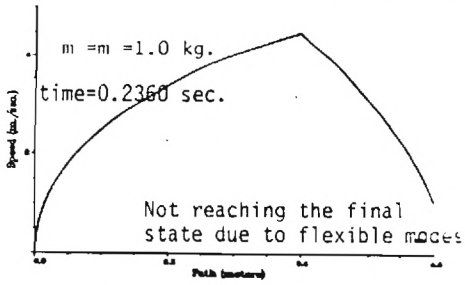

Fig. 6.a Trajectory of lightweight arms

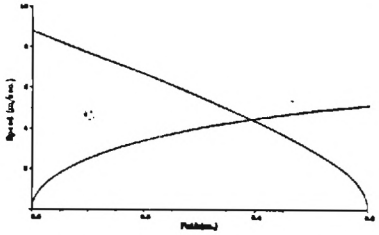

Fig. 6.b Finding the switching point

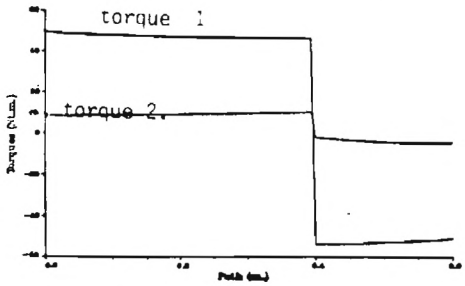

Fig. 6.c Torque histories of lightweight arms along path 1.

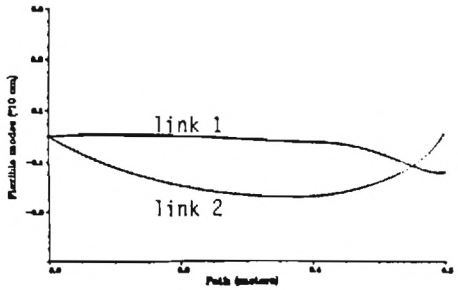

Fig. 6d. Flexible modes along path 1.

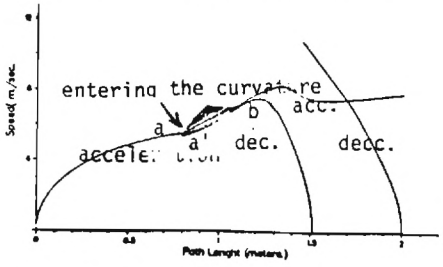

Fig. 7a. Finding the switching points for path 2.

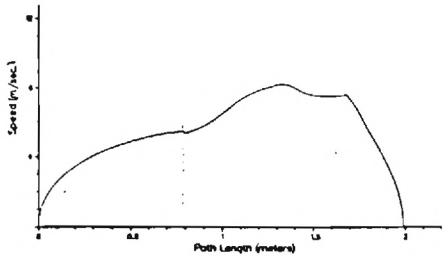

Fig. 7b. Trajectory for path 2.

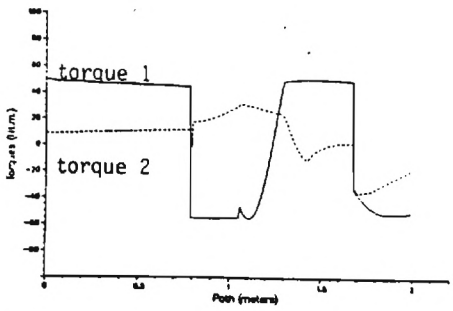

Fig. 7c. Torques along path 2.

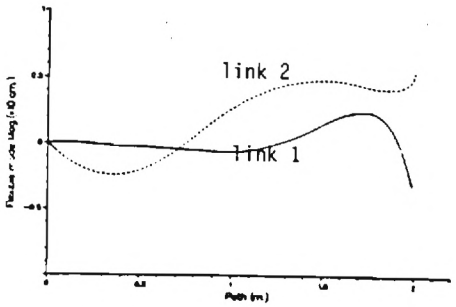

Fig. 7d. Flexible modes along path2.

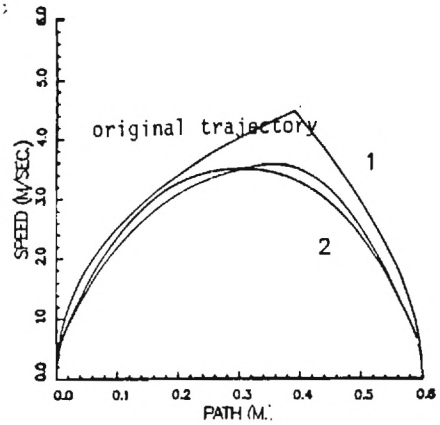

Fig. 8 Original and Modified Trajectories

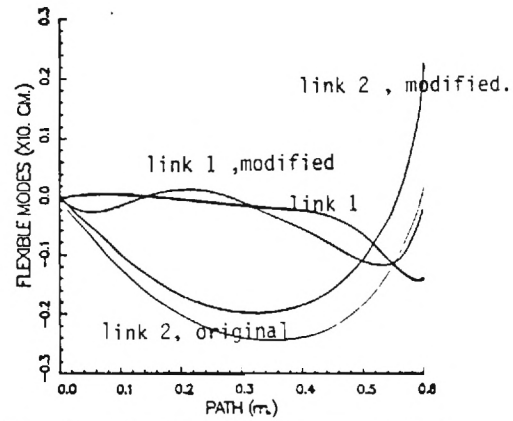

Fig. 9a. Flexible modes along original and modified trajectory 1.

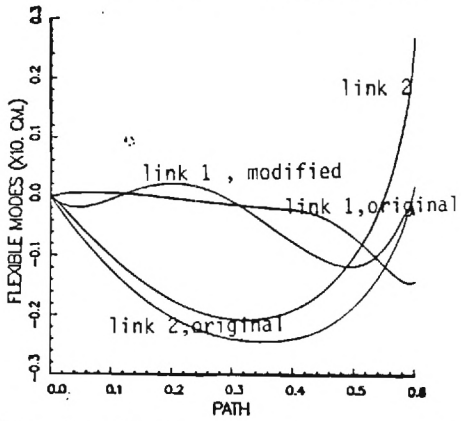

Fig. 9b. Flexible modes along original and modified trajectory 2.

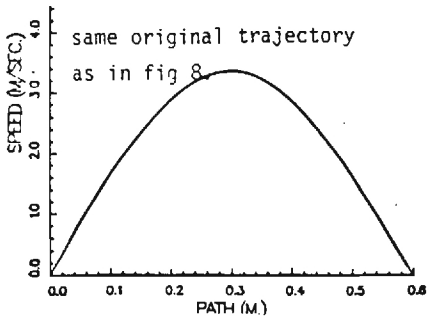

Fig. 10a. Modified trajectory 3.

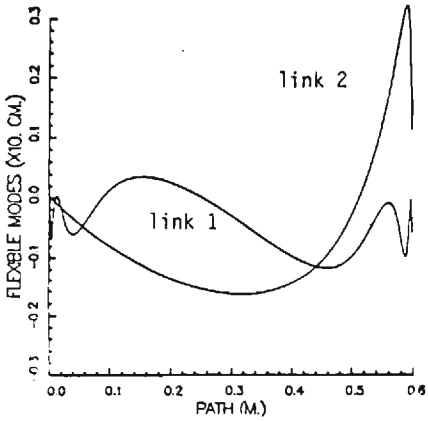

Fig. 10b. Flexible modes along modified trajectory 3.

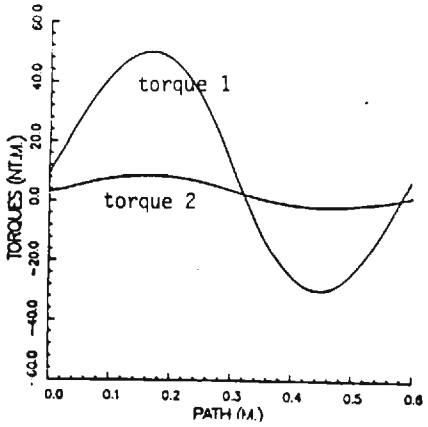

Fig. 10c. Torque histories along modified trajectory 3.

Proceedings of the 1986 IEEE International
Conference on Robotics and Automation,
April 7-10, 1986, San Francisco, CA

VERIFICATION OF A LINEAR DYNAMIC MODEL FOR FLEXIBLE ROBOTIC MANIPULATORS*

By Gordon G. Hastings, and Wayne J. Book

Department of Mechanical Engineering, Georgia Institute of Technology
Atlanta, Georgia

Abstract

This paper describes a linear state-space model for a flexible single link manipulator arm. The resultant model is compared to an experimental four foot long direct drive manipulator. The method employed to generate the model utilizes a separable formulation of assumed modes to represent the tranverse displacement due to bending. Lagrangian dynamics are applied to determine the kinetic and potential energies for the system. The resultant dynamic equations are then organized into a state space model suitable for use in linear control system design procedures. The performance of the model is considered for different model orders and assumed modes. Several important aspects of candidate mode selection, and results for different model order are discussed. The final section of the paper provides a brief summary and describes ongoing and future work.

Introduction

The material in this paper describes a linear model which forms the basis for investigating the control of flexible manipulators[1]. The initial sections discuss the modelling process, and verify parameters and algorithm implementation. The latter section compares simulation of the model to experimental measurements.

Model Generation

This sub-section describes the formation of a linear state space model for the flexible manipulator. The process for forming the model will be outlined in this section, a detailed description is contained in appendix A.

The first step of the process is to describe the position of every point along the flexible manipulator. A linear combination of vibratory modes to describe flexible deflections, and a rigid body motion of the center of mass is selected. A manipulator with a rigid body rotation and flexible "pinned-mass" mode is depicted in figure 1.

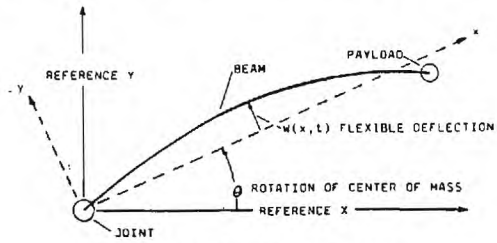

Flexible Manipulator
Figure 1

The flexible deflections are described by an infinite series of separable modes. Separability in this instance refers to describing the flexible deflections as a series modes which are products of two functions each a function of a single variable, one a function of a spatial varible, and the other a function of time. This is noted as:

$$w(x,t) = \sum \phi_i(x)\psi_i(t) \quad , \text{ for } i=1,2...n \qquad (1)$$

This separability is important in later phases of the process when the equations of motion are formed in terms of time varying variables only. Next the kinetic and potential energies are derived. The distributed character of the flexible manipulator is taken into account via integral expressions over the mass of the entire system in forming the energy expressions. The integral for calculating the kinetic energy, KE,has the following form;

$$KE = 1/2\int \dot{R}\cdot\dot{R}dm \qquad (2)$$

where $\dot{R}$, the absolute velocity vector, and mass range over the entire system. The potential energy, PE, of the system is stored in the flexible modes and can be attributed to "modal stifnesses", K_i, which are evaluated by integrals over the length as shown in equation A.12. Lagrange's equations of motion can be formed from the energies;

$$\frac{\partial}{\partial t}\left[\frac{\partial KE}{\partial \dot{q}_i}\right] - \frac{\partial PE}{\partial q_i} = Q_i \qquad (3)$$

where the q_i are the coordinates, and Q_i are the generalized work terms associated with each coordinate. Turning the computational crank on the various differentials and integrals as carried out in appendix A results in a coupled set of second order dynamic equations with familiar form;

$$[M][\ddot{z}] + [K][z] = [Q] \qquad (4)$$

$$z = [\theta,\psi_1(t),\psi_2(t),.....,\psi_n(t)] \qquad (5)$$

M is a mass matrix, K represents stiffness, and Q the input. The dynamic equations are easily organized into a state-space model as;

$$\begin{bmatrix} \dot{\theta} \\ \dot{\psi}_1 \\ \dot{\psi}_2 \\ \vdots \\ \ddot{\theta} \\ \ddot{\psi}_1 \\ \ddot{\psi}_2 \\ \vdots \end{bmatrix} = \left[\begin{array}{c|c} 0 & I \\ \hline M^{-1}K & 0 \end{array}\right] \begin{bmatrix} \theta \\ \psi_1 \\ \psi_2 \\ \vdots \\ \dot{\theta} \\ \dot{\psi}_1 \\ \dot{\psi}_2 \\ \vdots \end{bmatrix} + \begin{bmatrix} 0 \\ \hline M^{-1}Q \end{bmatrix} u \qquad (6)$$

*This material is based in part on work supported by the National Science Foundation under grant MEA-8303539 and by NASA grant NAG-1-623.

The input, u, into the system is torque applied by the motor at the joint, the generalized work terms, Q_i, are then related to the rotation of the joint with each variable. Examination of the form of the model reveals the expected result that the coupling between the modes, and the rigid body motion occurs from inertial terms of the mass matrix.

Equation (6) depicts a 2(n+1) order linear model where n is the number of included modes. Non-linear terms arise from the evaluation of equation 2 for the kinetic energy, and the specific assumptions employed to result in only linear terms is discussed in Apppendix A.

Mode Selection and Frequency Determinant

The approach being followed in this developement is called assumed modes methods[2], and the remaining task in generating a trial model is the selection of the flexible modes to be used in forming the constant mass and stiffness matricies.

The path chosen in this work is to select admissible functions as candidates which are solutions to closely related probems. These solutions are eigen-functions for selected "clamped-mass", and "pinned-mass" boundary value problems. Clamped describes a boundary condition where the joint is fixed against rotation, pinned describes a joint free to rotate, and -mass describes the condition of the payload at the other beam boundary. The admissible functions will then satisfy the differential equation, the essential or geometric boundary conditions, and the natural boundary conditions of the free vibration problem.

Appendix B describes the developement of the differential equation for a Bernoulli-Euler beam and solution of selected boundary value problems. The problem is formulated in terms of a frequency determinant for determination of the eigen-functions and the associated frequencies.

Experimental Setup

This section describes the experimental system used in examining the model. The system consists of a flexible arm with payload, DC torque motor with servo-amp, signal conditioning with A/D conversion for data acqusition, 16 bit computer system for implementation of control algorithms, and D/A conversion for torque signal output.

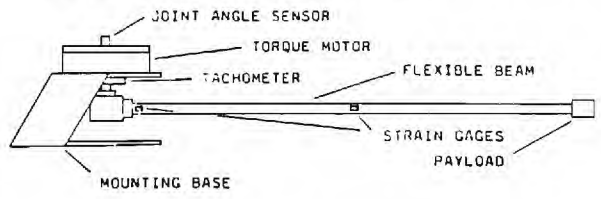

Flexible Beam Apparatus
Figure 2

The processor is equipped for hardware computation of floating point operations with a characteristic time for 32 bit multiplications of 19 microseconds. A torque motor is driven by a high internal gain DC servo-amp configured with a sense resistor on the motor output to act as a current source. The physical configuration of the flexible arm, torque motor, and sensors is represented in figure 2. Table 1 identifies the important parameters of the beam.

System Parameters
Table 1

Flexible Beam -	
Material	- Aluminum 6061-T6
Form	- Rectangular 3/4 x 3/16in
Length	- 48 in
Moment of Inertia	- 4.12E-4 in^4
EI Product	- 4120 $lbf-in^2$

Parameter and Program Verification

This section describes experiments conducted to verify system parameters and program implementation of the model generation process. Initally the frequencies determined via the Bernoulli-Euler beam equations with clamped-mass, and pinned-mass boundary conditions are compared to measured eigenvalues of the beam. This examines beam length, modulus, and density parameters, as well as, the suitability of the chosen boundary conditions.

Figure 3 shows the measured frequency response of strain at the base of the beam compared to random torques applied by the motor. The peaks correspond to "clamped-mass modes", while the valleys can be identified by the "pinned-mass" modes.

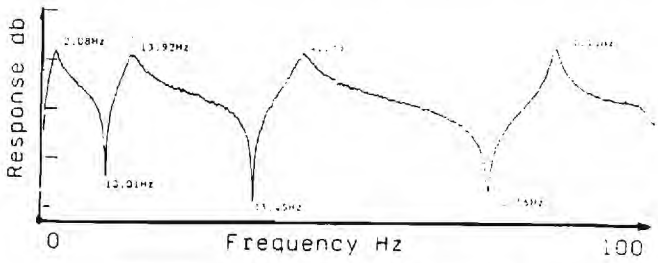

Frequency response for clamped beam
figure 3

The vibratory modes were additionaly calculated by the frequency determinant described in Appendix B. Table 2 compares the measured modal frequencies to those computed using the Bernoulli-Euler Beam. The application of the Bernoullid-Euler formulation to for the "clamped mass" case agrees very well with the measured frequencies, however, the "pinned-mass" conditions were not as accurate.

Comparison of Modal Frequencies(Hz)
Table 2

	Clamped-Mass		Pinned-Mass	
Mode	Measured	Calculated	Measured	Calculated
1	2.08	2.096	10.01	9.732
2	13.92	13.389	33.45	31.608
3	41.38	41.524	70.56	62.683
4	81.18	81.225		148.768
5		136.352		216.048

The the poorer agreement for the pinned case is attributed to the friction found in the joint hardware, this is a difficult condition to model and may have significant effect for the small amplitude motions used during the tests.

The next step checked the model generation algorithm. Normalization of the modal masses allowss the checking of the computations by examining the diagonal components of the stiffness matrix. The stiffnesses should be the square of the modal frequencies input to the process.

The algorithm was checked for both the clamped-mass modes and the pinned-mass modes. Table 3 presents a comparison of the modal frequencies input to the algorithm to the square root of the stiffnesses. The results are very good, however it was necessary to use higher precision computations for the higher modes.

Comparison of Frequencies Determined
by Stiffness Computations
Table 3

Clamped-mass		Pinned-Mass	
Input	Stiffness$^{1/2}$	Input	Stiffness$^{1/2}$
2.096Hz	2.096	9.732Hz	9.732
13.989	13.989	31.608	31.608
40.552	40.524	62.683	62.683
81.225	81.225	148.768	148.768
136.352	136.344	216.048	214.621

Dynamic Response Comparison

The previous section provides confidence that the beam parameters have been properly identified and modeled by the Bernoulli-Euler beam. The computational procedure has additionally been checked. The major questions concerning the model can now be investigated:

- Choosing the Modal Candidates
- Required Model Order
- Is a Linear Model of the Coupling Adequate

The following paragraphs describe simulations and experiments conducted to gain insight into the answer to these questions.

The simplest and best understood controller for flexible arms is a collocated controller, that is, a control system where the measurement and actuation is located at the same point. A collocated controller was implemented for the experimental system which applied a position gain to joint angle measurements, and a rate gain to angular velocity measurements.

The position gain was selected to provide the rigid body mode with a characteristic time of one second, and a rate gain providing a damping ratio of 0.7 was selected. Higher gains could be selected which stress the impact of flexibility on the control strategy, however, the chosen gains provide a good starting point well within the operating parameters of the system.

Figure 4 displays the measured response of the experimental system to a step change in desired angle. The strain at the beam base is also presented in the figure, while not used in the controller, it provides an indication of the relative modal amplitudes.

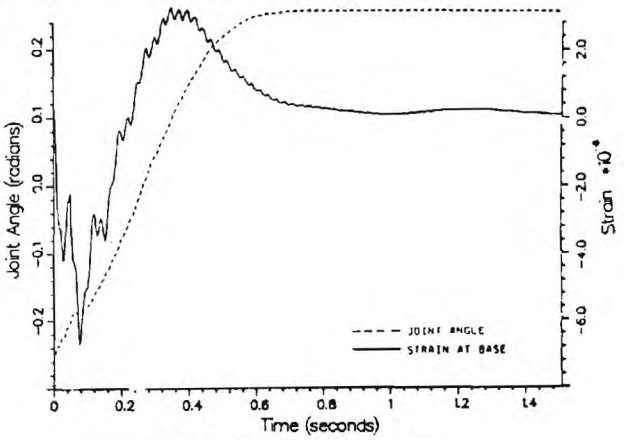

Measured Step Response
Figure 4

The dynamic model was discretized, and simulated for the step angle change. Small amounts of damping based on frequency response measurements were introduced into the model for the flexible modes. Additionally, a simple model for hysteretic joint friction was included in the digital simulation. Inclusion of modal damping and hysteresis in the simulations improved the agreement of the models especially in the time interval after the large initial transients had occured.

Figure 5 shows the results for a model implemented with five clamped-mass modes, while figure 6 presents a model using two clamped-mass modes. The last case simulated used five pinned-mass modes as inputs to the modeling process. This is presented in figure 7.

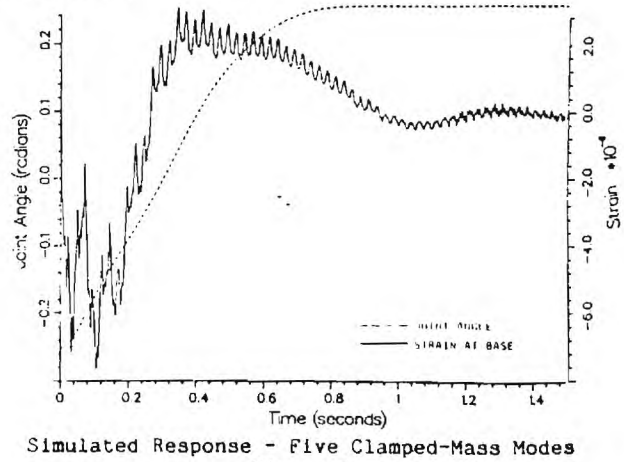

Simulated Response - Five Clamped-Mass Modes
Figure 5

The simulations based upon clamped-mass modes agree the best with measured responses. Suprisingly the model implemented with only two clamped-mass modes agrees almost as well if not better than the higher order model. This presentation maybe somewhat misleading as better determination of damping for the higher modes could provide better results. It

is apparent that a dominant portion of the response is adequately characterized by as few as two modes.

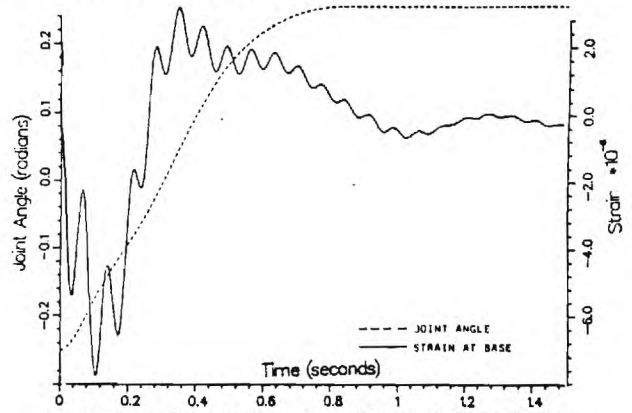

Simulated Response - Two Clamped-Mass Modes
Figure 6

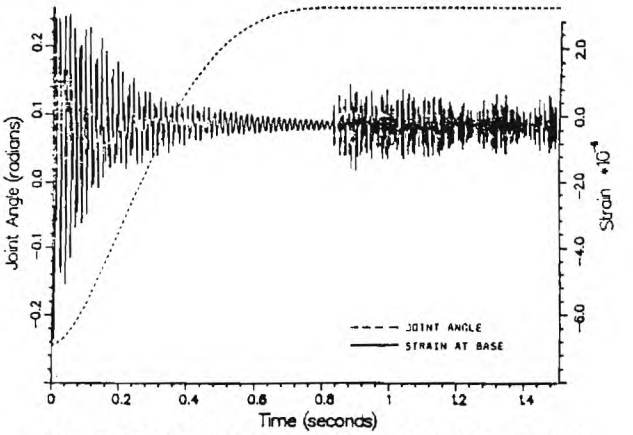

Simulated Response - Five Pinned-Mass Modes
Figure 7

Summary and Future Work

A modelling process to generate a linear model for use in controlling flexible manipulators was presented, and compared to experimental measurements for a position, and rate feedback controller. The model agreed favorably with the measured response for a selection of clamped-mass assumed modes. The dominant parts of the transient response were chararcterized by inclusion of as few as two assumed flexible modes.

The material collected here is part of a more comprehensive effort focusing on the control of flexible manipulators using feedback based on the modal variables, as well as joint position and velocity data. The selection of appropriate assumed modes must consider the feedback law, as the applied torque dominates the boundary condition at the base of the beam. Clamped-mass modes yielded good results for the simple collocated controller, however this may not prove true for more sophisticated controllers.

Current work examines the impact of optimal control laws on the model accuracy, and methods to integrate the feedback laws into the modal candidate selection.

APPENDIX A
FORMULATION OF DYNAMIC EQUATIONS

This section describes the generation of a dynamic model via application of Lagrange's equations to the flexible system[A1,A2]. The first step in this process is to select a suitable set of coordinates. The approach utilized selects one rigid body coordinate associated with the joint rotation, and flexible transverse displacements from a set of axes attached to the joint. This is depicted in figure 1. Then a position vector R to every point of the system can be can be constructed;

$$R = xi + w(x,t)j \qquad (A.1)$$

where i, j are unit vectors in the x, y directions. The absolute velocity of the position vector;

$$\dot{R} = \frac{\partial R}{\partial t} + \dot{\theta} x R \qquad (A.2a)$$

$$\dot{R} = x\dot{i} + \frac{\partial w(x,t)}{\partial t} j + \dot{\theta}(xj - w(x,t)i) \qquad (A.2b)$$

The kinetic energy of the system KE, can then be computed by integrating this expression over the entire mass of the flexible system M_s;

$$KE = 1/2 \int \dot{R} \cdot \dot{R} \, dm \qquad (A.3a)$$

$$\dot{R} \cdot \dot{R} = \left[\frac{\partial w(x,t)}{\partial t}\right]^2 + 2\theta \frac{\partial w(x,t)}{\partial t} x + \dot{\theta}^2 (x^2 + w^2(x,t)) \qquad (A.3b)$$

$$KE = 1/2 \int \{\left[\frac{\partial w(x,t)}{\partial t}\right]^2 + 2\dot{\theta}\frac{\partial w(x,t)}{\partial t} x + \dot{\theta}^2 (x^2 + w^2(x,t))\} dm \qquad (A.3c)$$

Next introduce the assumed mode series representation for the transverse deflections w(x,t);

$$w(\xi,t) = \sum \phi_i(\xi)\psi_i(t) \quad i = 1,2...n \qquad (A.4)$$

where $\xi = x/L$ a normalized length variable. Substitution for the transverse deflections results in;

$$KE = 1/2 \int [\sum \phi_i(\xi) \frac{d\psi_i}{dt}(t) \sum \phi_j(\xi) \frac{d\psi_j}{dt}(t) + 2\dot{\theta} L \xi \sum \phi_i(\xi) \frac{d\psi_i}{dt}(t) + \dot{\theta}^2((L\xi)^2 + \sum \phi_i(\xi)\psi_i(t) \sum \phi_j(\xi)\psi_j(t))] dm \qquad (A.5)$$

This integral can be separated into three integrals over the primary components of the beam, joint mass, beam mass, and payload. Evaluation of equation A.5 over the joint mass results in;

$$KE_m = 1/2 J_0 [\dot{\theta}^2 + \sum \frac{d\phi_i}{d\xi}(\xi) \frac{d\psi_i}{dt}(t) \sum \frac{d\phi_j}{d\xi}(\xi) \frac{d\psi_j}{dt}(t)] \qquad (A.5a)$$

Evaluation of equation (A.5) over the mass of the beam results in;

$$KE_b = 1/2 J_b \theta^2 + 1/2 \rho A_b L \int [\sum \phi_i(\xi) \frac{d\psi_i}{dt}(t) \sum \phi_j(\xi) \frac{d\psi_j}{dt}(t) + \xi L \phi_i(\xi) \frac{d\psi_i}{dt}(t)] d\xi \qquad (A.5b)$$

Notice that in evaluating;

$$1/2\rho A_b L\int[\dot\theta^2(x^2+\sum\phi_i(\xi)\psi_i(t)\sum\phi_j(\xi)\psi_j(t)]d\xi \quad (A.6)$$

rotary inertia of the cross section was neglected and the squared flexible deflections assumed negligible compared to the axial dimension squared. Finally the integral is evaluated over the mass of the payload as;

$$KE_p=1/2[M_pL^2+J_p]\dot\theta^2+1/2M_p\sum\phi_i(1)\frac{d\psi_i}{dt}(t)\sum\phi_j(1)\frac{d\psi_j}{dt}(t)+$$
$$1/2J_p\sum\frac{d\phi_i}{d\xi}(1)\frac{d\psi_i}{dt}(t)\sum\frac{d\phi_j}{d\xi}(1)\frac{d\psi_j}{dt}(t) \quad (A.7)$$

Next it is convenient to introduce an ortho-normal condition on the spatial mode functions.

$$1/2\rho A_b L\int[\sum\phi_i(\xi)\frac{d\psi_i}{dt}(t)\sum\phi_j(\xi)\frac{d\psi_j}{dt}(t)]d\xi +$$
$$1/2M_p\sum\phi_i(1)\frac{d\psi_i}{dt}(t)\sum\phi_j(1)\frac{d\psi_j}{dt}(t) +$$
$$1/2J_p\sum\frac{d\phi_i}{d\xi}(1)\frac{d\psi_i}{dt}(t)\sum\frac{d\phi_j}{d\xi}(1)\frac{d\psi_j}{dt}(t) = 1 \text{ , for } i=j$$
$$= 0 \text{ , for } i=j \quad (A.8)$$

The potential energy, PE, for the system is evaluated by the following integral expression;

$$PE = 1/2EI\int[\sum\frac{d^2\phi_i}{dx^2}(x)\psi_i(t)\sum\frac{d^2\phi_j}{dx^2}(\xi)\psi_j(t)dx \quad (A.9)$$

Applying the orthogonality condition on the mode functions, and substituting the normalized length variable yields;

$$PE = 1/2\frac{EI}{L^3}\int\sum[\frac{d^2\phi_i}{d\xi^2}(\xi)]^2\psi^2{}_i t)d\xi \quad (A.10)$$

Notation in the following sections can be greatly simplified if the following definitions are made for a "modal stiffness", K_i, for equation (A.10), and "moment of modal mass", W_i, for the last integrand in equation (A.5b) as;

$$K_i = 1/2\frac{EI}{L^3}\sum\psi^2{}_i(t)\int[\frac{d^2\phi_i}{d\xi^2}(\xi)]^2d\xi \quad (A.11)$$

$$W_i = \rho A_b{}^2\sum\psi_i(t)\int\xi\phi_i(\xi)d\xi \quad (A.12)$$

Then the kinetic energy for the system can be expressed as;

$$KE = 1/2\dot\theta^2[J_0+J_p+M_pL^2]+\dot\theta\sum\frac{d\psi_i}{dt}(t)[W_i+LM_p\phi(1)+$$
$$LJ_p\phi(1)]+1/2\sum[\frac{d\psi(t)}{dt}]^2 \quad (A.13)$$

To form the dynamic equation we form the Lagrangian of the energy expressions;

$$\frac{\partial}{\partial t}[\frac{\partial KE}{\partial\dot q_i}] - \frac{\partial PE}{\partial q_i} = Q_i \quad (A.14)$$

Where the q_i are the coordinates, and Q_i represents the work done by the input torque at the joint by each coordinate. The resultant equations can then be organized in matrix form;

$$[M][\ddot z] + [K][z] = [Q] \quad (A.15)$$

$$z = [\theta,\psi_1(t),\psi_2(t),\ldots,\psi_n(t)] \quad (A.16)$$

M =

$$\begin{bmatrix} J_0+J_b+J_p+M_pL^2 & W_1+LM_p\phi_1(1)+J_p\frac{d\phi_1}{d\xi}(1) & W_2+LM_p\phi_2(1)+J_p\frac{d\phi_2}{d\xi}(1) & \cdots \\ W_1+LM_p\phi_1(1)+J_p\frac{d\phi_1}{d\xi}(1) & 1 & 0 & \cdots \\ W_2+LM_p\phi_2(1)+J_p\frac{d\phi_2}{d\xi}(1) & 0 & 1 & \cdots \\ \vdots & \vdots & \vdots & \end{bmatrix} \quad (A.17)$$

$$K = \begin{bmatrix} 0 & 0 & 0 & \cdots \\ 0 & K_1 & 0 & \cdots \\ 0 & 0 & K_2 & \cdots \\ \cdot & \cdot & \cdot & \cdot \\ \cdot & \cdot & \cdot & \cdot \end{bmatrix} \quad Q = \begin{bmatrix} 1 \\ \frac{d\phi_1}{d\xi}(0) \\ \frac{d\phi_2}{d\xi}(0) \\ \cdot \\ \cdot \end{bmatrix} \quad (A.18,19)$$

This system is easily organized into a linear state-space model as shown in equation 6.

Appendix B
Bernoulli-Euler Beam Equations

This section describes the developement of a frequency determinant from Bernoulli-Euler beam theory which was used to derive candidate mode frequencies and the associated shapes. The homogeneous differential equation is presented first, followed by a discussion of the boundary conditions utilized. Lastly the frequency determinant is derived.

Differential Equation

The transverse displacement of the beam, w(x,t), shown in figure A-1 is a function of both the spatial variable along the beam, and time. Following the analysis attributed to Bernoulli and Euler gives rise to following fourth order partial differential equation.

$$EI\frac{\partial^4 w(\xi,t)}{\partial\xi^4} - \rho A_b L^4\frac{\partial^2 w(\xi,t)}{\partial t^2} = 0 \quad (B.1)$$

where: $\xi=x/L$

The next step applies the separability of equation (1) to obtain the following result;

$$EI\frac{d^4\phi(\xi)}{d\xi^4}\psi(t) - \rho A_b L^4\phi(\xi)\frac{d^2\psi(t)}{dt^2} = 0 \quad (B.2)$$

Searching for periodic time functions of the form $\psi(t)= e^{i\omega t}$ leads to the following formulation;

$$EI[\frac{d^4(\xi)}{d\xi^4} - \rho L^4 A\phi(\xi)\omega^2]\psi(t) = 0 \quad (B.3a)$$

This implies that the term in brackets must be equal to zero for all time t. This is expressed as:

$$\frac{d^4\phi(\xi)}{d\xi^4} - \beta^4\phi(\xi) = 0 \qquad (B.3b)$$

where the new parameter,

$$\beta^4 = \frac{\rho A_b L^4 \omega^2}{EI} \qquad (B.4)$$

has been substituted.

This is readily solved for $\phi(\xi)$:

$$\phi(\xi) = A\sin(\beta\xi) + B\cos(\beta\xi) + C\sinh(\beta\xi) + D\cosh(\beta\xi) \qquad (B.5)$$

Boundary Conditions

The solution for the spatial mode function $\phi(\xi)$ requires four independent boundary conditions be provided. The first and most obvious results from noting that there cannot be transverse displacement at the pinned joint, this takes the form;

$$\phi(\xi) = 0 \text{ , for } \xi = 0 \qquad (B.6)$$

The second condition is provided from a moment balance at joint, this is expressed as;

$$\frac{d^2\phi(\xi)}{d\xi^2} = \frac{-J_0\beta^4 d\phi(\xi)}{\rho A_b L^3 d\xi} \quad \text{for } \xi = 0 \qquad (B.7)$$

where the following substitution was made to eliminated the dependence on the frequency;

$$\omega^2 = \frac{\beta^4 EI}{\rho A_b L^4} \qquad (B.8)$$

Using this boundary condition results in pinned mode shapes for small joint inertias, additionally clamped mode shapes can be determined by inputing very large joint inertias. This provides more programming versatility than supplying one formulation of the frequency determinant for each type of boundary condition.

The third boundary condition is derived by resolving the shear force at the end of the beam against the inertial forces of the payload mass. This takes the following form;

$$\frac{d^3\phi(\xi)}{d\xi^3} = \frac{-M_p\beta^4\phi(\xi)}{\rho A_b L^3} \text{ , for } \xi = 1 \qquad (B.9)$$

The last boundary condition arises from a moment balance against the angular inertial forces of the payload.

$$\frac{d^2\phi(\xi)}{d\xi^2} = \frac{-J_p\beta^4 d\phi(\xi)}{\rho A_b L^3 d\xi} \quad \text{for } \xi = 1 \qquad (B.10)$$

Frequency Determinant

Application of the boundary conditions to the solution for $\phi(\xi)$ will result in a frequency determinant for the eigen-values β. Application of the first boundary condition for transverse displacement at the joint relates two of the constants in the solution;

$$B = -D \qquad (B.11)$$

The second boundary condition balancing the moment at the joint forms a relation between three of the of the constants;

$$2DJ_0 = -\rho A_b L^3 \beta^3 (A+C) \qquad (B.12)$$

The shear force balance at the payload relates all the constants of the solution;

$$A(M_p\frac{\beta}{A_bL}\sin\beta - \cos\beta) + B(\sin\beta + M_p\frac{\beta}{A_bL}\cos\beta) +$$
$$C(M_p\frac{\beta}{A_bL}\sinh\beta + \cosh\beta) + D(\sinh\beta + M_p\frac{\beta}{A_bL}\cosh\beta) = 0 \qquad (B.13)$$

The moment balance at the payload forms a similar relation;

$$-A(\sin\beta + J_p\frac{\beta^3}{A_bL^3}\cos\beta) + B(J_p\frac{\beta^3}{A_bL^3}\sin\beta - \cos\beta) +$$
$$C(\sinh\beta - J_p\frac{\beta^3}{A_bL}\cosh\beta) + D(-J_p\frac{\beta^3}{A_bL}\sinh\beta + \cosh\beta) = 0 \qquad (B.14)$$

The expressions (B.11- B.14) involve only the constants from the solution for the mode function and the parameter β. This can be configured in matrix form as;

$$F(\beta)\begin{matrix}A\\D\end{matrix} = 0 \qquad (B.15)$$

$$F_{11} = \sin\beta + \sinh\beta + J_{p^*}\beta^3(\cos\beta - \cosh\beta) \qquad (B.16)$$

$$F_{12} = \sin\beta - \sinh\beta + \frac{2\cosh\beta}{J_{0^*}\beta^3} + M_{p^*}\beta(\cos\beta - \cosh\beta) + \frac{2\sinh\beta}{J_{0^*}\beta^3} \qquad (B.17)$$

$$F_{21} = \cos\beta + \cosh\beta - M_{p^*}\beta(\sin\beta - \sinh\beta) \qquad (B.18)$$

$$F_{22} = -\cos\beta - \cosh\beta + \frac{2\sinh\beta}{J_{0^*}\beta^3} + J_{p^*}\beta^3(\sinh\beta - \sin\beta) -$$
$$2J_{p^*}\frac{\cosh\beta}{J_{0^*}\beta^3} \qquad (B.16)$$

Where the starred subscripts indicate modification by the appropriate area and length terms. The roots of the frequency determinant $\det[F(\beta_i)] = 0$ yield the characteristic values for the mode functions $\phi_i(\xi)$, and associated frequncies ω_i.

Table of Symbols

J_0 - Joint Inertia	J_p - Payload Inertia
M_p - Payload Mass	E - Modulus of Elasticity
A_b - Beam Area	I - Beam Area Inertia
L - Beam Length	ρ - Density per Length

Bibliography

1. G. Hastings, W. Book,"Experiments in the Optimal Control of a Flexible Manipulator", Proceedings ACC, Summer 1985.

2. L. Meirovitch,"Elements of Vibration Analysis",Mc-Graw Hill, 1975.

A1. J. Neto,"Automatic Control of a Vibrating Transverse Beam",MS Thesis, MIT, January 1972.

A2. V. Sangveraphunsiri,"The Optimal Control and Design of a Flexible Manipulator Arm", PhD Thesis, Georgia Institute of Tech., May 1984.

A BRACED END EFFECTOR
FOR A FLEXIBLE ROBOT MANIPULATOR

A THESIS

Presented to

The Faculty of the Division of Graduate Studies

By

Ray Lanier Holden

In Partial Fulfillment

of the Requirements for the Degree

Master of Science in Mechanical Engineering

Georgia Institute of Technology

February, 1986

ABSTRACT

Conventional robot manipulators are designed for rigidity, in order to minimize endpoint deflection and achieve positional accuracy. However, many manipulator tasks require accurate positioning only at certain points along the commanded trajectory. For gross motion, which may comprise a major portion of the task, deviations from the commanded trajectory are permissible and the robot's structural rigidity is not necessary.

An alternative strategy is to design a manipulator which is flexible for gross motion and rigid when the end effector performs fine motions. The manipulator is braced on the work surface, establishing a new base for the end effector. Deflections in the flexible part of the manipulator, caused by gravity and dynamic loads, are attenuated when the manipulator is braced, and the end effector's accuracy is greatly improved.

The design of a bracing end effector for a long-reach, flexible arm is presented. The end effector consists of a bracing structure and a rigid manipulator. Force exerted by the flexible arm affixes the bracing structure to the surface while the manipulator performs its task. The manipulator has three degrees of freedom, and features unlimited rotation around the bracing leg. Its maximum

reach is 56 inches and it has an operating payload of up to six pounds. Total end effector weight is approximately 62 pounds.

Manipulator and bracing structure geometries are based on requirements imposed by prospective end effector tasks and by compatibility with the large flexible arm. Possible applications include surface inspection, welding, painting, and water-jet cutting.

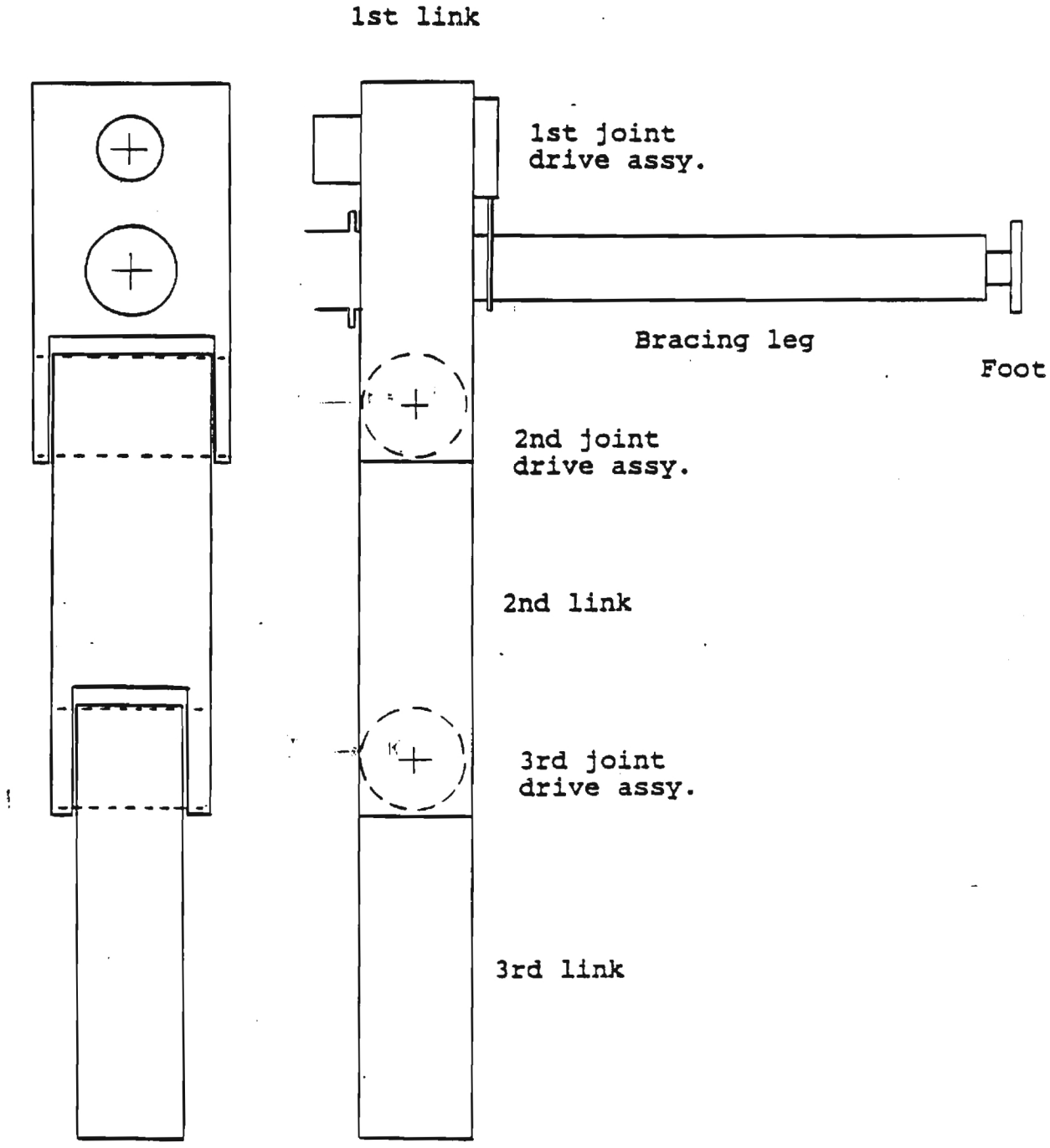

Figure 27. End effector schematic.

Table 8. End Effector Dimensions

1st Link	
1st joint to axis thru bracing leg	7.5 in.
Axis thru bracing leg to second joint	8.5 in.
Overall length	23.5 in.
Width	12.3 in.
Height	7.0 in.
Link center of mass to axis thru leg	2.5 in.
2nd Link	
2nd joint to 3rd joint	24.0 in.
Overall length	31.0 in.
Width	10.7 in.
Height	7.0 in.
Link center of mass to second joint	12.0 in.
3rd Link	
3rd joint to end	24.0 in.
Overall length	27.5 in.
Width	6.9 in.
Height	7.0 in.
Link center of mass to third joint	12.0 in.
Bracing Leg	36.0 in.

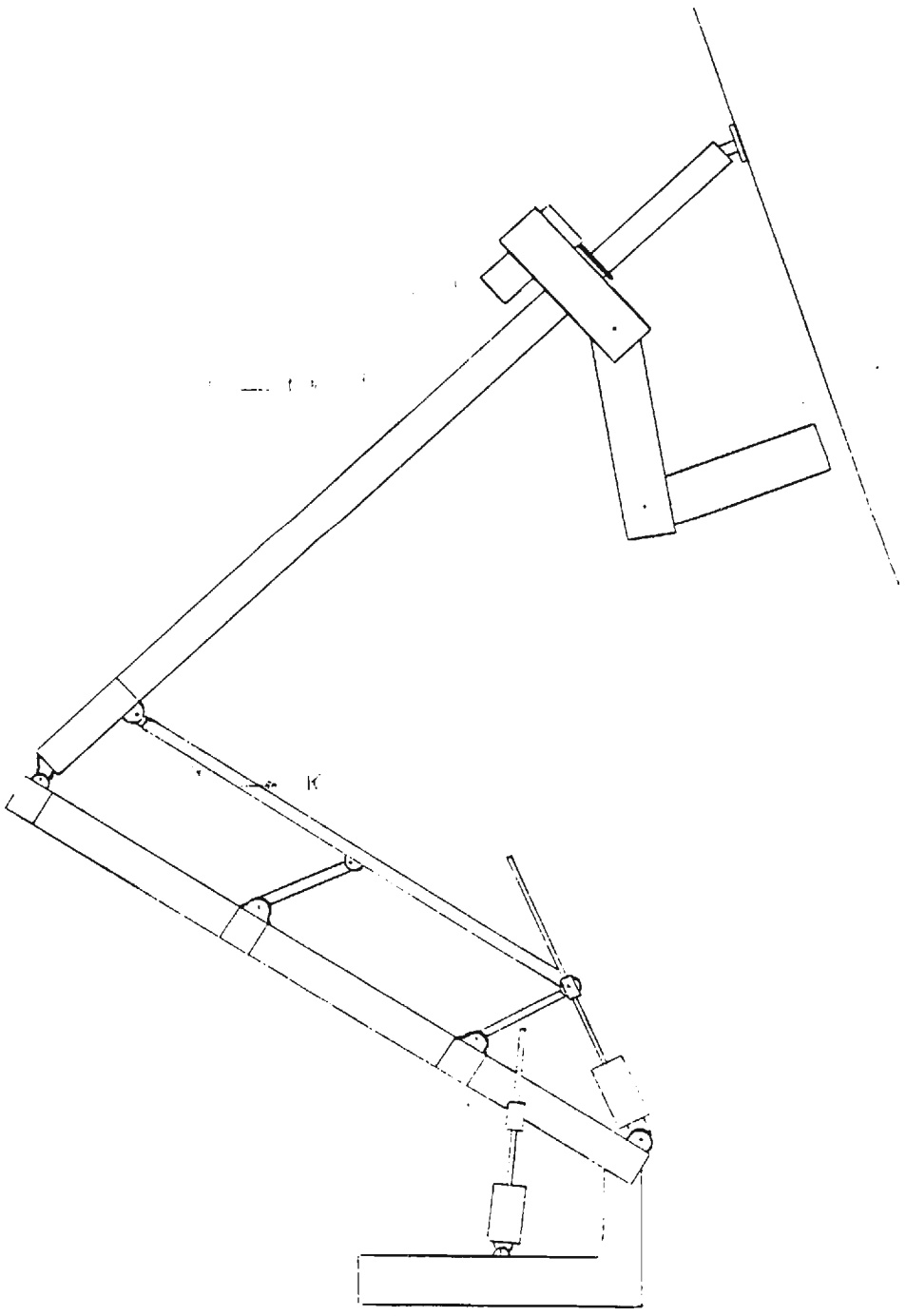

Figure 28. Large arm and end effector.

The Design and Construction of a Flexible Manipulator

Thomas Rowe Wilson

164 Pages

Directed by Dr. Wayne J. Book

The current practice in designing robot controllers is to assume that the links of the robot are rigid. Construction of rigid link robots requires either fairly short link lengths or extremely heavy design. Using the rigid link criteria, the construction of robots with large reaches is impractical due to required weight and actuator power. Through the use of modal control and the concept of "Bracing" the rigid link requirement can be discarded. Modal control accounts for deflection in the links and allows reasonably accurate control of the manipulator endpoint. Bracing allows the robot to perform precise manipulations on a worksurface located some considerable distance from the base of the robot. Bracing of the manipulator is similar to resting one's hand on the desk when writing to allow neater (more precise) script.

This thesis is concerned with designing a large manipulator arm to provide experimental apparatus on which to test the concepts of modal control and bracing. Included

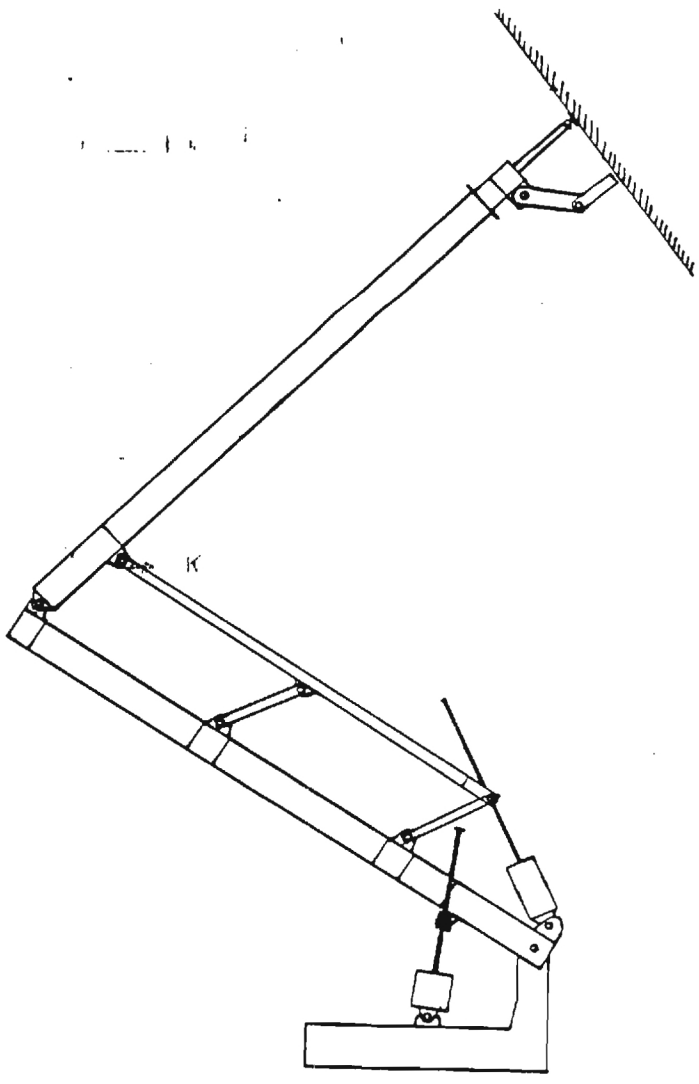

Figure 1-1. Robot Bracing Against Worksurface.